Stochastic Stability of Viscoelastic Systems

by

Qinghua Huang

A thesis
presented to the University of Waterloo
in fulfilment of the
thesis requirement for the degree of
Doctor of Philosophy
in
Civil Engineering

Waterloo, Ontario, Canada, 2008

Author's Declaration

I hereby declare that I am the sole author of this thesis. This is a true copy of the thesis, including any required final revisions, as accepted by my examiners.

I understand that my thesis may be made electronically available to the public.

Abstract

Many new materials used in mechanical and structural engineering exhibit viscoelastic properties, that is, stress depends on the past time history of strain, and vice versa. Investigating the behaviour of viscoelastic materials under dynamical loads is of great theoretical and practical importance for structural design, vibration reduction, and other engineering applications. The objective of this thesis is to find how viscoelasticity affects the stability of structures under random loads.

The time history dependence of viscoelasticity renders the equations of motion of viscoelastic bodies in the form of integro-partial differential equations, which are more difficult to study compared to those of elastic bodies.

The method of stochastic averaging, which has been proved to be an effective tool in the study of dynamical systems, is applied to simplify some single degree-of-freedom linear viscoelastic systems parametrically excited by wide-band noise and narrow-band noise. The solutions of the averaged systems are diffusion processes characterized by Itô differential equations. Therefore, the stability of the solutions is determined in the sense of the moment Lyapunov exponents and Lyapunov exponents, which characterize the moment stability and the almost-sure stability, respectively. The moment Lyapunov exponents may be obtained by solving the averaged Itô equations directly, or by solving the eigenvalue problems governing the moment Lyapunov exponents.

Monte Carlo simulation is applied to study the behaviour of stochastic dynamical systems numerically. Estimating the moments of solutions through sample average may lead to erroneous results under the circumstances that systems exhibit large deviations. An improved algorithm for simulating the moment Lyapunov exponents of linear homogeneous stochastic systems is presented. Under certain conditions, the logarithm of norm of a solution converges weakly to normal distribution after suitably normalized. This property, along with the results of Komlós-Major-Tusnády for sums of independent random variables, are applied to construct the algorithm. The numerical results obtained from the improved algorithm are used to determine the accuracy of the approximate analytical moment Lya-

punov exponents obtained from the averaged systems. In this way the effectiveness of the stochastic averaging method is confirmed.

The world is essentially nonlinear. A single degree-of-freedom viscoelastic system with cubic nonlinearity under wide-band noise excitation is studied in this thesis. The approximated nonlinear stochastic system is obtained through the stochastic averaging method. Stability and bifurcation properties of the averaged system are verified by numerical simulation. The existence of nonlinearity makes the system stable in one of the two stationary states.

Acknowledgments

First and foremost, I like to express my sincere appreciation to my supervisor, Professor Wei-Chau Xie, for his valuable advice, support and encouragement during the years of this research.

I like to extend my thanks to Professors A. J. Heunis, X. Z. Liu, S. Potapenko, and S. Narasimhan, for their suggestions and cares for my research.

Thanks also go to my friends, the family of Xianxun Yuan, the family of Wensheng Bu, Jinyu Zhu, Jun Liu, Tianjin Cheng, Richard Wiebe, Dongliang Lu, Xiaoguang Chen, Xiaohong Wang, Yuxin Liu, Ying An, Hongtao Liu, and other graduate students in the mechanics and structural engineering group, with whom I shared the unforgettable days in Waterloo.

The financial support by the Natural Sciences and Engineering Research Council of Canada through Grant No. OGPO131355 in the form of a Research Assistantship is greatly appreciated.

This thesis was made possible by the facilities of the Shared Hierarchical Academic Research Computing Network (SHARCNET: www.sharcnet.ca).

Last but not least, without the support and encouragement from my parents and sisters throughout these years, this thesis would not be possible.

TO

My Parents and Sisters

Contents

List of Figures

C H A P T E R 1

Introduction

1.1 Stability and Bifurcation of Stochastic Dynamical Systems

1.1.1 Stochastic Stability

Stability problems spread widely in physical sciences and engineering applications. For example, the vibration of buildings under wind and seismic loads should not be too large, or in better cases, diminish gradually as time passes by. Phenomenally, stable system means that its output should be under a preset level, provided that its input is small. If a system becomes unstable, its ouput will exceed a critical level or lose control even if the input is small enough.

Mathematically, a deterministic system with state vector $\mathbf{x} \in \mathcal{R}^d$ may be characterized by the differential equation

$$\dot{\mathbf{x}}(t) = \mathbf{A}(t, \mathbf{x}), \quad \mathbf{x}(0) = \mathbf{x}_0 \in \mathcal{R}^d. \tag{1.1.1}$$

If the mapping $\mathbf{A} : [0, \infty) \times \mathcal{R}^d \to \mathcal{R}^d$ is continuous, and locally Lipschitz with respect to $\mathbf{x}$, then equation (1.1.1) has a unique solution in the neighborhood of the initial point $(0, \mathbf{x}_0)$ [12], [49]. Since a shift transformation can always be applied, the trivial solution or zero equilibrium point of the transformed system is usually considered, without loss of generality, when studying the stability property of the corresponding solution for the

original system. Different types of stability for system (1.1.1) can be found in many classical references, such as [79], [18], and [120].

It is usual that a system is affected by some indetermined or random parameters, and external disturbances or noises. A vector stochastic process $\boldsymbol{\xi}(t)$, which describes the indetermined disturbances, may be introduced and thus leads to the so-called stochastic differential dynamical system

$$\dot{\mathbf{x}}(t) = \mathbf{A}(t, \mathbf{x}, \boldsymbol{\xi}(t)), \quad \mathbf{x}(0) = \mathbf{x}_0 \in \mathcal{R}^d. \tag{1.1.2}$$

The existence of $\boldsymbol{\xi}(t)$ makes the stochastic system different from the deterministic system since the state at any fixed time is not uniquely determined, thus the stability has to be defined first in order to investigate system (1.1.2) in a rigorous sense.

Similar to deterministic systems, the equilibrium point $\mathbf{x}^* = \mathbf{0}$ can be considered for system (1.1.2), without loss of generality, by applying a shift transformation, provided that it is a solution of the transformed system. The most frequently used stochastic stability concepts are almost-sure stability and moment stability, whose definitions follow Kushner [68], Khasminskii [58], and Arnold [8] below.

Almost-Sure (a.s.) Stability or Stability with Probability One (w.p.1)

The equilibrium point $\mathbf{x}^* = \mathbf{0}$ is stable with probability 1 (w.p.1) if, for any $\varepsilon > 0$ and $\rho > 0$, there exists $\delta(\varepsilon, \rho) > 0$ such that

$$\mathcal{P}\left\{ \sup_{t \geqslant 0} \left\| \mathbf{x}(t) \right\| \geqslant \varepsilon \right\} < \rho,$$

whenever $\left\| \mathbf{x}(0) \right\| < \delta$, where $\mathcal{P}\{\cdot\}$ denotes the probability, $\| \cdot \|$ denotes a suitable vector norm.

Almost-Sure Asymptotic Stability

The equilibrium point $\mathbf{x}^* = \mathbf{0}$ is asymptotically stable w.p.1 if and only if it is stable w.p.1 and

$$\mathcal{P}\left\{ \lim_{t \to \infty} \left\| \mathbf{x}(t) \right\| = 0 \right\} = 1.$$

Moment Stability

The equilibrium point $\mathbf{x}^* = \mathbf{0}$ is stable in the pth moment if, for any $\varepsilon > 0$, there exists $\delta > 0$ such that $\mathrm{E}\big[\|\mathbf{x}(t)\|^p\big] < \varepsilon$, for all $t \geqslant 0$ and $\|\mathbf{x}(0)\| < \delta$, where $\mathrm{E}[\,\cdot\,]$ denotes the expectation.

Lyapunov's direct method is widely used in studying the stability of deterministic systems. The idea is to find a function, that is positive everywhere, except at the origin where it takes zero value. This function is known as the Lyapunov function and can be treated as the total energy of the system. If the derivative of this function with respect to time is less than or equals to zero, it means that the total energy of the system is nonincreasing with time. In this sense the trivial equilibrium point is stable. More details on Lyapunov's direct method can be found in references such as [12] and [54].

With the theory of probability and stochastic processes, there is also the stochastic Lyapunov function theorem for determining the stability of stochastic dynamical systems, which has a close relation with the martingale theory, since the derivative of Lyapunov function may be evaluated in accordance with Itô's theorem. More details may be refered to the work by Kushner [68], Khasminskii [58], and Arnold [8]. Compared to deterministic cases, it is generally more difficult to find the Lyapunov functions for stochastic systems.

Although Lyapunov function theorem provides a method to determine the stochastic stability of dynamical systems, it is generally not an easy task to find the Lyapunov functions for stochastic systems. Therefore, other direct methods concerning with the stochastic stability, such as determining the Lyapunov exponents and the moment Lyapunov exponents of stochastic dynamical systems, are exploited.

For a linear system

$$\dot{\mathbf{x}}(t) = \mathbf{A}(t)\,\mathbf{x}(t), \quad \mathbf{x}(0) = \mathbf{x}_0 \neq \mathbf{0},$$

the Lyapunov exponents are defined by

$$\lambda_{\mathbf{x}(t)}(\mathbf{x}_0) = \lim_{t\to\infty} \frac{1}{t} \log \|\mathbf{x}(t; \mathbf{x}_0)\|, \tag{1.1.3}$$

which characterize the exponential rates of growth or decay of the solutions as $t \to \infty$. The Lyapunov exponents were first introduced by Lyapunov [78], and later advanced by Oseledec [89] to stochastic dynamical systems. Another approach to the Lyapunov exponents is the product of independent and identically distributed (i.i.d.) invertible random matrices (see,

e.g. [38], [39], [23]), which gives an alternative proof to Oseledec's multiplicative ergodic theorem. It is shown that $\lambda_{\mathbf{x}(t)}(\mathbf{x}_0)$ exist w.p.1 if $\mathbf{A}(t)$ is a stationary stochastic process with $\mathrm{E}\big[\|\mathbf{A}(t)\|\big] < \infty$. If moreover $\mathbf{A}(t)$ is ergodic, then $\lambda_{\mathbf{x}(t)}(\mathbf{x}_0)$ take only finitely many deterministic real values.

Hence, the Lyapunov exponents determine the almost-sure stability. If the largest Lyapunov exponent is negative, the solution will decay to zero exponentially as $t \to \infty$, and hence the system is asymptotically stable w.p.1. If the largest Lyapunov exponent is positive, the system is unstable w.p.1. Lyapunov exponents are widely used in stability analysis because they provide a criteria for asymptotic stability w.p.1, which has a better performance than stability w.p.1, when the state of a system is required to return to the equilibrium state under small stochastic perturbations.

Generally, convergence w.p.1 does not imply convergence in moments, and vice versa. Thus stability w.p.1 may not be enough in engineering applications if moment stability is required. The moment Lyapunov exponents are defined by

$$\Lambda_{\mathbf{x}(t)}(p; \mathbf{x}_0) = \lim_{t \to \infty} \frac{1}{t} \log \mathrm{E}\Big[\big\|\mathbf{x}(t; \mathbf{x}_0)\big\|^p\Big]. \tag{1.1.4}$$

$\Lambda_{\mathbf{x}(t)}(p; \mathbf{x}_0)$ determine the stability of the pth moments of the solutions of a dynamical system. The pth moments are asymptotically stable if $\Lambda_{\mathbf{x}(t)}(p; \mathbf{x}_0) < 0$.

The connection between the moment Lyapunov exponent and the Lyapunov exponent, i.e. the moment stability and the almost-sure stability, was established by Molchanov [81] and extended by Arnold *et al.* [9], [7], [5] for linear stochastic dynamical systems in the form of

$$\mathrm{d}\mathbf{x}(t) = \mathbf{B}_0(t, \mathbf{x})\,\mathrm{d}t + \sum_{i=1}^{r} \mathbf{B}_i(t, \mathbf{x})\,\mathrm{d}W_i,$$

and

$$\dot{\mathbf{x}}(t) = \mathbf{A}\big(\boldsymbol{\xi}(t)\big)\,\mathbf{x}(t),$$

where $\mathbf{A}$ is analytic and $\boldsymbol{\xi}(t)$ is a stationary ergodic diffusion process. It has been proved that, if the non-degenerate conditions hold, $\lambda_{\mathbf{x}(t)}(\mathbf{x}_0)$ and $\Lambda_{\mathbf{x}(t)}(p; \mathbf{x}_0)$ are independent of the non-zero initial condition $\mathbf{x}_0$, and $\lambda_{\mathbf{x}(t)}(\mathbf{x}_0) = \lambda^{\max}_{\mathbf{x}(t)}$ almost-surely with $\lambda^{\max}_{\mathbf{x}(t)}$ being the largest (top) Lyapunov exponent. Moreover, $\Lambda_{\mathbf{x}(t)}(p)$ is a convex analytic function in p with $\Lambda_{\mathbf{x}(t)}(0) = 0$ and $\Lambda'_{\mathbf{x}(t)}(0) = \lambda^{\max}_{\mathbf{x}(t)}$.

The stability index $\delta_{\mathbf{x}(t)}$, which is the non-trivial zero of $\Lambda_{\mathbf{x}(t)}(p)$, i.e. $\Lambda_{\mathbf{x}(t)}(\delta_{\mathbf{x}(t)})=0$, characterizes the stability range of the moment. With the convexity of $\Lambda_{\mathbf{x}(t)}(p)$ and $\Lambda_{\mathbf{x}(t)}(0)=0$, if $\delta_{\mathbf{x}(t)}<0$, then $\Lambda_{\mathbf{x}(t)}(p)>0$ for all $p>0$, which means all the pth moments ($p>0$) are unstable. Therefore, only $\delta_{\mathbf{x}(t)}>0$ is meaningful in applications. When $0<p<\delta_{\mathbf{x}(t)}$, the pth moment is asymptotically stable.

From Jensen's inequality, it can be concluded that higher moment stability implies lower moment stability. However, following Markov's inequality and Chebyshev's inequality, the stability of pth moment ($p>0$) implies only weak stochastic stability, i.e.

$$\lim_{\|\mathbf{x}(0)\|\to 0}\sup_{t\geqslant 0}\mathcal{P}\left\{\|\mathbf{x}(t)\|\geqslant\varepsilon\right\}=0,\quad \text{for all } \varepsilon>0, \tag{1.1.5}$$

which is weaker than the definition of almost-sure stability. These two stability concepts are equivalent for linear autonomous systems [58], [8]. But for a general system, there is no such result. Therefore it is important to determine both the largest Lyapunov exponent (almost-sure stability) and the moment Lyapunov exponent (moment stability) in order to have a complete picture of the dynamical stability of stochastic system (1.1.2).

1.1.2 Stochastic Bifurcation

The deterministic bifurcation theory studies the stability of equilibrium points of a family of deterministic paramerized systems

$$\dot{\mathbf{x}}(t)=\mathbf{A}(\mathbf{x};\boldsymbol{\alpha}),\quad \mathbf{x}\in\mathcal{R}^d,\quad \boldsymbol{\alpha}\in\mathcal{R}^m, \tag{1.1.6}$$

with $\boldsymbol{\alpha}$ being the m-dimensional parameter. The equilibrium solutions of equation (1.1.6) are determined by $\mathbf{A}(\mathbf{x};\boldsymbol{\alpha})=\mathbf{0}$ when $\boldsymbol{\alpha}$ varies. If the Fréchet derivative $D_{\mathbf{x}}\mathbf{A}(\mathbf{x};\boldsymbol{\alpha})$ with respect to $\mathbf{x}$ has zero eigenvalue at some equilibrium point $(\mathbf{x}_0,\boldsymbol{\alpha}_0)$, some branches of the equilibrium solutions may change their stability properties. In this case it is said that bifurcation occurs [45], [113].

For general stochastic dynamic systems (1.1.2), the solutions are stochastic processes. It is interesting to study a class of solutions that are Markovian, stationary, and ergodic processes.

Markov property says that the future is independent of the past when the present is known. It is known that a solution of system (1.1.2) is a Markov process provided that

$\boldsymbol{\xi}(t)$ is a family of independent random vectors which are also independent of $\mathbf{x}_0$ [8]. The transition probability function $\bar{P}(s, \mathbf{X}, t, B)$ of a Markov process $\mathbf{x}(t)$ defined on a probability space $(\Omega, \bar{F}, \bar{P})$ is a conditional distribution given by

$$\bar{P}(s, \mathbf{X}, t, B) = \bar{P}\left\{\mathbf{x}(t) \in B \,\middle|\, \mathbf{x}(s) = \mathbf{X}\right\},$$

where $0 \leqslant s \leqslant t < \infty$, $\mathbf{X} \in \bar{R}^d$, $B \in \bar{\mathcal{B}}^d$, $\bar{\mathcal{B}}^d$ is the Boral sigma-algebra. The transition probability satisfies the Chapman-Kolmogorov equation [40], [105]

$$\bar{P}(s, \mathbf{X}, t, B) = \int_{\bar{R}^d} \bar{P}(\tau, \mathbf{y}, t, B) \bar{P}(s, \mathbf{X}, \tau, \mathrm{d}\mathbf{y}). \tag{1.1.7}$$

Using this equation, all finite-dimensional distributions of a Markov process can be determined from the initial distribution and the transition probability; thus all the properties of the process are known. A Markov process is homogeneous in time t if its transition probability is stationary or invariant under time shift, that is,

$$\bar{P}(s, \mathbf{X}, t, B) = \bar{P}(s+u, \mathbf{X}, t+u, B).$$

In this case it can be written that $\bar{P}(s, \mathbf{X}, t, B) = \bar{P}(t-s, \mathbf{X}, B)$.

A stochastic process $\mathbf{x}(t)$ is (strict) stationary if, for any sequence of $t_1, t_2, \cdots, t_n$ and arbitrary h, the joint distribution of random vectors $\mathbf{x}(t_1), \mathbf{x}(t_2), \cdots, \mathbf{x}(t_n)$ are the same as that of $\mathbf{x}(t_1+h), \mathbf{x}(t_2+h), \cdots, \mathbf{x}(t_n+h)$. This means that all joint probability distributions of a stationary process are invariant under time shift. Thus stationary processes play a significant role in applications. The necessary and sufficient conditions for a Markov process to be a stationary process are (see, e.g. [58], [8]) that, $\mathbf{x}(t)$ is homogeneous, and an invariant distribution ϱ exists such that

$$\varrho(B) = \int_{\bar{R}^d} \bar{P}(t, \mathbf{y}, B) \varrho(\mathrm{d}\mathbf{y}), \quad \text{for all } B \in \bar{\mathcal{B}}^d,\ t \geqslant 0. \tag{1.1.8}$$

This invariant distribution is the stationary limit distribution of $\mathbf{x}(t)$ and is independent of the initial distribution [8].

For a stationary Markov process, it is reasonable to expect further that the ergodic property holds, i.e. the space average of a function can be evaluated by the time average along the trajectories almost everywhere [18], [11], [101]. This requires that ([41], [102]), the

invariant probability measure ϱ is unique, and for every bounded $\mathcal{B}$-measurable function $f : \Omega \to B$,

$$\lim_{T\to\infty} \frac{1}{T} \int_0^T f(\mathbf{x}(t))\,\mathrm{d}t = \int_{\mathcal{R}^d} f(\mathbf{x})\,\varrho(\mathrm{d}\mathbf{x}). \tag{1.1.9}$$

If system (1.1.2) is linear, it is obvious that the trivial solution is a stationary solution and its stability can be determined in the sense of Lyapunov exponents and moment Lyapunov exponents. Consider a general stochastic dynamical system of the form

$$\dot{\mathbf{x}}(t) = \mathbf{A}(\mathbf{x}, \boldsymbol{\xi}(t); \boldsymbol{\alpha}), \quad \mathbf{x} \in \mathcal{R}^d, \quad \boldsymbol{\alpha} \in \mathcal{R}^m, \tag{1.1.10}$$

where $\boldsymbol{\alpha}$ denotes the m-dimensional parameter. Without loss of generality, assume that $\mathbf{x} = \mathbf{0}$ is a stationary solution, since a shift transformation can always be applied. Similar to deterministic systems, the stability of this trivial solution can be investigated by linearizing equation (1.1.10) at $\mathbf{x} = \mathbf{0}$ with respect to $\mathbf{x}$,

$$\dot{\mathbf{v}} = D_{\mathbf{x}}\mathbf{A}(\mathbf{0}, \boldsymbol{\xi}(t); \boldsymbol{\alpha})\mathbf{v} = \tilde{\mathbf{A}}(\boldsymbol{\xi}(t); \boldsymbol{\alpha})\mathbf{v}. \tag{1.1.11}$$

If the linearization is applied directly for the non-trivial stationary solution $\mathbf{x}_{st}(t)$, then the equation for the perturbed variable $\mathbf{v} = \mathbf{x} - \mathbf{x}_{st}$ becomes

$$\begin{aligned} \dot{\mathbf{v}} &= D_{\mathbf{x}}\mathbf{A}(\mathbf{x}_{st}(t), \boldsymbol{\xi}(t); \boldsymbol{\alpha})\mathbf{v}, \\ \dot{\mathbf{x}}_{st}(t) &= \mathbf{A}(\mathbf{x}_{st}(t), \boldsymbol{\xi}(t); \boldsymbol{\alpha}). \end{aligned} \tag{1.1.12}$$

Obviously, the equations for the perturbed variable $\mathbf{v}$ in (1.1.11) and (1.1.12) are linear and homogeneous. Thus the stability of the trivial or non-trivial solutions may be determined by the Lyapunov exponents and moment Lyapunov exponents for a given $\boldsymbol{\alpha}$. Moreover, the Lyapunov exponents can be the indicators of stochastic bifurcation, that is, when $\boldsymbol{\alpha}$ varies, change of the sign of the largest Lyapunov exponent indicates change in the stability of the trivial solution. This type of bifurcation is called stochastic dynamical bifurcation, or D-bifurcation [10].

It is possible that, when the parameter $\boldsymbol{\alpha}$ varies, the stability of a stationary solution does not change, but the invariant distribution ϱ of the stationary solution has a "qualitative change". This phenomena is called stochastic phenomenological bifurcation, or P-bifurcation [10], [87], although some researchers doubt that if it should be called a bifurcation, since the stability of the solution keeps unchanged and it is not obvious to define

a "qualitative change" [24]. The relation between P-bifurcation and stability index, i.e. the non-trivial zero of moment Lyapunov exponents, can be found in [10].

1.2 Approximate Method for Stochastic Dynamical Systems

For the general stochastic dynamical system (1.1.2), it is difficult to find the solution or even to determine if a solution exists. Therefore approximate methods have to be applied so that system (1.1.2) can be converted to or approximated by some types of system which may be more easily studied.

1.2.1 Method of Stochastic Averaging

The method of averaging, after it was developed by Krylov, Bogoliubov and Mitropolskii [66], [20], has been widely used in investigating deterministic dynamical systems. The principle is to separate the variables of the system into two parts, slow-varying variables and fast-varying variables. Then the terms related to the slow-varying variables may be approximately replaced by some simpler forms. After this simplification the solution of the approximate dynamical system may be obtained.

Consider the following deterministic system

$$\dot{\mathbf{x}}(t) = \varepsilon \mathbf{A}(t, \mathbf{x}, \varepsilon), \tag{1.2.1}$$

where $0 < \varepsilon \ll 1$ is a small parameter. If $\mathbf{A}$ is T-periodic in t, $\mathbf{A}$ and its derivatives are continuous and bounded, system (1.2.1) can be approximated in the first-order by the averaged system

$$\dot{\mathbf{y}}(t) = \varepsilon \bar{\mathbf{A}}_T(\mathbf{y}), \tag{1.2.2}$$

where

$$\bar{\mathbf{A}}_T(\mathbf{y}) = \frac{1}{T}\int_{\tau}^{\tau+T} \mathbf{A}(t, \mathbf{y}, 0)\mathrm{d}t = \underset{t}{\mathscr{M}}\left\{\mathbf{A}(t, \mathbf{y}, 0)\right\}. \tag{1.2.3}$$

Under the above conditions and approximation, $\left\|\mathbf{x}(t) - \mathbf{y}(t)\right\| = \mathcal{O}(\varepsilon)$ on the time scale ε^{-1} as $\varepsilon \to 0$.

In more general cases, the averaging operator $\underset{t}{\mathscr{M}}\{\cdot\}$ defined in (1.2.3) may be extended to the form

$$\underset{t}{\mathscr{M}}\{\cdot\} = \lim_{T\to\infty}\frac{1}{T}\int_{\tau}^{\tau+T}\{\cdot\}\,\mathrm{d}t, \tag{1.2.4}$$

provided that the limit exists. The standard averaging operator in (1.2.3) requires that the functions being averaged be periodic. However, the functions to be averaged in (1.2.4) are not necessarily periodic, although a better approximation is obtained if these functions are almost periodic. The extension of the averaging operator enlarges the cases where averaging method can be applied. Additional discussion can be found in [97], [76], [82].

A more complex case is the integro-differential system in the form of

$$\dot{\mathbf{x}}(t) = \varepsilon\,\mathbf{A}(t,\mathbf{x}) + \varepsilon\int_0^t \mathbf{H}(t,s,\mathbf{x}(s))\,\mathrm{d}s, \tag{1.2.5}$$

where $\mathbf{A}$ and $\mathbf{H}$ are continuous for all $t, s \geqslant 0$ and $\mathbf{x}$. The averaging method due to Larionov [69] shows that, if there exists the limit

$$\lim_{T\to\infty}\frac{1}{T}\int_0^T\left[\mathbf{A}(t,\mathbf{x}) + \int_0^t \mathbf{H}(t,s,\mathbf{x}(s))\,\mathrm{d}s\right]\mathrm{d}t = \hat{\mathbf{A}}(\mathbf{x}), \tag{1.2.6}$$

in which $\mathbf{A}(t,\mathbf{x})$, $\mathbf{H}(t,s,\mathbf{x}(s))$, $\hat{\mathbf{A}}(\mathbf{x})$ satisfy the Lipschitz condition with respect to $\mathbf{x}$, the solution to the differential equation

$$\dot{\mathbf{y}}(t) = \varepsilon\,\hat{\mathbf{A}}(\mathbf{y}), \quad \mathbf{y}(0) = \mathbf{x}(0), \tag{1.2.7}$$

is defined for $t \geqslant 0$, and, for any finite time interval $[t_1, t_2]$ along the trajectory $\mathbf{y}$,

$$\left|\int_{t_1}^{t_2}\hat{\mathbf{A}}(\mathbf{y}(s))\,\mathrm{d}s\right| \leqslant C(t_2 - t_1),$$

with C being a constant, then the solution of equation (1.2.5) can be approximated by the solution of (1.2.7) over a time interval of order $\varepsilon^{-1/2}$.

If the second-order averaging for deterministic system (1.2.1) is considered, $\mathbf{x}$ is expressed as $\mathbf{x}(t) = \mathbf{y}(t) + \varepsilon\mathbf{x}_1(t,\mathbf{y})$, and $\mathbf{A}(t,\mathbf{x},\varepsilon)$ is expanded as Taylor series in terms of the small parameter ε. Then it can be obtained, by substituting $\mathbf{x}(t)$ into equation (1.2.1),

$$\dot{\mathbf{y}}(t) = \varepsilon\left[\mathbf{I} + \varepsilon\frac{\partial\mathbf{x}_1(t,\mathbf{y})}{\partial\mathbf{y}}\right]^{-1}\left\{\left[\mathbf{A}(t,\mathbf{y},0) - \frac{\partial\mathbf{x}_1(t,\mathbf{y})}{\partial t}\right] + \varepsilon\frac{\partial\mathbf{A}(t,\mathbf{y},0)}{\partial\varepsilon}\right\} + o(\varepsilon^2). \tag{1.2.8}$$

Expanding the matrices in equation (1.2.8) and neglecting the higher-order terms result in the second-order averaged equation

$$\dot{\mathbf{y}}(t) = \varepsilon \left[\mathbf{A}(t, \mathbf{y}, 0) - \frac{\partial \mathbf{x}_1(t, \mathbf{y})}{\partial t} \right] + \varepsilon^2 \mathbf{B}(t, \mathbf{y}, \mathbf{x}_1). \tag{1.2.9}$$

To solve the averaged equation (1.2.9),

$$\frac{\partial \mathbf{x}_1(t, \mathbf{y})}{\partial t} = \mathbf{A}(t, \mathbf{y}, 0) - \bar{\mathbf{A}}_T(\mathbf{y}) \tag{1.2.10}$$

may be chosen. After $\mathbf{x}_1$ is obtained from equation (1.2.10), equation (1.2.9) can be solved for $\mathbf{y}(t)$. Similar procedures can be followed in order to obtain higher-order averaging approximations.

The averaging method for stochastic differential equations was proposed by Stratonovich [106], [107] and developed by Khasminskii [57], [56]. For a stochastic system

$$\dot{\mathbf{x}}(t) = \varepsilon \mathbf{A}(t, \mathbf{x}, \boldsymbol{\xi}(t), \varepsilon), \quad \mathbf{x}(0) = \mathbf{x}_0, \tag{1.2.11}$$

where $0 < \varepsilon \ll 1$ is a small parameter, $\boldsymbol{\xi}(t)$ is a zero mean value, stationary stochastic process. If as $\varepsilon \to 0$, $\mathbf{A}(t, \mathbf{x}, \boldsymbol{\xi}(t), \varepsilon)$ can be expressed uniformly in $t, \mathbf{x}, \boldsymbol{\xi}$ as

$$\mathbf{A}(t, \mathbf{x}, \boldsymbol{\xi}(t), \varepsilon) = \mathbf{A}_0(t, \mathbf{x}, \boldsymbol{\xi}(t)) + \varepsilon \mathbf{A}_1(t, \mathbf{x}) + o(\varepsilon), \tag{1.2.12}$$

where $\mathbf{A}_0$, $\mathbf{A}_1$ and their first- and second-order derivatives with respect to $\mathbf{x}$ are smooth and bounded functions, $\mathbf{A}$, $\mathbf{A}_0$ and $\mathbf{A}_1$ are measurable for fixed $\mathbf{x}$ and ε, and the correlation function $\mathrm{E}\big[\boldsymbol{\xi}(t)\boldsymbol{\xi}(t+\tau)\big]$ decays to zero fast enough as τ increases, or $\boldsymbol{\xi}(t)$ is a wide-band process, then system (1.2.11) can be approximated uniformly in weak sense (see, e.g. [56], [34], [103], [102]) on the time scale ε^{-2} by a Markov diffusion process $\bar{\mathbf{x}}(t)$ satisfying

$$\mathrm{d}\bar{\mathbf{x}}(t) = \varepsilon^2 \mathbf{m}(\bar{\mathbf{x}})\,\mathrm{d}t + \varepsilon \boldsymbol{\sigma}(\bar{\mathbf{x}})\,\mathrm{d}\mathbf{W}(t), \tag{1.2.13}$$

provided that the following limits exist

$$\begin{aligned} \mathbf{m}(\bar{\mathbf{x}}) &= \mathop{\mathscr{M}}_{t} \left\{ \mathbf{A}_1 + \int_{-\infty}^{0} \mathrm{E}\Big[\frac{\partial \mathbf{A}_0}{\partial \mathbf{x}} \mathbf{A}_{0\tau} \Big] \mathrm{d}\tau \right\}, \\ \boldsymbol{\sigma}(\bar{\mathbf{x}}) \boldsymbol{\sigma}^T(\bar{\mathbf{x}}) &= \mathop{\mathscr{M}}_{t} \left\{ \int_{-\infty}^{\infty} \mathrm{E}\big[\mathbf{A}_0 \mathbf{A}_{0\tau}^T \big] \mathrm{d}\tau \right\}, \end{aligned} \tag{1.2.14}$$

where $\mathbf{A}_{0\tau} = \mathbf{A}_0(t+\tau, \mathbf{x}, \boldsymbol{\xi}(t+\tau))$.

Stochastic version of higher-order averaging may follow the same procedure as the deterministic case. In fact, the weak convergence of stochastic averaging as $\varepsilon \to 0$ is the result of the functional central limit theorem for stochastic processes [34], [103], [102]. The conditions for weak convergence of averaging principle are very general assumptions, which are considered to be satisfied in many physical and engineering applications.

It is also stated ([57], [34], [35], [103], [102]) that, if $\mathbf{A}(t, \mathbf{x}, \boldsymbol{\xi}(t), 0)$ in equation (1.2.11) satisfies the strong law of large numbers for fixed $\mathbf{x}$, i.e.

$$\bar{\mathbf{A}}(\mathbf{x}) = \lim_{T\to\infty} \frac{1}{T} \int_0^T \mathrm{E}\big[\mathbf{A}(t, \mathbf{x}, \boldsymbol{\xi}(t), 0)\big]\,\mathrm{d}t, \tag{1.2.15}$$

then the averaging principle leads to convergence w.p.1 to the solution of a deterministic system

$$\dot{\mathbf{x}}(t) = \varepsilon\,\bar{\mathbf{A}}(\mathbf{x}), \quad \mathbf{x}(0) = \mathbf{x}_0, \tag{1.2.16}$$

on time interval of order ε^{-1} as $\varepsilon \to 0$. The difference between the solutions of the original system (1.2.11) and the averaged system (1.2.16), after normalized by $\sqrt{\varepsilon}$, converges weakly to a Gaussian Markov process over a wider time interval of order ε^{-2}. Similar almost-sure convergence results are also established in [47], [64], [65] under some slightly more restrictive conditions.

By applying the stochastic averaging method, the state variables of the original stochastic dynamical system will be approximated by a new set of averaged variables which are Markov processes. The transition density functions of the averaged variables can be obtained from the Fokker-Plank-Kolmogorov equation, and thus the properties of the approximate solution are known.

Although stochastic averaging principle only ensures that the approximate solution given by equation (1.2.13) converges in distribution to the true solution of equation (1.2.11) over a finite time interval, it still provides a useful approach when the true solution is difficult to obtain. The accuracy of the approximate solutions may be verified by experiments or simulations in practice.

1.2.2 Existence and Uniqueness of Solutions of Stochastic Differential Equations

From Section 1.2.1 it is known that a general stochastic dynamical system may be approximated by the Itô stochatic differential equation

$$\mathrm{d}\mathbf{x}(t) = \mathbf{m}(\mathbf{x})\,\mathrm{d}t + \boldsymbol{\sigma}(\mathbf{x})\,\mathrm{d}\mathbf{W}(t). \tag{1.2.17}$$

Before studying the stability of its solution, it should be confirmed that a solution exists.

For this purpose, the following more general form of equation can be considered

$$\mathrm{d}\mathbf{x}(t) = \mathbf{m}(t,\mathbf{x})\,\mathrm{d}t + \boldsymbol{\sigma}(t,\mathbf{x})\,\mathrm{d}\mathbf{W}(t), \quad \mathbf{x}(0) = \mathbf{x}_0 \in \mathcal{R}^d, \ \ 0 \leqslant t \leqslant T < \infty, \tag{1.2.18}$$

where $\mathbf{m}$ is a d-dimensional vector, $\boldsymbol{\sigma}$ is a $d \times r$ matrix, and $\mathbf{W}$ is a r-dimensional vector Wiener process. Equation (1.2.18) is a formal expression of stochastic integral

$$\mathbf{x}(t) = \mathbf{x}_0 + \int_0^t \mathbf{m}(s,\mathbf{x}(s))\,\mathrm{d}s + \int_0^t \boldsymbol{\sigma}(s,\mathbf{x}(s))\,\mathrm{d}\mathbf{W}(s). \tag{1.2.19}$$

It has been shown ([58], [115], [41], [8], [36]) that, if $\mathbf{m}(t,\mathbf{x})$ and $\boldsymbol{\sigma}(t,\mathbf{x})$ are measurable on $[0,T]\times\mathcal{R}^d$ and, for all $t\in[0,T]$, $\mathbf{x},\mathbf{y}\in\mathcal{R}^d$, satisfy the Lipschitz condition

$$\big\|\mathbf{m}(t,\mathbf{x}) - \mathbf{m}(t,\mathbf{y})\big\| + \big\|\boldsymbol{\sigma}(t,\mathbf{x}) - \boldsymbol{\sigma}(t,\mathbf{y})\big\| \leqslant K\big\|\mathbf{x}-\mathbf{y}\big\|, \tag{1.2.20}$$

and the restriction on growth condition

$$\big\|\mathbf{m}(t,\mathbf{x})\big\|^2 + \big\|\boldsymbol{\sigma}(t,\mathbf{x})\big\|^2 \leqslant K^2\big(1 + \big\|\mathbf{x}\big\|^2\big), \tag{1.2.21}$$

where $K>0$ is a constant and $\|\boldsymbol{\sigma}\|^2 = \mathrm{tr}\left(\boldsymbol{\sigma}\boldsymbol{\sigma}^T\right)$, then equation (1.2.18) has a unique solution continuous w.p.1 on $[0,T]$ satisfying the given initial condition. For the special case when equation (1.2.18) is linear, which finds wide applications in physics and engineering, it has a unique solution continuous w.p.1.

The solution of equation (1.2.18) is a diffusion process with $\mathbf{m}(t,\mathbf{x})$ being the drift coefficient and $\mathbf{b}(t,\mathbf{x}) = \boldsymbol{\sigma}(t,\mathbf{x})\boldsymbol{\sigma}(t,\mathbf{x})^T$ being the diffusion coefficient. Diffusion process is a special case of Markov processes with continuous sample functions and usually serve as the theoretical model of physical diffusion phenomena. If its transition density function $q(t,\mathbf{x};\,t_0,\mathbf{x}_0)$ has continuous derivative with respect to t and continuous second-order

derivatives with respect to $\mathbf{x}$, then for fixed $\mathbf{x}_0$ and t_0 such that $t_0 \leqslant t$, q satisfies the well-known Fokker-Plank or Forward Kolmogorov equation (FPK equation) [8]

$$\frac{\partial q}{\partial t} + \sum_{i=1}^{d} \frac{\partial \big[m_i(t,\mathbf{x})q\big]}{\partial x_i} - \frac{1}{2}\sum_{i=1}^{d}\sum_{j=1}^{d} \frac{\partial^2 \big[b_{ij}(t,\mathbf{x})q\big]}{\partial x_i \partial x_j} = 0, \tag{1.2.22}$$

with the initial condition

$$q(t,\mathbf{x};\, t_0,\mathbf{x}_0) \to \delta(\mathbf{x}-\mathbf{x}_0), \quad \text{as } t \downarrow t_0, \tag{1.2.23}$$

where m_i and b_{ij}, $i,j=1,2,\cdots,d$ are the elements of $\mathbf{m}$ and $\mathbf{b}$. It can be seen ([41], [8]) that, every Markov diffusion process is uniquely determined by its infinitesimal generator defined by

$$\mathscr{G}_t = \sum_{i=1}^{d} m_i(t,\mathbf{x})\frac{\partial}{\partial x_i} + \frac{1}{2}\sum_{i=1}^{d}\sum_{j=1}^{d} b_{ij}(t,\mathbf{x})\frac{\partial^2}{\partial x_i \partial x_j}. \tag{1.2.24}$$

The stability property of a diffusion process may be determined through its transition density function, since the density function of state vector $\mathbf{x}$ at time t can be obtained by the Chapman-Kolmogorov equation (1.1.7) using the initial distribution. However, the Fokker-Plank-Kolmogorov equation (1.2.22) is not always easy to solve. Hence it is necessary to find other ways to analyse the stability property of equation (1.2.18).

It is shown ([81], [9], [7], [5], [111]) that, for a linear stochastic system, the pth moment Lyapunov exponent $\Lambda(p)$ is the principal eigenvalue of the differential eigenvalue problem

$$\mathscr{L}(p)T(p) = \Lambda(p)T(p),$$

where $\mathscr{L}(p)$ is a differential operator associated with the system parameters, $T(p)$ is the corresponding non-negative eigenfunction. Solving this eigenvalue problem by methods such as perturbation, the pth moment Lyapunov exponent can be obtained.

1.3 Noise Models and Monte Carlo Simulation

1.3.1 Wide-band and Narrow-band Noises

In oder to study the properties of dynamical systems under the perturbation of noise, suitable mathematical models for different types of noises have to be established. With

the application of stochastic integrals, noises may be defined as the solutions of certain stochastic differential equations, since the existence, uniqueness, and Markov properties of solutions are based on the properties of the governing equations.

Gaussian white noise process $\xi(t)$ is the formal derivative of the Wiener process given by

$$\xi(t)\,\mathrm{d}t = \sqrt{S_0}\,\mathrm{d}W(t), \tag{1.3.1}$$

with constant power spectral density $S(\omega) = S_0$. Such noise does not exist in reality since its power is infinity. However, it provides a very simple and useful mathematical idealization for wide-band noise.

A real noise, or more specifically an Ornstein-Uhlenbeck process, is defined by

$$\mathrm{d}\xi(t) = -\alpha\xi(t)\,\mathrm{d}t + \sigma\,\mathrm{d}W(t), \tag{1.3.2}$$

with power spectral density

$$S(\omega) = \frac{\sigma^2}{\alpha^2 + \omega^2}. \tag{1.3.3}$$

Ornstein-Uhlenbeck process is stationary and Gaussian [40]. From (1.3.3) it can be seen that its power mainly concentrates in lower frequency band. When α increases, the spectrum becomes "flatter", which means it may be considered as an approximate model of wide-band noise by suitably choosing α and σ.

The more general definition of "real noise" is defined as a stationary ergodic diffusion vector process $\boldsymbol{\xi}(t)$, which is described by the Stratonovich stochastic differential equation

$$\mathrm{d}\boldsymbol{\xi}(t) = \mathbf{Q}_0\big(\boldsymbol{\xi}(t)\big)\,\mathrm{d}t + \sum_{i=1}^{r} \mathbf{Q}_i\big(\boldsymbol{\xi}(t)\big) \circ \mathrm{d}W_i,$$

with $\mathbf{Q}_i$, $i = 0, 1, \ldots, r$, being smooth [9]. Such noise may not be Gaussian but may be more suitable to describe noises in the real world.

The bounded noise process was introduced by Stratonovich [106]. It overcomes the shortcoming of Ornstein-Uhlenbeck process, which is not bounded. The unit bounded noise is given by

$$\xi(t) = \cos\big[\nu t + \sigma W(t) + \theta\big], \tag{1.3.4}$$

where θ is a uniformly distributed random number in $[0, 2\pi)$ and is independent of $W(t)$. Using Itô's Lemma, it can be seen that $\xi(t)$ is the solution of the Itô differential equation

$$\mathrm{d}\xi(t) = -\Big(\nu\sqrt{1-\xi^2} + \frac{1}{2}\sigma^2\xi\Big)\,\mathrm{d}t - \sigma\sqrt{1-\xi^2}\,\mathrm{d}W(t), \tag{1.3.5}$$

or equivalently, the Stratonovich stochastic differential equation

$$\mathrm{d}\xi(t) = -\nu\sqrt{1-\xi^2}\,\mathrm{d}t - \sigma\sqrt{1-\xi^2}\circ\mathrm{d}W(t). \tag{1.3.6}$$

Thus the bounded noise is a special kind of non-Gaussian general "real noises". The power spectral density of the unit bounded noise is

$$S(\omega) = \frac{\sigma^2\big(\omega^2+\nu^2+\frac{1}{4}\sigma^4\big)}{2\big[(\omega+\nu)^2+\frac{1}{4}\sigma^4\big]\big[(\omega-\nu)^2+\frac{1}{4}\sigma^4\big]}. \tag{1.3.7}$$

Equation (1.3.7) shows that the power of the bounded noise can be controlled by adjusting the values of ν and σ, and it mainly distributes in the neighborhood of ν. Hence the bounded noise is a very good realistic model of narrow-band noise and is widely used in many engineering applications.

1.3.2 Monte Carlo Simulation

For Itô stochastic differential equations, the complete behaviour of solutions can be obtained by solving the determininstic Fokker-Planck-Kolmogorov equations for the transition probability density functions. However, in many cases such procedures may have great practical difficulies, although it can be done analytically or numerically in principle. Therefore, direct numerical approaches to the corresponding Itô equations may have to be applied. Moreover, the generation of noises may be obtained by computer simulation of stochastic differential equations.

There are two types of discrete schemes, strong approximation scheme and weak approximation scheme. The difference between them is the way they converge to the exact solution [60], [80].

A strong approximation scheme with order γ requires that the error of approximation satisfies

$$\epsilon(h) = \mathrm{E}\big[\,\|\mathbf{x}(T) - \mathbf{x}^h(T)\|\,\big] \leqslant Ch^\gamma, \tag{1.3.8}$$

where $\mathbf{x}$ is the exact solution, $\mathbf{x}^h$ is the discrete approximation, $h>0$ is the time step, T is the total length of time of simulation, C and γ are positive constants, and C is independent of h.

Weak schemes do not require path-wise approximation but focus on obtaining more information about the probability measure. Hence for a weak scheme whose approximation converges weakly with order $\gamma>0$ to the exact solution, the error of approximation only needs to satisfy

$$\epsilon(h) = \left|\mathsf{E}\left[g(\mathbf{x}(T))\right] - \mathsf{E}\left[g(\mathbf{x}^h(T))\right]\right| \leqslant Ch^\gamma, \tag{1.3.9}$$

where $g(x)$ is a continuously differentiable function with derivative at least of the order of $2(\gamma+1)$.

The direct numerical simulation schemes and their features are always associated with the properties of Wiener process and Itô differential equation. The simplest numerical scheme, the Euler scheme, for system (1.2.18) is

$$\mathbf{x}^{k+1} = \mathbf{x}^k + \mathbf{m}(t_k, \mathbf{x}^k)\, h + \boldsymbol{\sigma}(t_k, \mathbf{x}^k)\, \Delta\mathbf{W}^k, \quad k = 0, 1, 2, \cdots, \tag{1.3.10}$$

which is obtained from the stochastic Taylor expansion of stochastic integral [60], [59]. The superscript k means the value at the kth iteration. Time step $h=t_{k+1}-t_k$, and $\Delta\mathbf{W}^k$ satisfies the l-dimensional Gaussian distribution with zero mean and covariance matrix $h\mathbf{I}$. The Euler schemes are strong approximation schemes of order 0.5 and weak approximation schemes with order 1.0, and are widely used in applications due to their simple forms. Similar to Euler scheme, higher order schemes can also be constructed through the stochastic Taylor expansion.

1.4 Viscoelasticity and Integro-differential Equations

1.4.1 Equations of Motion for Linear Viscoelastic Bodies

Viscoelasticity has been observed in a number of materials, such as polymers, composites, metals, and alloys at high temperatures. Investigating the behaviour of viscoelastic materials under dynamical loads is of great help for engineering applications.

Generally speaking, elastic materials have the capacity to store mechanical energy without dissipation because they have the property to recover to the original states after they are

unloaded. On the other hand, Newtonian viscous fluid cannot store mechanical energy except in non-hydrostatic stress state. However, some materials both store and dissipate mechanical energy; such property is called viscoelasticity. In classical elasticity, there are no strain-rate effects. That is the strain at time t depends only on the stress at time t, and vice versa. However, for viscoelastic materials, stress is not a function of instantaneous strain but depends on the past time history of strain; this dependent relation also holds for strain. It has been observed that, typically, the strain of viscoelastic material under constant stress increases with time in creep test, while the stress decreases with time under constant strain in relaxation test.

In the case of linear aging viscoelasticity, where aging means the mechanical properties of a given material change with its age, the relation between uniaxial strain $\varepsilon(t)$ and stress $\sigma(t)$ can be expressed as Stieltjes integrals, according to the Riesz's representation theorem [33], [25],

$$\varepsilon(t) = \int_{-\infty}^{t} F(t,\tau)\,\mathrm{d}\sigma(\tau), \qquad \sigma(t) = \int_{-\infty}^{t} G(t,\tau)\,\mathrm{d}\varepsilon(\tau), \tag{1.4.1}$$

where $F(t,\tau)$ is called the creep function, and $G(t,\tau)$ is the relaxation function. In the complicated strain and stress states, the integral representation will be

$$\varepsilon_{ij}(t) = \int_{-\infty}^{t} F_{ijkl}(t,\tau)\,\mathrm{d}\sigma_{kl}(\tau), \qquad \sigma_{ij}(t) = \int_{-\infty}^{t} G_{ijkl}(t,\tau)\,\mathrm{d}\varepsilon_{kl}(\tau), \tag{1.4.2}$$

where $\{\varepsilon_{ij}(t)\}=\boldsymbol{\varepsilon}(t)$ is the strain tensor and $\{\sigma_{ij}(t)\}=\boldsymbol{\sigma}(t)$ is the stress tensor. Correspondingly, $F_{ijkl}(t,\tau)$ is the tensorial creep function and $G_{ijkl}(t,\tau)$ is the tensorial relaxation function.

For linear non-aging materials, the time when they are loaded can be selected as the time origin without loss of generality. Therefore, the creep function and the relaxation function are only determined by the time difference $t-\tau$. If the creep function, relaxation function, strain, and stress are further assumed to be differentiable, then the constitutive relation reduces to

$$\begin{aligned}
\varepsilon_{ij}(t) &= \int_0^t F_{ijkl}(t-\tau)\,\mathrm{d}\sigma_{kl}(\tau) = F_{ijkl}(0)\sigma_{kl}(t) + \int_0^t \dot{F}_{ijkl}(t-\tau)\sigma_{kl}(\tau)\,\mathrm{d}\tau,\\
\sigma_{ij}(t) &= \int_0^t G_{ijkl}(t-\tau)\,\mathrm{d}\varepsilon_{kl}(\tau) = G_{ijkl}(0)\varepsilon_{kl}(t) + \int_0^t \dot{G}_{ijkl}(t-\tau)\varepsilon_{kl}(\tau)\,\mathrm{d}\tau,
\end{aligned} \tag{1.4.3}$$

where $G_{ijkl}(0)$ is the instantaneous elastic modulus. The conditions

$$\int_0^{+\infty} \left\| \dot{G}_{ijkl}(t) \right\| \mathrm{d}t < \infty, \qquad \int_0^{+\infty} t \left\| \dot{G}_{ijkl}(t) \right\| \mathrm{d}t < \infty \tag{1.4.4}$$

ensure that the equilibrium elastic modulus $G_{ijkl}(+\infty)$ exists. There are also differential representations of the constitutive relation. They include the derivatives of strain and stress, which describe their dependence on time history. These two types of representation are equivalent [25].

One choice of relaxation and creep functions under uniaxial strain state often used is

$$G(t) = E\mathrm{e}^{-\frac{t}{\lambda}}, \qquad F(t) = \frac{1}{E}\left(1 + \frac{t}{\lambda}\right), \tag{1.4.5}$$

where E is the general elastic modulus, λ is known as the relaxation time. Equation (1.4.5) describes the stress relaxation and creep phenomena and is associated with the well-known differential Maxwell model [25], [32]. Furthermore, the generalized Maxwell model, which consists of a sequence of differential Maxwell units coupled in parallel, can be used as an approximation to most linear viscoelastic behavior as close as possible [96], [32]. Obviousely, the relaxation function for generalized Maxwell model will be given by

$$G(t) = \sum_{j=1}^{M} E_j \mathrm{e}^{-t/\lambda_j}, \tag{1.4.6}$$

where M is the number of Maxwell units in the parallel chain.

The linear theory is often used under the assumption of infinitesimal deformation. However, for some materials, such as concrete subjected to high stresses or partial unloading [27], the deformation is beyond the range where superposition and, therefore, linearity are valid. As a result, the general theory of nonlinear viscoelasticity has to be applied. However, the constitutive relation for nolinear viscoelastic materials is far more complicated and is still under development. Generally it is defined through the deformation gradient but not strain, and there may be many choices due to the variety of materials. Green-Rivlin theory [43] is a common approach in determining the mechanical properties of viscoelastic solids.

From linear elasticity theory, the governing equations for the dynamic response of an elastic body with boundary and initial data are given by, using Newton's Second Law [37],

$$\begin{aligned}
\rho\frac{\partial^2 u_i}{\partial t^2}-\frac{\partial \sigma_{ij}}{\partial x_j} &= f_i(\mathbf{x},t), && \text{in } \bar{\mathcal{D}}\times[0,T), \qquad (1.4.7)\\
u_i &= 0, && \text{on } \partial\bar{\mathcal{D}}_u\times[0,T),\\
\sigma_{ij}\nu_j &= g_i, && \text{on } \partial\bar{\mathcal{D}}_\sigma\times[0,T),\\
u_i(\mathbf{x},0) &= u_{i0}, && \text{in } \bar{\mathcal{D}},\\
\frac{\partial u_i(\mathbf{x},0)}{\partial t} &= u_{i1}, && \text{in } \bar{\mathcal{D}}, \qquad (1.4.8)
\end{aligned}$$

where $i=1,2,3$, ρ is the mass density of the elastic body, $\mathbf{u}(\mathbf{x},t)=(u_1,u_2,u_3)$ is the displacement vector, $\mathbf{x}\in\bar{\mathcal{D}}\subset\mathcal{R}^3$, $\partial\bar{\mathcal{D}}=\partial\bar{\mathcal{D}}_u\oplus\partial\bar{\mathcal{D}}_\sigma$ is the boundary of $\bar{\mathcal{D}}$, $\mathbf{f}(\mathbf{x},t)=(f_1,f_2,f_3)$ is the body force, and $\boldsymbol{\nu}=(\nu_1,\nu_2,\nu_3)$ is the unit outward vector normal to $\partial\bar{\mathcal{D}}_\sigma$. If viscoelasticity is considered, then from the constitutive relationship (1.4.3) one has the integro-partial differential equation

$$\rho\frac{\partial^2 u_i}{\partial t^2}-\int_0^t G_{ijkl}(t-\tau)\frac{\partial^2\varepsilon_{kl}(\mathbf{u}(\mathbf{x},\tau))}{\partial x_j\partial\tau}\,\mathrm{d}\tau=f_i,\quad \text{in } \bar{\mathcal{D}}\times[0,T),$$

or

$$\rho\frac{\partial^2 u_i}{\partial t^2}-G_{ijkl}(0)\frac{\partial\varepsilon_{kl}(\mathbf{u}(\mathbf{x},t))}{\partial x_j}-\int_0^t \dot{G}_{ijkl}(t-\tau)\frac{\partial\varepsilon_{kl}(\mathbf{u}(\mathbf{x},\tau))}{\partial x_j}\,\mathrm{d}\tau=f_i, \qquad (1.4.9)$$

combining with the boundary and initial conditions in equations (1.4.8). Under the assumption of small deformation, the symmetric strain tensor is given by [37]

$$\varepsilon_{ij}(\mathbf{x},t)=\frac{1}{2}\left[\frac{\partial u_i(\mathbf{x},t)}{\partial x_j}+\frac{\partial u_j(\mathbf{x},t)}{\partial x_i}\right],\quad i,j=1,2,3. \qquad (1.4.10)$$

Substituting equation (1.4.10) into (1.4.9) leads to the general form of equations of motion for viscoelastic dynamical system with the displacement vector $\mathbf{u}(\mathbf{x},t)$ as variables.

1.4.2 Stability of Integro-Differential Equations

Stability of elastic structures under deterministic loads has been investigated by many researchers for decades [21], [22], [121], [72]. Stability of elastic structures under random loads can also be found in some references such as [75], [73], [119]. However, the study of

stability of viscoelastic structures is in its infancy, since it is more difficult to study the stability of integro-partial differential equations, and moreover, the constitutive relationships for viscoelastic materials are also under development.

For one-dimensional small deformation problems, the governing equation of motion reduces to hyperbolic partial differential equation of the form

$$\rho\frac{\partial^2 u(x,t)}{\partial t^2} - E\frac{\partial^2 u(x,t)}{\partial x^2} = f(x,t), \tag{1.4.11}$$

for elastic case, and

$$\rho\frac{\partial^2 u(x,t)}{\partial t^2} - \int_0^t G(t-\tau)\frac{\partial^3 u(x,\tau)}{\partial x^2 \partial \tau}d\tau = f(x,t),$$

or

$$\rho\frac{\partial^2 u(x,t)}{\partial t^2} - G(0)\frac{\partial^2 u(x,t)}{\partial x^2} - \int_0^t \dot{G}(t-\tau)\frac{\partial^2 u(x,\tau)}{\partial x^2}d\tau = f(x,t), \tag{1.4.12}$$

for linear viscoelastic case. Thus studying the dynamic response of a viscoelastic body may lead to studying an integro-partial differential equation of the type

$$u_{tt}(x,t) = \left[\phi(u_x(x,t))\right]_x - \int_0^t H(t-\tau)\left[\psi(u_x(x,\tau))\right]_x \,\mathrm{d}\tau + f(x,t). \tag{1.4.13}$$

Note that equation (1.4.13) includes the linear and nonlinear viscoelastic constitutive relationship. When one takes $\phi(x) = c_1 x$ and $\psi(x) = c_2 x$, where c_1 and c_2 are constants, equation (1.4.13) can be converted to (1.4.12) easily.

The stability of equation (1.4.13) in deterministic cases has been studied by some researchers. If the viscoelasticity vanishes, i.e. $H(t) \equiv 0$, equation (1.4.13) describes the one-dimensional nonlinear elastic response when ϕ is nonlinear, and it is known that generally the corresponding initial-boundary value problem does not have globally smooth solution for any nonzero initial and boundary data. However, for the cases when viscoelasticity exists, the results given in [28], [29], [19] show that, for materials with linear viscoelasticity, i.e. ϕ and ψ are linear functions, the initial-boundary value problems associated with equation (1.4.13) have globally defined smooth solutions, provided that the initial data in equations (1.4.8) and forcing function f are suitably smooth and small, and these solutions tend to zero as $t \to \infty$. Furthermore, if $H(t)$ is an exponential kernel, i.e. Maxwell viscoelastic model, the initial data and f need not be small to ensure that the response reduces to zero

with time [51]. This implies that viscoelasticity has the similar effect as damping and helps to stabilize structures.

1.5 Scope of the Thesis

Study on the stability of dynamical systems in engineering mechanics arises from the investigation of responses of strucures subjected to dynamic loads. Although there are numerous works on the stability of elastic structures, research on the stability of viscoelastic structures, especially for the cases under random loads, appears to be limited. Due to the wide applications of viscoelastic materials, research in this area is of great importance.

This thesis focuses on the stability of viscoelastic systems under stochastic perturbations. The main goal is to obtain the Lyapunov exponents and moment Lyapunov exponents of certain models of viscoelastic systems. These models may be simplifications of realistic structures, such as buildings subjected to earthquake or wind loads. After the Lyapunov and moment Lyapunov exponents are known, the stability of these systems may be improved by adjusting or optimizing system parameters.

This chapter presents the preliminary backgrounds which will be applied to the study of stochastic stability. Stochastic differential equations provide the mathematical models for realistic stochastic phenomena, on which analytical and numerical methods can be applied to investigate the properties of these systems. Generally speaking, the methods of averaging and perturbation are two important methods for obtaining approximate solutions of dynamical systems. Numerical methods may be employed when the analytical methods are difficult to apply, or when the analytical approximations need to be validated.

Chapter 2 presents a new algorithm on simulation of moment Lyapunov exponents for linear homogeneous stochastic systems. Since numerical simulation results can be used to verify the accuracy of approximate analytical solutions of stochastic systems, an accurate and efficient algorithm is necessary.

In Chapter 3, an example of single degree-of-freedom (SDOF) linear viscoelastic system is established. Then the method of stochastic averaging, both the first- and the second-order,

is applied to determine the moment Lyapunov exponents of the sytem under wide-band and narrow-band noise excitations.

In Chapter 4, a SDOF nonlinear viscoelastic system is considered. The system is simplified using the method of stochastic averaging. Lyapunov exponents for the trivial and non-trivial stationary solutions are then obtained. Stochastic bifurcation phenomena associated with the nonlinear system are studied.

Chapter 5 presents some conclusions from this study and directions for future research.

CHAPTER 2

Monte Carlo Simulation of Moment Lyapunov Exponents

As introduced in Chapter 1, the moment Lyapunov exponents characterize the moment stability of a stochastic dynamical system. Although it is quite straightforward to set up the partial differential eigenvalue problem with the pth moment Lyapunov exponent $\Lambda(p)$ as the principal eigenvalue ([9], [7], [5], [111], see also [119]), the actual solution of the eigenvalue problem is very difficult. For certain simple two-dimensional or four-dimensional systems, approximate analytical methods, such as stochastic averaging or perturbation, have been applied to obtain approximate analytical results of the moment Lyapunov exponent $\Lambda(p)$ (see, e.g. [4], [55], [84], [86], [116], [117]). In general, numerical approaches, such as Monte Carlo simulations, have to be applied to determine the moment Lyapunov exponents. Furthermore, even when approximate analytical results are available, their accuracies have to be verified by numerical simulations.

When investigating the stability of a general stochastic dynamical system, it is usual to consider the corresponding linearized system near its stationary solution as presented in Section 1.1.2. The linearized system is homogeneous. This shows the importance of linear homogeneous systems in the study of stochastic dynamical systems.

There are some references discussing the numerical approximation of Lyapunov exponents, such as [109], [110], [44]. However, there seems to be only one numerical algorithm

for determining the moment Lyapunov exponents using Monte Carlo simulation published so far [118], which is described briefly in Section 2.1.

2.1 Numerical Algorithm Using Sample Norm

Consider a general d-dimensional linear homogeneous stochastic dynamical system

$$\dot{\mathbf{X}}(t) = \mathbf{A}\big(\boldsymbol{\xi}(t)\big)\,\mathbf{X}(t), \quad \mathbf{X}(0) = \mathbf{X}_0. \tag{2.1.1}$$

In the cases that $\boldsymbol{\xi}(t)$ is described by Itô or Stratonovich stochastic differential equations, equation (2.1.1) is solved using an appropriate numerical discretization scheme with a time step h. To have an accurate estimation of the pth moment, $\mathsf{E}\big[\|\mathbf{X}(t)\|^p\big]$, a large number of sample realizations must be simulated, since the evaluation of expectation is determined by the sample average.

When system (2.1.1) is stable, the solution decays exponentially in time, whereas, when it is unstable, the solution grows exponentially with time. To avoid float-point data overflow or underflow, it is essential to devise an appropriate scheme to normalize the solutions regularly during simulation. In practice, there is no need to normalize the solution at every iteration. Suppose the solution is normalized after every K iterations, or after every time period $T_N = Kh$.

Let $\mathcal{S}^{d-1}$ be the unit sphere in d-dimensional space $\mathcal{R}^d$. For a given initial condition $\mathbf{X}(0) = \mathbf{X}_0 \in \mathcal{S}^{d-1}$, i.e. $\|\mathbf{X}_0\| = 1$, and simulation time $T = MT_N$, one has

$$\|\mathbf{X}(T)\| = \|\mathbf{X}(T, \mathbf{X}_0)\| = \prod_{m=1}^{M} \frac{\|\mathbf{X}(mT_N, \mathbf{X}_0)\|}{\|\mathbf{X}\big((m-1)T_N, \mathbf{X}_0\big)\|}. \tag{2.1.2}$$

Since equation (2.1.1) is linear homogeneous, it can be seen that

$$\mathbf{X}_m(t) = \frac{\mathbf{X}\big((m-1)T_N + t, \mathbf{X}_0\big)}{\|\mathbf{X}\big((m-1)T_N, \mathbf{X}_0\big)\|}, \quad m = 1,\ 2,\ \ldots \tag{2.1.3}$$

solves equation (2.1.1) with the initial condition

$$\mathbf{X}_m(0) = \frac{\mathbf{X}\big((m-1)T_N, \mathbf{X}_0\big)}{\|\mathbf{X}\big((m-1)T_N, \mathbf{X}_0\big)\|} \in \mathcal{S}^{d-1}. \tag{2.1.4}$$

Thus

$$\left\|\mathbf{X}(T)\right\| = \prod_{m=1}^{M} \left\|\mathbf{X}_m(T_N)\right\|. \tag{2.1.5}$$

Equations (2.1.3) and (2.1.4) indicate that normalization procedure can be performed for every time period T_N such that the solution of the stochastic differentials always restarts from initial conditions with unit norm right after the normalization (see Figure 2.1).

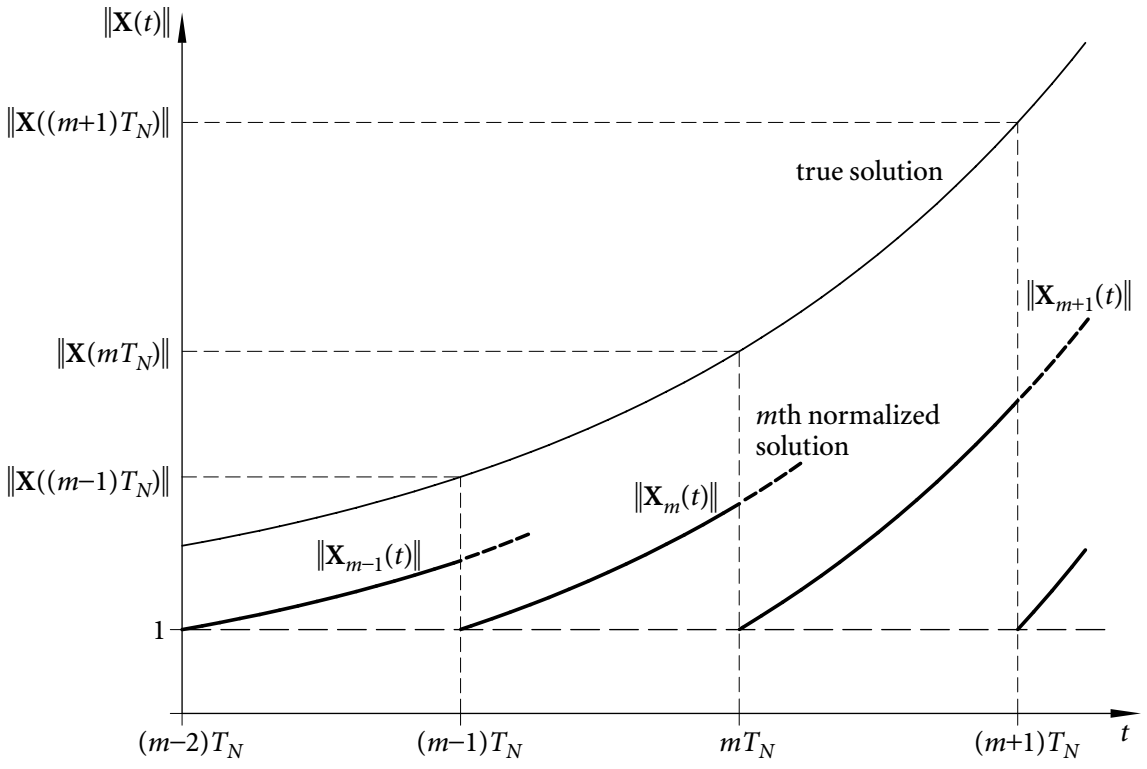

Figure 2.1 Growth of the solution and normalization

Let $\bar{\mathbf{X}}^h$ denote the solution from an appropriate numerical discretization scheme with time step h. For a large simulation time T with M large, the pth moment Lyapunov exponent should be approximated as

$$\bar{\Lambda}^h(p) = \frac{1}{T}\log \mathsf{E}\left[\left\|\bar{\mathbf{X}}^h(T)\right\|^p\right] = \frac{1}{MT_N}\log \mathsf{E}\left[\prod_{m=1}^{M}\left\|\bar{\mathbf{X}}^h_m(T_N)\right\|^p\right]. \tag{2.1.6}$$

In the algorithm in Xie [118], the pth moment Lyapunov exponent is evaluated as

$$\bar{\Lambda}^h(p) = \frac{1}{MT_N} \log \prod_{m=1}^{M} \mathrm{E}\left[\left\|\bar{\mathbf{X}}_m^h(T_N)\right\|^p\right], \tag{2.1.7}$$

where the expectation is determined by the sample average

$$\mathrm{E}\left[\left\|\bar{\mathbf{X}}_m^h(T_N)\right\|^p\right] = \frac{1}{N}\sum_{s=1}^{N} \left\|\bar{\mathbf{X}}_m^{h,s}(T_N)\right\|^p, \tag{2.1.8}$$

with N being the sample size for simulation, and $\bar{\mathbf{X}}_m^{h,s}$ the sth sample path of $\bar{\mathbf{X}}_m^h$.

It is obvious that equations (2.1.6) and (2.1.7) are different since all $\left\|\bar{\mathbf{X}}_m^h(T_N)\right\|$ are dependent and thus the order of the expectation operation and the product operation cannot be exchanged. Noticing that equation (2.1.7) can be rewritten as

$$\bar{\Lambda}^h(p) = \frac{1}{M}\sum_{m=1}^{M} \frac{1}{T_N} \log \mathrm{E}\left[\left\|\bar{\mathbf{X}}_m^h(T_N)\right\|^p\right], \tag{2.1.9}$$

it actually gives the average of M moment Lyapunov exponents simulated for a time period of T_N rather than the moment Lyapunov exponent simulated for a long time period of $T = MT_N$. Theoretically, the larger the value of T_N, the more accurate the approximation. Unfortunately, to avoid float-point data overflow and underflow, the value of T_N cannot be very large. Although each simulation of the moment Lyapunov exponent for a relatively short time period of T_N may not be accurate, for some systems the algorithm based on equation (2.1.7) yields satisfactory results because of the Central Limit Theorem. However, there are systems for which equation (2.1.7) leads to erroneous results.

One possible revision to correct the insufficiency of algorithm (2.1.7) for linear homogeneous systems is to normalize the solutions by their expectations, but not their norms as in equation (2.1.3). With unit norm initial condition and the definition

$$\bar{\mathbf{Y}}_m^h(t) = \frac{\bar{\mathbf{X}}^h\big((m-1)T_N + t, \mathbf{X}_0\big)}{\mathrm{E}\left[\left\|\bar{\mathbf{X}}^h\big((m-1)T_N, \mathbf{X}_0\big)\right\|\right]}, \quad m = 1, 2, \ldots, \tag{2.1.10}$$

the approximate moment Lyapunov exponents at time T are given by

$$\begin{aligned}\bar{\Lambda}^h(p) &= \frac{1}{MT_N}\log\left\{\frac{\mathsf{E}\big[\|\bar{\mathbf{X}}^h(MT_N)\|^p\big]}{\mathsf{E}\big[\|\bar{\mathbf{X}}^h\big((M-1)T_N\big)\|\big]^p}\prod_{m=1}^{M-1}\frac{\mathsf{E}\big[\|\bar{\mathbf{X}}^h(mT_N)\|\big]^p}{\mathsf{E}\big[\|\bar{\mathbf{X}}^h\big((m-1)T_N\big)\|\big]^p}\right\}\\ &= \frac{1}{MT_N}\log\mathsf{E}\left[\left\|\frac{\bar{\mathbf{X}}^h(MT_N)}{\mathsf{E}\big[\|\bar{\mathbf{X}}^h\big((M-1)T_N\big)\|\big]}\right\|^p\right]\\ &\quad+\frac{1}{MT_N}\sum_{m=1}^{M-1}p\log\mathsf{E}\left[\left\|\frac{\bar{\mathbf{X}}^h(mT_N)}{\mathsf{E}\big[\|\bar{\mathbf{X}}^h\big((m-1)T_N\big)\|\big]}\right\|\right]\\ &= \frac{1}{MT_N}\left\{\log\mathsf{E}\big[\|\bar{\mathbf{Y}}^h_M(T_N)\|^p\big]+\sum_{m=1}^{M-1}p\log\mathsf{E}\big[\|\bar{\mathbf{Y}}^h_m(T_N)\|\big]\right\}.\end{aligned}\tag{2.1.11}$$

The solution of equation (2.1.1) may be a diffusion process and its variance may increase significantly with time. Although equation (2.1.11) is exact theoretically when M approaches infinity, there are two main sources that will lead to significant numerical errors.

First, according to the Central Limit Theorem, for independent and identically distributed (i.i.d.) random variables $x_1, x_2, \ldots$ with the same mean value μ and variance σ^2, the distribution of sample average $\bar{x}=\big(\sum_{s=1}^N x_s\big)/N$ tends to the normal distribution $\mathcal{N}(\mu,\sigma^2/N)$. This means that equation (2.1.8) will not give acceptable results of the expected values when the variances of the solutions are so large that it is impossible to reduce the error of estimation to an acceptable level with a finite number of samples.

Second, due to the finite lengths of floating-point representations in computers, when two numbers are summed up, the smaller one will be neglected if the difference of their exponent bits exceeds the limit. If a system is unstable, its solution grows exponentially with time. Even when the system is stable and the chance that the solution takes extremely large values may be rare, once it happens, all the contributions from other samples will be eliminated. Thus this truncated error in estimating the expectations will be dominant in simulations with large variances.

To illustrate, consider the first-order linear homogeneous stochastic system

$$\mathrm{d}x(t) = ax(t)\,\mathrm{d}t + \sigma x(t)\,\mathrm{d}W(t),\tag{2.1.12}$$

where a and σ are real constants. The solution of system (2.1.12) is given by

$$x(t) = x(0)\exp\left\{\left(a-\frac{1}{2}\sigma^2\right)t + \sigma W(t)\right\}.$$

The pth moment Lyapunov exponent can be easily determined as

$$\Lambda(p) = \lim_{t\to\infty}\frac{1}{t}\log \mathrm{E}\left[|x(t)|^p\right] = \frac{p}{2}\left[(p-1)\sigma^2 + 2a\right],$$

and the variance of norm is

$$\mathrm{Var}\left[|x(t)|\right] = \mathrm{E}\left[|x(t)|^2\right] - \left\{\mathrm{E}\left[|x(t)|\right]\right\}^2 = \mathrm{e}^{2at}(\mathrm{e}^{\sigma^2 t} - 1).$$

Figure 2.2 shows the numerical results of the moment Lyapunov exponents for $a=0$, $\sigma=1$, and different values of the total time of simulation T, in which equation (2.1.12) is solved numerically using the explicit Euler scheme. The time step for iteration is $h=0.001$, the sample size is $N=5000$ and equation (2.1.11), i.e. the revised algorithm, is used to determine the approximate moment Lyapunov exponents. It is obvious that the longer the time T for simulation, the worse the results. Because the variance of $|x(t)|$ increases exponentially with time, it is impossible to get an accurate estimate of the pth moment using sample average from finite sample sizes N for t large.

2.2 Estimation of the Expectation through Logarithm of Norm

Because of the possible large errors in simulating moment Lyapunov exponents with increasing time of simulation, it is required to develop a new algorithm to overcome the difficulty in estimating the moments. Since the errors are caused by large variances of the solutions, it is clear that how to reduce the variances in order to obtain a good estimation of the moments using a finite number of samples is the key.

There exists variance reduction techniques in Monte Carlo simulation [60], [80]. These methods construct either an alternate correction process or a new random variable to reduce the variance of estimation through the sample average. However, in order to have the best effect, the solution to the equation to be simulated should be known in advance. In practice, one has to guess and choose the required functions for estimation. Thus it is not easy to say how much these techniques will improve the results.

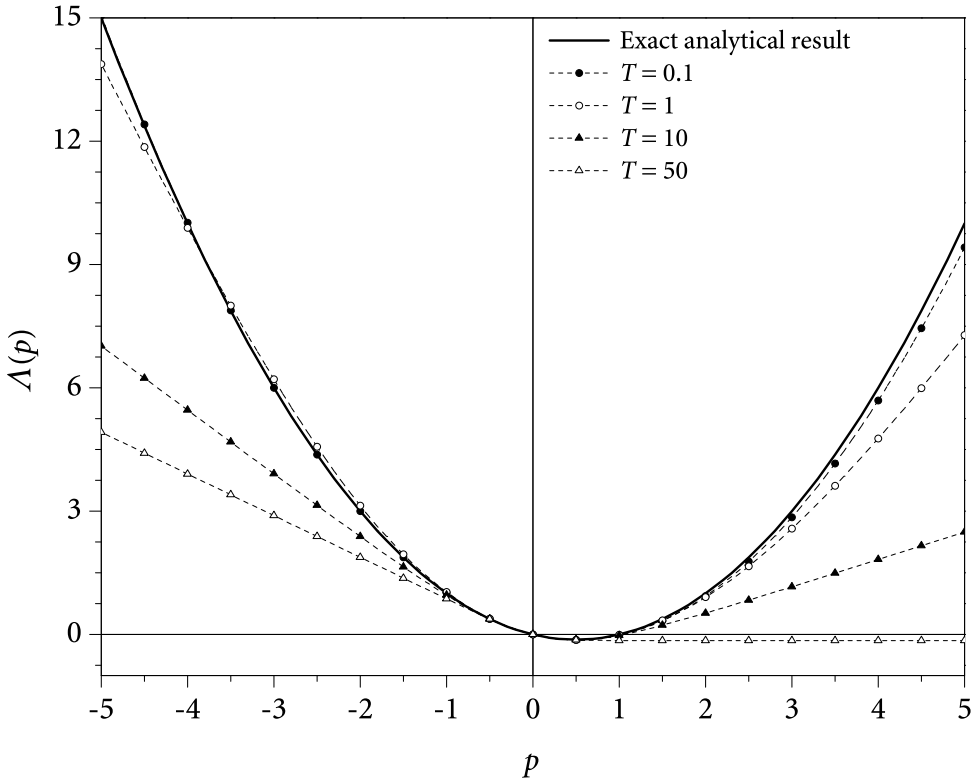

Figure 2.2 Simulation of moment Lyapunov exponents for a first-orderlinear system

Notice that

$$\log \mathrm{E}\left[\left\|\mathbf{X}(T)\right\|^{p}\right] = \log \mathrm{E}\left[\mathrm{e}^{p\log\left\|\mathbf{X}(T)\right\|}\right] = C(p), \tag{2.2.1}$$

where $C(p)$ is the cumulant generating function of $\log\left\|\mathbf{X}(T)\right\|$. In the special case when $\log\left\|\mathbf{X}(T)\right\|$ is normal, $C(p)$ takes the simple form

$$C(p) = p\,\mathrm{E}\left[\log\left\|\mathbf{X}(T)\right\|\right] + \frac{1}{2}p^{2}\,\mathrm{Var}\left[\log\left\|\mathbf{X}(T)\right\|\right], \tag{2.2.2}$$

where $\mathrm{Var}[\,\cdot\,]$ denotes the variance. Therefore it may be possible to use the statistical properties of $\log\left\|\mathbf{X}(T)\right\|$ in estimating the moment Lyapunov exponents.

2.2.1 Asymptotic Normality of Logarithm of Norm

Since the simulation of stochastic dynamical systems is based on the theory of stochastic integrals, it is natural to start with the following d-dimensional Itô stochastic differential

equation

$$\mathrm{d}\mathbf{X}(t) = \mathbf{B}_0(\mathbf{X}, t)\,\mathrm{d}t + \sum_{i=1}^{r} \mathbf{B}_i(\mathbf{X}, t)\,\mathrm{d}W_i. \tag{2.2.3}$$

When the system is linear homogeneous with constant coefficients, equation (2.2.3) takes the form

$$\mathrm{d}\mathbf{X}(t) = \mathbf{B}_0\,\mathbf{X}(t)\,\mathrm{d}t + \sum_{i=1}^{r} \mathbf{B}_i\,\mathbf{X}(t)\,\mathrm{d}W_i, \tag{2.2.4}$$

where $\mathbf{B}_i$, $i=0, 1, \ldots, r$, are $d\times d$ constant matrices. Let $\rho(t)=\log\|\mathbf{X}(t)\|$ and λ be the largest Lyapunov exponent. It has been shown ([58], p. 243) that the limit distribution of $\big(\rho(t)-\lambda t\big)\big/\sqrt{\mathrm{Var}\,[\rho(t)]}$ is standard normal as $t\to\infty$ if $\mathrm{Var}\,[\rho(t)]\to\infty$, and there exists a constant $\alpha>0$ such that, for any vector $\mathbf{Y}$,

$$\sum_{i=1}^{r} \big(\mathbf{Y}^T\mathbf{B}_i\mathbf{X}\big)^2 \geqslant \alpha\|\mathbf{X}\|^2\|\mathbf{Y}\|^2 \tag{2.2.5}$$

is satisfied.

However, in applications, there are many cases that the non-degenerate condition (2.2.5) is not satisfied. An extended result by Arnold *et al.* [7] shows that, for any $\mathbf{X}(0)\neq\mathbf{0}$,

$$\lim_{t\to\infty}\frac{1}{t}\rho(t)=\lambda \quad \text{a.s.}, \qquad \lim_{t\to\infty}\frac{1}{t}\log \mathrm{E}\Big[\|\mathbf{X}(t)\|^p\Big]=\Lambda(p), \tag{2.2.6}$$

and the normalized $\rho(t)$ converges weakly to Gaussian distribution with

$$\frac{\rho(t)-\lambda t}{\sqrt{t}} \xrightarrow{\ D\ } \mathcal{N}\big(0, \Lambda''(0)\big), \quad t\to\infty, \tag{2.2.7}$$

provided that

$$\dim \mathcal{LA}\big(\mathbf{g}_i : 0\leqslant i\leqslant r\big)(\mathbf{s}) = d-1, \quad \text{for all } \mathbf{s}\in\mathcal{PJ}^{d-1}, \tag{2.2.8}$$

where $\mathcal{LA}(\mathbf{g}_i)$ denotes the Lie algebra generated by the set of vector fields $\mathbf{g}_i$, dim the dimension, $\mathcal{PJ}^{d-1}$ the projective space obtained from $\mathcal{S}^{d-1}$ by identifying $\mathbf{s}$ and $-\mathbf{s}$, and $\mathbf{g}_i$ are given by

$$\mathbf{g}_0(\mathbf{s}) = \mathbf{g}\bigg(\mathbf{B}_0 - \frac{1}{2}\sum_{i=1}^{r}\mathbf{B}_i^2,\ \mathbf{s}\bigg), \quad \mathbf{g}_i(\mathbf{s}) = \mathbf{g}(\mathbf{B}_i,\ \mathbf{s}), \quad i=1,\ 2,\ \ldots,\ r, \tag{2.2.9}$$

in which $\mathbf{g}$ is defined as, for any $d\times d$ matrix $\mathbf{B}$ and $\mathbf{s}\in\mathcal{S}^{d-1}$,

$$\mathbf{g}(\mathbf{B},\mathbf{s})=\big(\mathbf{B}-(\mathbf{s}^T\mathbf{B}\mathbf{s})\mathbf{I}\big)\mathbf{s}=\mathbf{B}\mathbf{s}-(\mathbf{s}^T\mathbf{B}\mathbf{s})\mathbf{s}. \tag{2.2.10}$$

It is obvious that $\mathbf{g}(\mathbf{B},\mathbf{s})$ is the orthonormal component of vector $\mathbf{B}\mathbf{s}$ with respect to $\mathbf{s}$.

The linear homogeneous system with constant coefficients, i.e. equation (2.2.4), can be converted to the Stratonovich form. Thus it can describe the stochastic dynamical system

$$\dot{\mathbf{X}}(t)=\left(\mathbf{B}_0-\frac{1}{2}\sum_{i=1}^{r}\mathbf{B}_i^2+\sum_{i=1}^{r}\mathbf{B}_i\xi_i(t)\right)\mathbf{X}(t)=\mathbf{A}\big(\boldsymbol{\xi}(t)\big)\,\mathbf{X}(t),$$

with $\xi_i(t)$, $i=1,\,2,\,\ldots,\,r$, being unit Gaussian white noises. It is very likely that noise $\boldsymbol{\xi}(t)$ takes other forms. The result obtained by Arnold *et al.* [9], [5] solves this problem under some conditions.

Return to the general d-dimensional linear homogeneous system (2.1.1), with $\mathbf{A}$ being an analytic function and $\boldsymbol{\xi}(t)$ being a vector stochastic process on a connected smooth manifold $\mathcal{M}$ described by Stratonovich stochastic differential equation

$$\mathrm{d}\boldsymbol{\xi}(t)=\mathbf{Q}_0\big(\boldsymbol{\xi}(t)\big)\,\mathrm{d}t+\sum_{i=1}^{r}\mathbf{Q}_i\big(\boldsymbol{\xi}(t)\big)\circ\mathrm{d}W_i, \tag{2.2.11}$$

where $\mathbf{Q}_i$, $i=0,\,1,\,\ldots,\,r$, are smooth. If

$$\dim\mathcal{LA}\big(\mathbf{Q}_i:1\leqslant i\leqslant r\big)(\boldsymbol{\xi})=\dim\mathcal{M},\quad\text{for all }\boldsymbol{\xi}\in\mathcal{M}, \tag{2.2.12}$$

$$\dim\mathcal{LA}\big(\mathbf{g}\big(\mathbf{A}(\boldsymbol{\xi}),\mathbf{s}\big):\boldsymbol{\xi}\in\mathcal{M}\big)(\mathbf{s})=d-1,\quad\text{for all }\mathbf{s}\in\mathcal{PJ}^{d-1}, \tag{2.2.13}$$

then, for any $\mathbf{X}(0)\neq\mathbf{0}$, equations (2.2.6) and (2.2.7) are still true. Condition (2.2.12) ensures that $\boldsymbol{\xi}(t)$ is a stationary ergodic diffusion process with a unique smooth and positive invariant density ϱ on manifold $\mathcal{M}$ [5]. Fortunately, condition (2.2.13) is satisfied for most problems frequently considered in engineering applications [9]. Moreover, conditions (2.2.12) and (2.2.13) can be replaced by

$$\dim\mathcal{LA}\Big(\mathbf{Q}_0+\mathbf{g}(\mathbf{A},\mathbf{s})+\frac{\partial}{\partial t},\ \mathbf{Q}_1,\ \ldots,\ \mathbf{Q}_r\Big)(\boldsymbol{\xi},\mathbf{s},t)=\dim\mathcal{M}+d,$$
$$\text{for all }(\boldsymbol{\xi},\mathbf{s},t)\in\mathcal{M}\times\mathcal{PJ}^{d-1}\times\mathcal{R}, \tag{2.2.14}$$

As a result of equations (2.2.6) and (2.2.7), one can write [4]

$$\Lambda(p) = \lambda p + \frac{1}{2}\Lambda''(0)p^2 + o(p^2). \tag{2.2.15}$$

2.2.2 Estimation through Logarithm of Norm

Suppose $\|\mathbf{X}(T)\|$ is obtained for linear homogeneous systems (2.2.4) or (2.1.1), and the corresponding system satisfies conditions (2.2.8), or (2.2.12) and (2.2.13). When T is large enough and $\mathbf{X}(0) \neq \mathbf{0}$, $\rho(T) = \log\|\mathbf{X}(T)\|$ is near Gaussian according to the discussion in Section 2.2.1.

Let $\bar{\mathbf{X}}^h(T)$ still be the solution at time T obtained from an appropriate numerical discretization scheme with time step h, and $\bar{\mathbf{X}}^{h,s}(T)$, $s = 1, 2, \ldots, N$, be the different samples of $\bar{\mathbf{X}}^h(T)$. Then $\bar{\mathbf{X}}^{h,s}(T)$ can be treated as independent and identically distributed (i.i.d.) random vectors with the same distribution as $\bar{\mathbf{X}}^h(T)$. Thus the pth moment Lyapunov exponent is approximated as

$$\begin{aligned}\bar{\Lambda}^h(p) &= \frac{1}{T}\log \mathsf{E}\left[\left\|\bar{\mathbf{X}}^h(T)\right\|^p\right] = \frac{1}{NT}\log\left\{\prod_{s=1}^{N}\mathsf{E}\left[\left\|\bar{\mathbf{X}}^{h,s}(T)\right\|^p\right]\right\} \\ &= \frac{1}{NT}\log \mathsf{E}\left[\exp\left(p\sum_{s=1}^{N}\log\left\|\bar{\mathbf{X}}^{h,s}(T)\right\|\right)\right].\end{aligned} \tag{2.2.16}$$

By defining

$$\begin{aligned}&\bar{\rho}^h(T) = \log\left\|\bar{\mathbf{X}}^h(T)\right\|, \\ &\bar{\mu}_T^h = \mathsf{E}\left[\bar{\rho}^h(T)\right], \qquad \left(\bar{\sigma}_T^h\right)^2 = \mathsf{Var}\left[\bar{\rho}^h(T)\right], \\ &\hat{\rho}^{h,s}(T) = \frac{\bar{\rho}^{h,s}(T) - \bar{\mu}_T^h}{\bar{\sigma}_T^h}, \qquad R_N = \sum_{s=1}^{N}\hat{\rho}^{h,s}(T),\end{aligned} \tag{2.2.17}$$

equation (2.2.16) becomes

$$\bar{\Lambda}^h(p) = \frac{1}{NT}\log \mathsf{E}\left[\exp\left(p\bar{\mu}_T^h N + p\bar{\sigma}_T^h R_N\right)\right] = p\frac{\bar{\mu}_T^h}{T} + \frac{1}{NT}\log \mathsf{E}\left[e^{p\bar{\sigma}_T^h R_N}\right]. \tag{2.2.18}$$

With the notation

$$\zeta_N = \frac{R_N}{\sqrt{N}}, \tag{2.2.19}$$

equation (2.2.18) is converted to

$$\bar{\Lambda}^h(p) = p\frac{\bar{\mu}_T^h}{T} + \frac{1}{NT}\log \mathrm{E}\left[\mathrm{e}^{\sqrt{N}p\bar{\sigma}_T^h\zeta_N}\right]. \tag{2.2.20}$$

Let $F_\zeta^{*N}(x)$ be the cumulative distribution function of ζ_N, then $F_\zeta^{*N}(x)$ tends to the standard normal distribution of $\mathcal{N}(0,1)$ as $N\to\infty$ according to the Central Limit Theorem, i.e. $F_\zeta^{*N}(x)\to\Phi(x)$ uniformly, where $\Phi(x)$ is the standard normal distribution function

$$\Phi(x) = \frac{1}{\sqrt{2\pi}}\int_{-\infty}^{x}\exp\left(-\frac{y^2}{2}\right)\mathrm{d}y.$$

Using the Edgeworth expansion theorem for distribution [42], [31], one may have

$$F_\zeta^{*N}(x) = \Phi(x) + \sum_{k=3}^{\infty} c_k\,\Phi^{(k)}(x), \tag{2.2.21}$$

where $\Phi^{(k)}(x)$ is the kth derivative of $\Phi(x)$, and the coefficients c_k can be determined by the equality of moments on both sides of equation (2.2.21). Notice that ζ_N has zero mean and unit variance. If the kth central moment of $\hat{\rho}^h(T)$ is $\bar{\mu}_k^h$, for $k\geqslant 3$, then using integration by parts, it is easy to deduce from equation (2.2.21) that

$$c_3 = -\frac{1}{6}\frac{\bar{\mu}_3^h}{\sqrt{N}\left(\bar{\sigma}_T^h\right)^3}, \quad c_4 = \frac{1}{24}\frac{\bar{\mu}_4^h - 3\left(\bar{\sigma}_T^h\right)^4}{N\left(\bar{\sigma}_T^h\right)^4}, \quad \cdots.$$

Therefore equation (2.2.20) yields

$$\begin{aligned}
\bar{\Lambda}^h(p) &= p\frac{\bar{\mu}_T^h}{T} + \frac{1}{NT}\log\int_{-\infty}^{\infty}\mathrm{e}^{\sqrt{N}p\bar{\sigma}_T^h x}\mathrm{d}F_\zeta^{*N}(x)\\
&= p\frac{\bar{\mu}_T^h}{T} + \frac{1}{NT}\log\left\{\mathrm{e}^{\frac{1}{2}Np^2(\bar{\sigma}_T^h)^2}\left[1 - N^{3/2}p^3\left(\bar{\sigma}_T^h\right)^3 c_3 + N^2p^4\left(\bar{\sigma}_T^h\right)^4 c_4 + \cdots\right]\right\}\\
&= p\frac{\bar{\mu}_T^h}{T} + \frac{1}{2}p^2\frac{\left(\bar{\sigma}_T^h\right)^2}{T} + \frac{1}{NT}\log\left\{1 + \frac{1}{6}Np^3\bar{\mu}_3^h + \frac{1}{24}Np^4\left[\bar{\mu}_4^h - 3\left(\bar{\sigma}_T^h\right)^4\right] + \cdots\right\}.
\end{aligned} \tag{2.2.22}$$

The tail distribution of $F_\zeta^{*N}(x)$ is of paramount significance, since it is required to determine the expectation of $\mathrm{e}^{\sqrt{N}p\bar{\sigma}_T^h\zeta_N}$ in equation (2.2.20) from a finite sample size N in simulation. This means that accurate higher-order moments of $\bar{\rho}^h(T)$ are required in order to obtain a good approximation of $\mathrm{E}\left[\mathrm{e}^{\sqrt{N}p\bar{\sigma}_T^h\zeta_N}\right]$. However, it is very difficult to do so in

practice. If only lower-order moments are considered, the estimation error of moments may make the sum of a finite number of terms within the argument of the last logarithm in equation (2.2.22) be negative when N becomes large, which will lead to invalid operation in simulation. Despite there are many methods to estimate the distribution of a random variable in statistics, for example, the saddle point approximation [100], [13], [61], the kernal function estimation [30], these methods only ensure the uniform approximation of the probability density function, which is not enough to obtain a good approximation of the expectation of $\mathrm{e}^{\sqrt{N}p\bar{\sigma}_T^h\zeta_N}$. Therefore, the distribution of $\bar{\rho}^h(T)$ has to be considered to find an appropriate estimation.

Noticing that equation (2.2.2) is true for normal distribution, one may attempt to see if the last logarithm term in equation (2.2.22) can be dropped in simulation since the distribution of the normalized $\bar{\rho}^h(T)$ approaches normal as T goes to infinity, just as indicated by equation (2.2.7). Actually, $\bar{\rho}^h(T)$ obtained from simulation always takes values within some finite interval $[A, B]$. If the truncation of $\bar{\rho}^h(T)$, i.e. $\bar{\rho}^h(T)\mathbf{1}_{[A,B]}$, is considered, where $\mathbf{1}_{[A,B]}$ is the indicator function of $[A, B]$, $\mathrm{E}\big[\mathrm{e}^{p\bar{\rho}^h(T)\mathbf{1}_{[A,B]}}\big]$ approaches $\mathrm{E}\big[\mathrm{e}^{p\bar{\rho}^h(T)}\big]$ as close as possible when $A\to-\infty$ and $B\to\infty$. Helly's second theorem ([77], pp.45, see also [53]) shows that the value of $\mathrm{E}\big[\mathrm{e}^{p\bar{\rho}^h(T)\mathbf{1}_{[A,B]}}\big]$ can be approximated by evaluating the expectation using normal distribution when T is large enough. These reasons provide a support that $\mathrm{E}\big[\mathrm{e}^{p\bar{\rho}^h(T)}\big]$ may be estimated by taking $\bar{\rho}^h(T)$ as a normal random variable.

From the definition of $\hat{\rho}^{h,s}(T)$, it can be seen that $\hat{\rho}^{h,s}(T)$, $s=1, 2, \ldots, N$, are i.i.d. random variables with $\mathrm{E}\big[\hat{\rho}^{h,s}(T)\big]=0$, $\mathrm{Var}\big[\hat{\rho}^{h,s}(T)\big]=1$. Moreover, using equation (2.2.1), it is obvious that the existence of moment Lyapunov exponents ensures that $\mathrm{E}\big[\mathrm{e}^{\eta\hat{\rho}^{h,s}(T)}\big]<\infty$ for $|\eta|\leqslant\eta_0$, where η_0 is some constant. Then according to the theorem proved by Komlós *et al.* [62], [63], a sequence of standard normal random variables z_s, $s=1, 2, \ldots, N$, can be constructed such that, for every N and all $x>0$, the partial sums $R_k=\sum_{s=1}^{k}\hat{\rho}^{h,s}(T)$ and $V_k=\sum_{s=1}^{k}z_s$ satisfy

$$\mathcal{P}\left\{\max_{k\leqslant N}|R_k-V_k|>C_0\log N+x\right\}<\delta_0\mathrm{e}^{-\delta x}, \tag{2.2.23}$$

where C_0, δ, δ_0 depend only on the distribution of $\hat{\rho}^{h,s}(T)$, and δ can be as large as possible by choosing C_0 large enough. Thus it follows $\left|R_N - V_N\right| = \mathcal{O}(\log N)$ almost-surely for every N [62], [63].

Considering the near normality of $\hat{\rho}^{h,s}(T)$ and the finite sample size, events with zero probability are treated as not likely to occur in simulation. This means that R_N is replaced by $V_N + \mathcal{O}(\log N)$ in the evaluation of expectation and thus equation (2.2.18) is approximated as

$$\begin{aligned}\bar{\Lambda}^h(p) &= p\frac{\bar{\mu}_T^h}{T} + \frac{1}{NT}\log \mathsf{E}\left[\mathrm{e}^{p\bar{\sigma}_T^h\left\{V_N + \mathcal{O}(\log N)\right\}}\right] \\ &= p\frac{\bar{\mu}_T^h}{T} + \frac{1}{2}p^2\frac{\left(\bar{\sigma}_T^h\right)^2}{T} + \mathcal{O}\left(\frac{\log N}{N}\right). \end{aligned} \tag{2.2.24}$$

Hence, when the sample size N is large enough, by neglecting the last term in equation (2.2.24) and estimating the mean and variance of logarithm of norm, the pth moment Lyapunov exponent is given by

$$\bar{\Lambda}^h(p) = \frac{1}{T}\left\{p\,\mathsf{E}\left[\log\left\|\bar{\mathbf{X}}^h(T)\right\|\right] + \frac{1}{2}p^2\,\mathrm{Var}\left[\log\left\|\bar{\mathbf{X}}^h(T)\right\|\right]\right\}. \tag{2.2.25}$$

It is obvious that the variance of $\log\left\|\bar{\mathbf{X}}^h(T)\right\|$ will be much smaller than the variance of $\left\|\bar{\mathbf{X}}^h(T)\right\|$ when $\left\|\bar{\mathbf{X}}^h(T)\right\|$ becomes large; therefore obtaining a good estimation of the pth moment Lyapunov exponent through sample average is possible.

From equation (2.2.25) one also sees that the largest Lyapunov exponent can be approximated as

$$\bar{\lambda}^h = \frac{1}{T}\mathsf{E}\left[\log\left\|\bar{\mathbf{X}}^h(T)\right\|\right], \tag{2.2.26}$$

which is the same result as given by Talay [109].

2.3 Algorithm for Linear Homogeneous Stochastic Systems

2.3.1 Implementation of Algorithm

Following equation (2.2.25), an algorithm for simulating the moment Lyapunov exponents of linear homogeneous stochastic dynamical system (2.2.4)

$$\mathrm{d}\mathbf{X}(t) = \mathbf{B}_0\,\mathbf{X}(t)\,\mathrm{d}t + \sum_{i=1}^{r} \mathbf{B}_i\,\mathbf{X}(t)\,\mathrm{d}W_i,$$

or equivalently, in the Stratonovich's form,

$$\mathrm{d}\mathbf{X}(t) = \left(\mathbf{B}_0 - \frac{1}{2}\sum_{i=1}^{r} \mathbf{B}_i^2\right)\mathbf{X}(t)\,\mathrm{d}t + \sum_{i=1}^{r} \mathbf{B}_i\,\mathbf{X}(t) \circ \mathrm{d}W_i,$$

and system (2.1.1)

$$\begin{aligned}
\dot{\mathbf{X}}(t) &= \mathbf{A}\big(\boldsymbol{\xi}(t)\big)\,\mathbf{X}(t),\\
\mathrm{d}\boldsymbol{\xi}(t) &= \mathbf{Q}_0\big(\boldsymbol{\xi}(t)\big)\,\mathrm{d}t + \sum_{i=1}^{r} \mathbf{Q}_i\big(\boldsymbol{\xi}(t)\big) \circ \mathrm{d}W_i,
\end{aligned}$$

can be described as follows. Since the simulation requires the statistical properties of logarithm of the norm, the normalization operation described in Section 2.1 can be applied.

Step 1. Use an appropriate time discrete approximation, such as the Euler scheme, to discretize system (2.2.4) or (2.1.1) with time step h. Details of various numerical schemes for solving stochastic differential equations can be found in [60].

Step 2. Set the initial conditions of the state vector $\bar{\mathbf{X}}^h\big(t, \bar{\mathbf{X}}^h(0)\big)$ by $\bar{\mathbf{X}}^h(0) \in \mathbf{S}^{d-1}$, i.e.

$$\big\|\bar{\mathbf{X}}^{h,s}(0)\big\| = 1, \quad s = 1, 2, \ldots, N,$$

where N is the sample size, $\|\mathbf{X}\| = \sqrt{\mathbf{X}^T\mathbf{X}}$ is the Euclidean norm of vector $\mathbf{X}$.

Step 3. Solve the discretized system iteratively. Apply the normalization procedure as described in Section 2.1, i.e. normalization is performed after every K iterations or after every time period $T_N = Kh$. At the mth normalization, or at $t = mT_N$, the sth sample is normalized using equation (2.1.4), i.e.

$$\bar{\mathbf{X}}_{m+1}^{h,s}(0) = \frac{\bar{\mathbf{X}}^{h,s}\big(mT_N, \bar{\mathbf{X}}^{h,s}(0)\big)}{\big\|\bar{\mathbf{X}}^{h,s}\big(mT_N, \bar{\mathbf{X}}^{h,s}(0)\big)\big\|} = \frac{\bar{\mathbf{X}}_m^{h,s}\big(T_N, \bar{\mathbf{X}}_m^{h,s}(0)\big)}{\big\|\bar{\mathbf{X}}_m^{h,s}\big(T_N, \bar{\mathbf{X}}_m^{h,s}(0)\big)\big\|}, \quad m = 1, 2, \ldots.$$

Simulation is then continued with the initial condition $\bar{\mathbf{X}}^{h,s}_{m+1}(0)$ with $\|\bar{\mathbf{X}}^{h,s}_{m+1}(0)\|=1$ for another K iterations.

Step 4. Defining

$$\bar{\rho}^{h,s}(mT_N)=\log\|\bar{\mathbf{X}}^{h,s}(mT_N,\bar{\mathbf{X}}^{h,s}(0))\|,\quad \bar{\rho}^{h,s}_m(T_N)=\log\|\bar{\mathbf{X}}^{h,s}_m(T_N,\bar{\mathbf{X}}^{h,s}_m(0))\|,$$

then, using equation (2.1.5),

$$\begin{aligned}\bar{\rho}^{h,s}(MT_N)&=\log\|\bar{\mathbf{X}}^{h,s}(MT_N,\bar{\mathbf{X}}^{h,s}(0))\|\\&=\log\left[\prod_{m=1}^{M}\|\bar{\mathbf{X}}^{h,s}_m(T_N,\bar{\mathbf{X}}^{h,s}_m(0))\|\right]=\sum_{m=1}^{M}\bar{\rho}^{h,s}_m(T_N).\end{aligned}$$

Step 5. After KM iterations, i.e. at time $T=MKh$, use the following equations

$$\begin{aligned}&\mathrm{E}\left[\log\|\bar{\mathbf{X}}^h(T)\|\right]=\mathrm{E}\left[\bar{\rho}^h(T)\right]=\frac{1}{N}\sum_{s=1}^{N}\bar{\rho}^{h,s}(T)=\bar{\mu}^h_T,\\&\mathrm{Var}\left[\log\|\bar{\mathbf{X}}^h(T)\|\right]=\mathrm{Var}\left[\bar{\rho}^h(T)\right]=\frac{1}{N-1}\sum_{s=1}^{N}\left[\bar{\rho}^{h,s}(T)^2-\left(\bar{\mu}^h_T\right)^2\right]=\left(\bar{\sigma}^h_T\right)^2,\end{aligned}\tag{2.3.1}$$

to estimate the mean and variance of $\log\|\bar{\mathbf{X}}^h(T)\|$.

Step 6. Use equation (2.2.25), combining with equations (2.3.1), i.e.

$$\bar{\Lambda}^h(p)=\frac{1}{T}\left[p\bar{\mu}^h_T+\frac{1}{2}p^2\left(\bar{\sigma}^h_T\right)^2\right],\tag{2.3.2}$$

to calculate the moment Lyapunov exponents for all values of p of interest.

It is known from statistics [26] that the estimators for $\bar{\mu}^h_T$ and $\left(\bar{\sigma}^h_T\right)^2$ in equations (2.3.1) have accuracy of order $1/N$. As introduced in Section 1.3.2, Euler scheme is a weak approximation scheme with order 1.0. Thus if Euler scheme is applied to discretize the system, the error of approximations for $\mathrm{E}\left[\log\|\mathbf{X}(T)\|\right]$ and $\mathrm{Var}\left[\log\|\mathbf{X}(T)\|\right]$ is of order $\mathcal{O}(h)$. Combining these results with equations (2.2.15) and (2.2.24), when T is large enough, the error of algorithm presented in this section for simulating the moment Lyapunov exponents is approximately

$$\left|\bar{\Lambda}^h(p)-\Lambda(p)\right|=o(p^2)+\mathcal{O}(h)+\mathcal{O}\left(\frac{\log N}{N}\right).\tag{2.3.3}$$

It should be mentioned that, although higher order schemes lead to more accurate results, it is easier to implement the Monte Carlo simulation using the Euler scheme due to its simple

form, especially when the system is high dimensional and complicated. Moreover, Romberg extrapolation may be applied to increase the accuracy of the results to $\mathcal{O}(h^2)$ using the Euler scheme [108].

Before the algorithm presented in this section can be applied, conditions (2.2.8) (for system (2.2.4)), (2.2.12) and (2.2.13), or (2.2.14) (for system (2.1.1)) need to be satisfied. According to the definition of Lie algebra ([52] and [88]), $\mathcal{LA}(\mathbf{g}_i)$ is actually a vector space generated by the set of vectors $\mathbf{g}_i$, thus dim $\mathcal{LA}(\mathbf{g}_i)(\mathbf{s})$ can be determined by the dimension of this vector space. It turns out that condition (2.2.8) is satisfied, provided that the space spanned by vectors $\{\mathbf{g}_i : 0 \leqslant i \leqslant r\}$ has dimension d, i.e. the set of vectors $\{\mathbf{g}_i : 0 \leqslant i \leqslant r\}$ has rank d, since $\mathbf{s} \in \bar{\mathcal{P}}\mathcal{J}^{d-1}$. For system (2.1.1), condition (2.2.13) is satisfied for the special case [5]

$$\mathbf{A}(\boldsymbol{\xi}) = \begin{bmatrix} 0 & 1 & 0 & \cdots & 0 \\ 0 & 0 & 1 & \cdots & 0 \\ \vdots & & & & \vdots \\ 0 & 0 & 0 & \cdots & 1 \\ a_1(\boldsymbol{\xi}) & a_2(\boldsymbol{\xi}) & a_3(\boldsymbol{\xi}) & \cdots & a_d(\boldsymbol{\xi}) \end{bmatrix}. \tag{2.3.4}$$

In particular, when $d = 2$, equation (2.3.4) stands for the general second-order oscillator

$$\ddot{q}(t) - a_2(\boldsymbol{\xi})\,\dot{q}(t) - a_1(\boldsymbol{\xi})\,q(t) = 0. \tag{2.3.5}$$

If $a_2(\boldsymbol{\xi})$ is constant, equation (2.3.5) becomes

$$\ddot{q}(t) + \beta\,\dot{q}(t) + f\big(\boldsymbol{\xi}(t)\big)\,q(t) = 0, \tag{2.3.6}$$

which describes the motion of a damped oscillator under noise perturbation. For equation (2.3.6), one has

$$\mathbf{A}\big(\boldsymbol{\xi}(t)\big) = \begin{bmatrix} 0 & 1 \\ -f\big(\boldsymbol{\xi}(t)\big) & -\beta \end{bmatrix}. \tag{2.3.7}$$

When $f(\boldsymbol{\xi})$ is not a constant function, the vectors $\mathbf{g}\big(\mathbf{A}(\boldsymbol{\xi}), \mathbf{s}\big)$ are not in the same direction for different values of $\boldsymbol{\xi}$. Thus it can be easily verified that condition (2.2.13) is true.

It is stated in reference [5] that most systems considered in physics and engineering satisfy the required conditions to ensure the existence of the moment Lyapunov exponents and the

asymptotic normality of logarithm of norm. This means that the algorithm in this section may be applied directly in most cases, and the asymptotic normality of the logarithm of norm may be verified through the histogram estimation obtained in simulation.

2.3.2 Speedup of Simulation

To obtain a more accurate estimation of the mean and variance of $\log\left\|\bar{\mathbf{X}}^h(T)\right\|$ from equations (2.3.1), large sample size N has to be used. Moreover, time for simulation T has to be large enough to get a good approximation of moment Lyapunov exponents according to the definition. This means iteration times in solving the system will be extremely large. Since the simulation of different samples can be implemented independently, parallel computation using MPI (Message Passing Interface) or OpenMP application program interface will be a great benefit to the simulation of moment Lyapunov exponents.

Message passing is a programming standard used widely on multiprocessing computer systems with distributed memory, where each processor runs the codes on its own memory. When it is required to communicate among processors, messages and data will be sent through a programming interface, namely the Message Passing Interface [104].

Let T_s be the serial execution time of simulation on a single processor. If the simulation task is distributed uniformly to a multiprocessing system with m processors, then the execution time on each processor will be T_s/m. Moreover, if the communication time among processors during simulation is T_c, then according to Amdahl's timing model [92], [112], the speedup of simulation is defined as

$$Spd(m) = \frac{T_s}{T_s/m + T_c} = \frac{m}{1 + mT_c/T_s}. \tag{2.3.8}$$

It can be seen that, if $T_c \ll T_s$, the speedup is almost m. When m is large, the execution time of simulation will be reduced greatly.

From the steps of the algorithm presented in Section 2.3.1, the iteration procedure for solving the discretized system in **Step 3** is the most time-consuming part. This part of simulation can be distributed to multiprocessors, and each processor can run the iteration procedure of some samples independently without knowing the information on other processors. Only in **Step 5**, the logarithm of norm simulated by different processors needs

to be gathered to evaluate the mean and variance. Thus the communication time among processors is only the time of sending a small amount of data to a processor, which is obviousely far less than the iteration time in simulation. Since $T_c \ll T_s$ is satisfied, parallel computation using MPI is extremely suitable for the simulation of moment Lyapunov exponents. For more information about programming with MPI and OpenMP, one can refer to http://www.mpiweb.org and http://www.openmp.org.

2.4 Examples in Application

The Monte Carlo simulation algorithm presented in Section 2.3 is applicable to linear homogeneous stochastic dynamical systems, which have wide applications in engineering mechanics, such as oscillators under parametric excitations of noises. In this section, moment Lyapunov exponents of three single degree-of-freedom systems under white noise, real noise, and bounded noise excitations, respectively, are determined. The numerical results of simulation are compared with known approximate analytical results.

2.4.1 An Oscillator under White Noise Excitation

Consider the following two-dimensional oscillator under the excitation of white noises

$$\ddot{q}(t) + \left[2\varepsilon\beta + \varepsilon^{1/2}\sigma_2\zeta_2(t)\right]\dot{q}(t) + \omega^2\left[1 + \varepsilon^{1/2}\sigma_1\zeta_1(t)\right]q(t) = 0, \tag{2.4.1}$$

where $\zeta_1(t)$ and $\zeta_2(t)$ are unit Gaussian white noise processes, $0 < \varepsilon \ll 1$ is a small parameter. Approximate moment Lyapunov exponents can be obtained by the method of perturbation ([55], see also [119]), which is given by

$$\Lambda(p) = \varepsilon p\left(-\beta + \frac{p+2}{16}\omega^2\sigma_1^2 + \frac{3p+2}{16}\sigma_2^2\right) + \mathcal{O}(\varepsilon^3). \tag{2.4.2}$$

Equation (2.4.1) can be converted to the Itô differential equations

$$\begin{Bmatrix} x_1 \\ x_2 \end{Bmatrix} = \begin{bmatrix} 0 & 1 \\ -\omega^2 & -\varepsilon\left(2\beta - \frac{1}{2}\sigma_2^2\right) \end{bmatrix}\begin{Bmatrix} x_1 \\ x_2 \end{Bmatrix} \mathrm{d}t + \begin{bmatrix} 0 & 0 \\ -\varepsilon^{1/2}\omega^2\sigma_1 & 0 \end{bmatrix}\begin{Bmatrix} x_1 \\ x_2 \end{Bmatrix} \mathrm{d}W_1(t) + \begin{bmatrix} 0 & 0 \\ 0 & -\varepsilon^{1/2}\sigma_2 \end{bmatrix}\begin{Bmatrix} x_1 \\ x_2 \end{Bmatrix} \mathrm{d}W_2(t), \tag{2.4.3}$$

where $x_1(t)=q(t)$, $x_2(t)=\dot{q}(t)$. It is obvious that system (2.4.3) is of the form (2.2.4) with $d=2, r=2$, and

$$\mathbf{B}_0=\begin{bmatrix} 0 & 1 \\ -\omega^2 & -\varepsilon\left(2\beta-\frac{1}{2}\sigma_2^2\right)\end{bmatrix},\quad \mathbf{B}_1=\begin{bmatrix} 0 & 0 \\ -\varepsilon^{1/2}\omega^2\sigma_1 & 0\end{bmatrix},\quad \mathbf{B}_2=\begin{bmatrix} 0 & 0 \\ 0 & -\varepsilon^{1/2}\sigma_2\end{bmatrix}.$$

Using equation (2.2.10), it can be verified that the set of vectors $\{\mathbf{g}_0, \mathbf{g}_1, \mathbf{g}_2\}$ spans a space with dimension 2 since all $\mathbf{g}_i$, $i=0, 1, 2$, are two dimensional vectors. Thus for $\mathbf{s}\in\mathcal{PJ}^{d-1}$, condition (2.2.8) is satisfied. Therefore the algorithm presented in Section 2.3 can be applied to simulate the moment Lyapunov exponents.

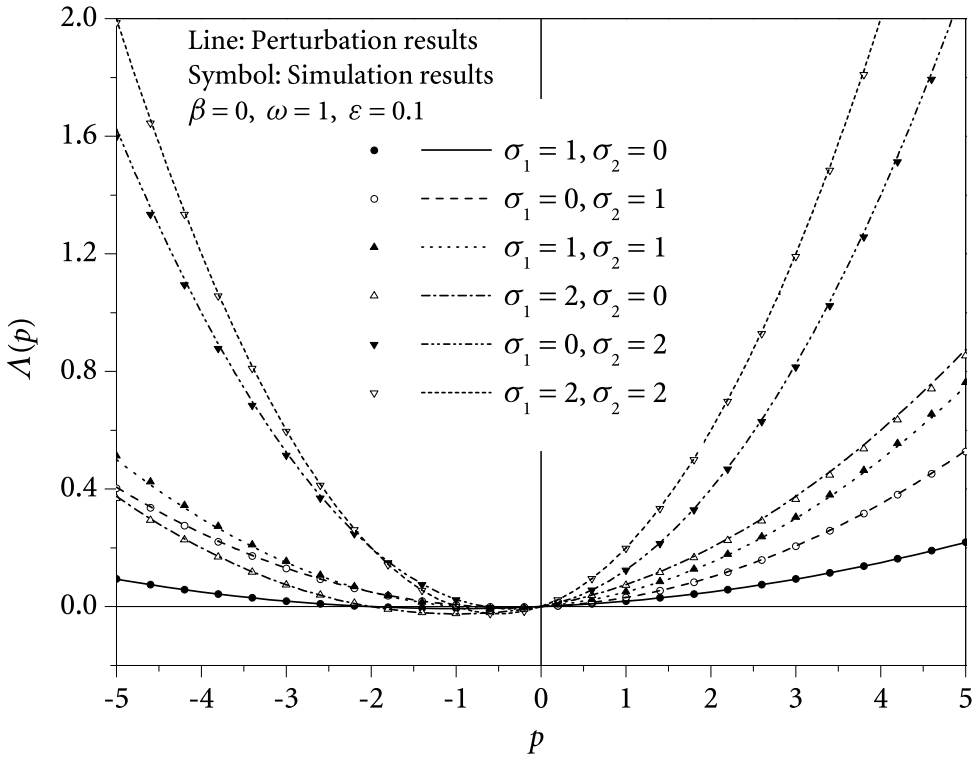

Figure 2.3 Moment Lyapunov exponents under white noise excitation ($\varepsilon=0.1$)

The explicit Euler scheme is applied for the simulation

$$x_1^{k+1}=x_1^k+x_2^k\cdot h,$$

$$x_2^{k+1}=x_2^k+\left[-\omega^2x_1^k-\varepsilon\left(2\beta-\frac{1}{2}\sigma_2^2\right)x_2^k\right]\cdot h-\varepsilon^{1/2}\omega^2\sigma_1x_1^k\cdot\Delta W_1^k-\varepsilon^{1/2}\sigma_2\cdot\Delta W_2^k.$$

The damping coefficient is set to $\beta = 0$, and $\omega = 1$. The sample size is $N = 10000$, time step $h = 0.0001$, and the number of iterations is $MK = 5 \times 10^7$, i.e. the total length of time of simulation is $T = 5000$.

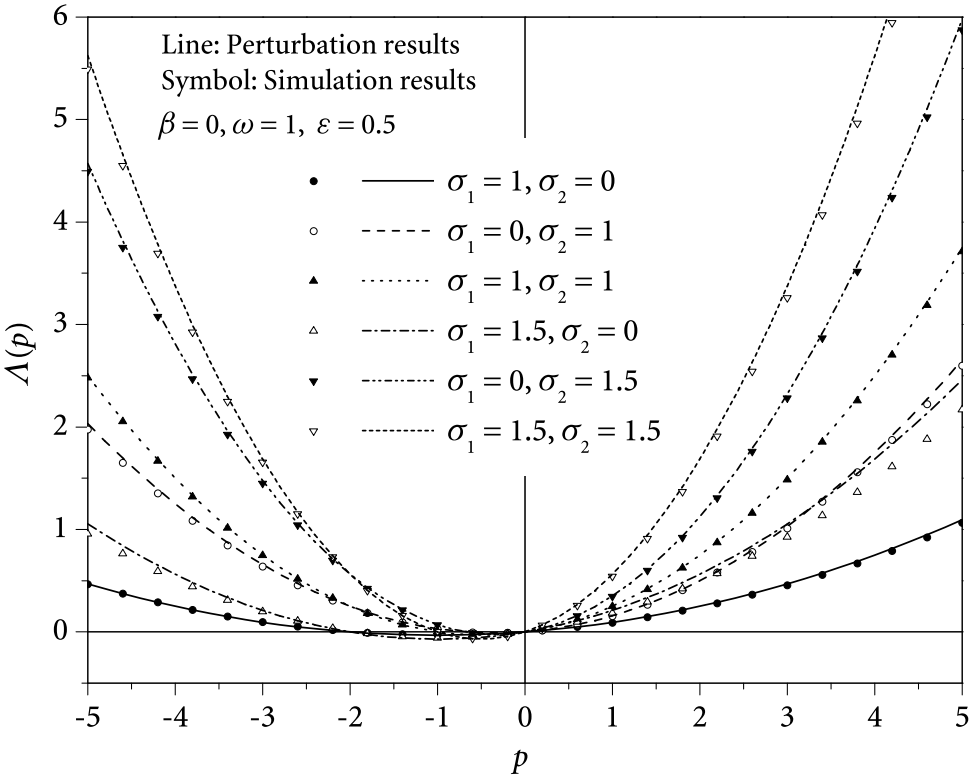

Figure 2.4 Moment Lyapunov exponents under white noise excitation ($\varepsilon = 0.5$)

Figures 2.3 and 2.4 show the comparison of approximate analytical moment Lyapunov exponents given by equation (2.4.2) and the Monte Carlo simulation results for different values of σ_1, σ_2, and ε. It can be seen that the approximate analytical results agree rather well with the simulation results in most cases, implying that the algorithm in Section 2.3 works well as predicted.

To illustrate the asymptotic normality of logarithm of norm, the normalized histograms of $\log \|\mathbf{x}(T)\|$ for some typical values of σ_1 and σ_2 are plotted in Figure 2.5. The correspond-

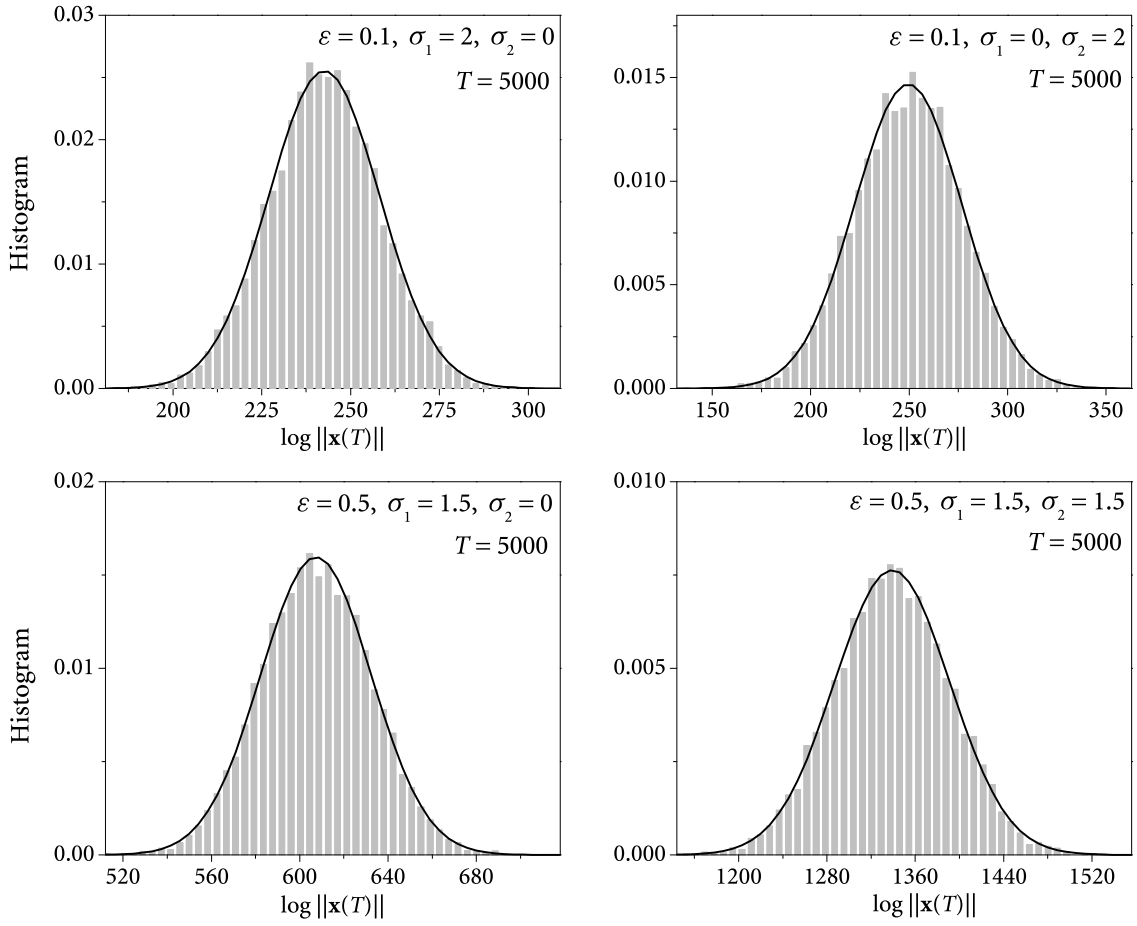

Figure 2.5 Histograms of logarithm of norm compared with normal density approximations under white noise excitation

ing normal density approximations given by

$$\bar{\varphi}(x) = \frac{1}{\sqrt{2\pi}\bar{\sigma}_T^h} \exp\left[-\frac{\left(x-\bar{\mu}_T^h\right)^2}{2\left(\bar{\sigma}_T^h\right)^2}\right], \tag{2.4.4}$$

are also shown in the same figure for comparison. It appears that, as the time of simulation T is large enough, the distribution of $\log\|\mathbf{x}(T)\|$ does approach normal distribution. This is also a complementary evidence that system (2.4.1) is eligible for the new algorithm when simulating the moment Lyapunov exponents.

2.4.2 An Oscillator under Real Noise Excitation

Consider an oscillator under the excitation of real noise or Ornstein-Uhlenbeck process $\zeta(t)$:

$$\begin{aligned} &\ddot{q}(t) + 2\varepsilon\beta\dot{q}(t) + \omega^2\left[1 - \varepsilon^{1/2}\zeta(t)\right]q(t) = 0, \\ &\mathrm{d}\zeta(t) = -\alpha\zeta(t)\,\mathrm{d}t + \sigma\,\mathrm{d}W(t). \end{aligned} \tag{2.4.5}$$

Xie ([116], see also [119]) determined the approximate moment Lyapunov exponents using the method of perturbation as

$$\Lambda(p) = -\varepsilon p\beta + p(p+2)\left[\varepsilon\frac{\sigma^2\omega^2}{16(\alpha^2+4\omega^2)} + \varepsilon^2\frac{(\alpha^4+22\alpha^2\omega^2+48\omega^4)\sigma^4\omega^4}{32\alpha(\alpha^2+\omega^2)(\alpha^2+4\omega^2)^3}\right] + \mathcal{O}(\varepsilon^3). \tag{2.4.6}$$

Obviously, system (2.4.5) can be simulated using the algorithm presented since it takes the form of equation (2.3.6) with $f(x) = \omega^2 - \varepsilon^{1/2}\omega^2 x$.

Letting

$$x_1(t) = q(t), \quad x_2(t) = \dot{q}(t), \quad x_3(t) = \zeta(t), \tag{2.4.7}$$

system (2.4.5) can be converted to the Itô differential equations

$$\begin{Bmatrix} x_1 \\ x_2 \\ x_3 \end{Bmatrix} = \begin{Bmatrix} x_2 \\ -\omega^2 x_1 - 2\varepsilon\beta x_2 + \varepsilon^{1/2}\omega^2 x_3 x_1 \\ -\alpha x_3 \end{Bmatrix}\mathrm{d}t + \begin{Bmatrix} 0 \\ 0 \\ \sigma \end{Bmatrix}\mathrm{d}W(t). \tag{2.4.8}$$

The iteration equations using explicit Euler scheme are then given by

$$\begin{aligned} x_1^{k+1} &= x_1^k + x_2^k \cdot h, \\ x_2^{k+1} &= x_2^k + (-\omega^2 x_1^k - 2\varepsilon\beta x_2^k + \varepsilon^{1/2}\omega^2 x_3^k x_1^k) \cdot h, \\ x_3^{k+1} &= x_3^k - \alpha x_3^k \cdot h + \sigma \cdot \Delta W^k. \end{aligned}$$

The state vector is $(x_1, x_2)^T$, i.e. the norm for evaluating the moment Lyapunov exponents is $\|\mathbf{x}(t)\| = \left(x_1^2+x_2^2\right)^{1/2}$. The sample size for estimating the expected value is $N = 20000$, time step $h = 0.0001$, and the total length of time of simulation is $T = 5000$, i.e. the number of iterations is $MK = 5\times 10^7$.

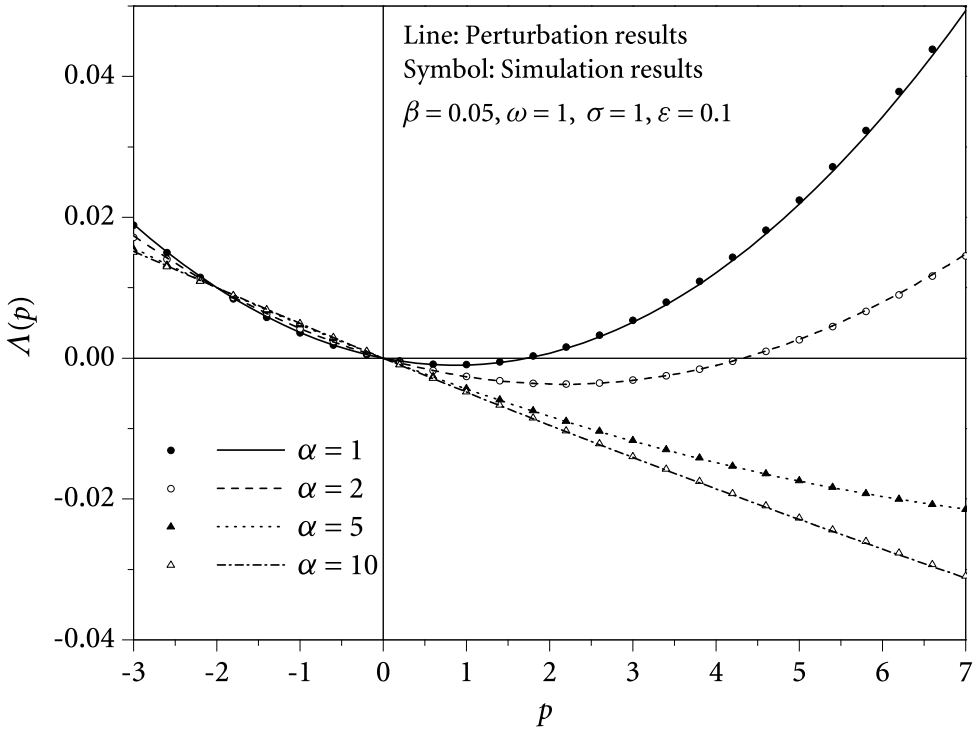

Figure 2.6 Moment Lyapunov exponents under real noise excitation for different α

Figures 2.6 and 2.7 show typical results of the moment Lyapunov exponents for different values of α and σ, with the parameters taken as $\varepsilon = 0.1$, $\beta = 0.05$, $\omega = 1$. It can be seen that when σ is small, i.e. the noise intensity is weak, and for different values of α, the approximate results from the perturbation method agree well with the simulation results. This is reasonable since the analytical approximations are obtained by weak noise expansion of eigenvalue problem governing the moment Lyapunov exponents.

The normalized histograms of $\log\|\mathbf{x}(T)\|$ are plotted in Figure 2.8 with selected values of α and σ. It can be seen that the histograms agree with the normal density functions in all cases; this fact implies that the simulated moment Lyapunov exponents using the algorithm in Section 2.3 are more reliable if the approximated analytical results from perturbation method do not agree well with the simulation results.

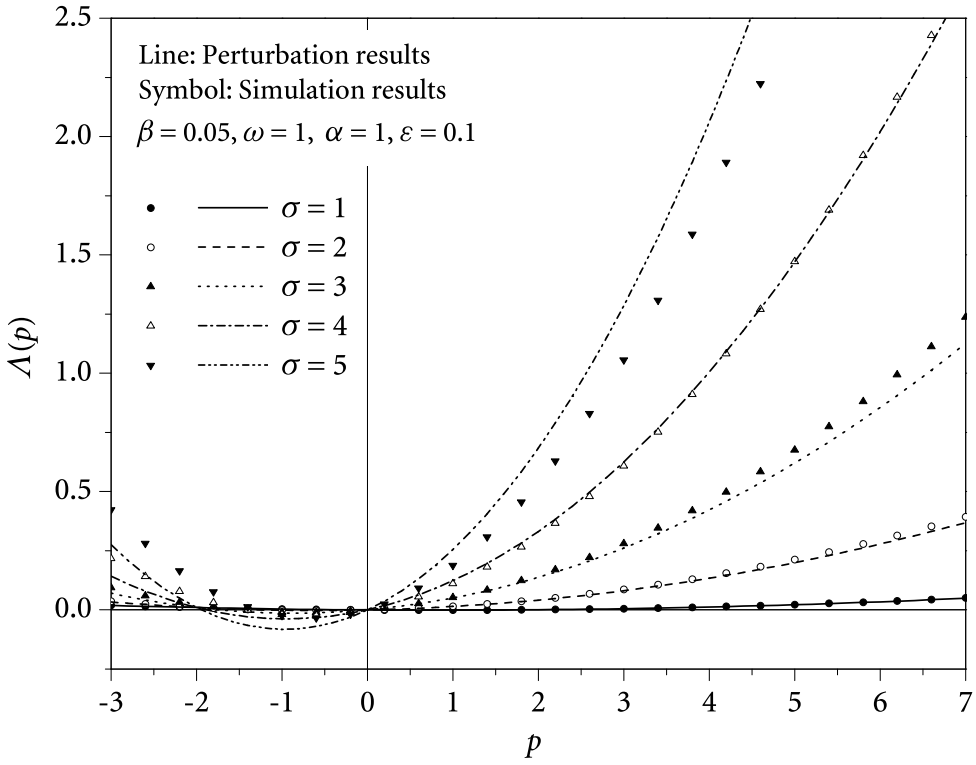

Figure 2.7 Moment Lyapunov exponents under real noise excitation for different σ

2.4.3 An Oscillator under Bounded Noise Excitation

Consider an oscillator under the excitation of bounded noise,

$$\begin{aligned} &\ddot{q}(t) + 2\varepsilon\beta\dot{q}(t) + \omega^2\left[1 - \varepsilon\mu\cos\zeta(t)\right]q(t) = 0, \\ &\mathrm{d}\zeta(t) = \nu\mathrm{d}t + \varepsilon^{1/2}\sigma\,\mathrm{d}W(t). \end{aligned} \tag{2.4.9}$$

Xie ([117], see also [119]) determined the approximate moment Lyapunov exponents using the method of perturbation as

$$\Lambda(p) = -\varepsilon p\beta + \frac{\varepsilon^3 p(p+2)\omega^4\mu^2\sigma^2\left[\nu^2+4(\omega^2-\varepsilon^2\beta^2)+\frac{1}{4}\varepsilon^2\sigma^4\right]}{32(\omega^2-\varepsilon^2\beta^2)\left[\left(2\sqrt{\omega^2-\varepsilon^2\beta^2}+\nu\right)^2+\frac{1}{4}\varepsilon^2\sigma^4\right]\left[\left(2\sqrt{\omega^2-\varepsilon^2\beta^2}-\nu\right)^2+\frac{1}{4}\varepsilon^2\sigma^4\right]}$$
$$+ o(\varepsilon^3) \tag{2.4.10}$$

Similar to the real noise case, condition (2.2.13) is satisfied with $f(x)=\omega^2 - \varepsilon\mu\omega^2 x$ in the form of equation (2.3.6). And the bounded noise $\cos\zeta(t)$ satisfies condition (2.2.12)

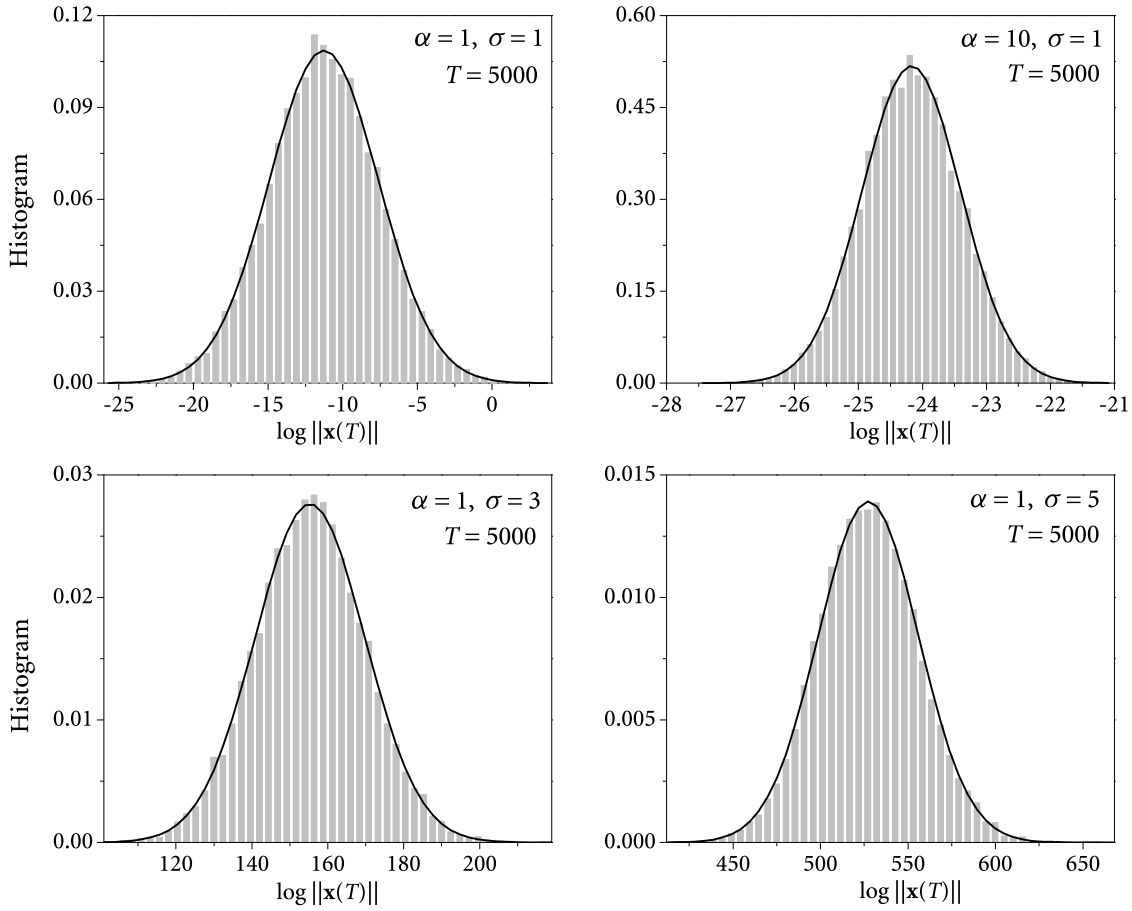

Figure 2.8 Histograms of logarithm of norm compared with normal density approximations under real noise excitation

according to equations (1.3.5) and (1.3.6). Therefore the algorithm presented in Section 2.3 can be applied. Using the same notation as (2.4.7), the Itô differential equations for system (2.4.9) become

$$\begin{Bmatrix} x_1 \\ x_2 \\ x_3 \end{Bmatrix} = \begin{Bmatrix} x_2 \\ -\omega^2 x_1 - 2\varepsilon\beta x_2 + \varepsilon\omega^2 \mu x_1 \cos x_3 \\ \nu \end{Bmatrix} \mathrm{d}t + \begin{Bmatrix} 0 \\ 0 \\ \varepsilon^{1/2}\sigma \end{Bmatrix} \mathrm{d}W(t). \tag{2.4.11}$$

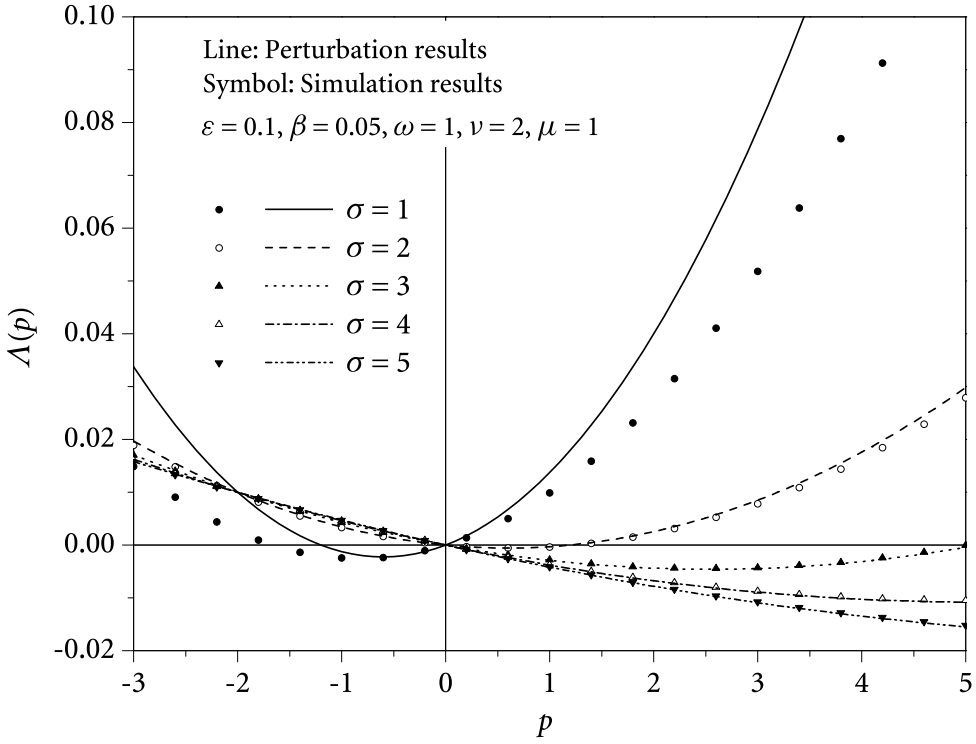

Figure 2.9 Moment Lyapunov exponents under bounded noise excitation for different σ

The iteration equations using explicit Euler scheme are then given by

$$
\begin{aligned}
x_1^{k+1} &= x_1^k + x_2^k \cdot h, \\
x_2^{k+1} &= x_2^k + \left(-\omega^2 x_1^k - 2\varepsilon\beta x_2^k + \varepsilon^{1/2}\omega^2 \mu x_1^k \cos x_3^k \right) \cdot h, \\
x_3^{k+1} &= x_3^k + \nu \cdot h + \varepsilon^{1/2}\sigma \cdot \Delta W^k.
\end{aligned}
$$

The norm for evaluating the moment Lyapunov exponents is $\|\mathbf{x}(t)\| = \left(x_1^2 + x_2^2\right)^{1/2}$. The sample size for estimating the expected value is $N = 20000$, time step $h = 0.0001$, and the total length of time of simulation is $T = 5000$, i.e. the number of iterations is $MK = 5 \times 10^7$.

Typical results of the moment Lyapunov exponents for different values of σ and μ are shown in Figures 2.9 and 2.10, with the parameters taken as $\varepsilon = 0.1$, $\beta = 0.05$, $\omega = 1$, $\nu = 2$. It can be seen that the approximate results from perturbation method agree well with the simulation results for small μ and large σ. This is the result that, in the eigenvalue problem governing the moment Lyapunov exponents, the approximate analysis using perturbation

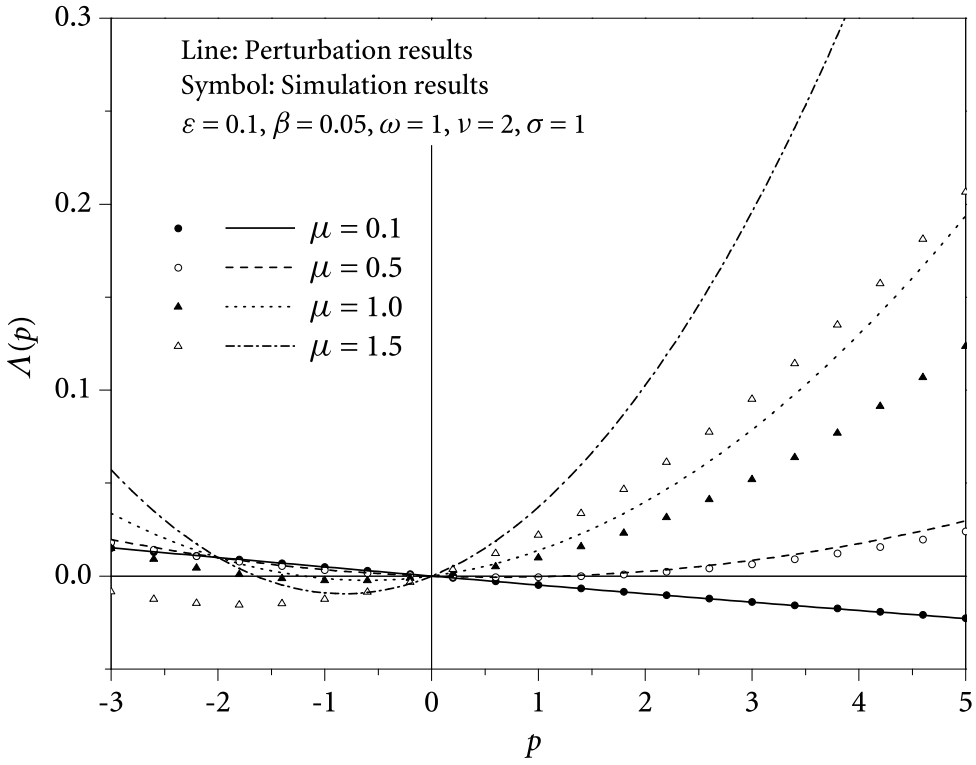

Figure 2.10 Moment Lyapunov exponents under bounded noise excitation for different μ

method requires $\varepsilon\mu$ be small enough and $\varepsilon\sigma^2$ be in the order $\mathcal{O}(1)$. The discrepancy between perturbation and simulation for small σ and relatively large μ shows that some better approximation methods have to be considered.

Figure 2.11 shows the asymptotic normality of $\log\|\mathbf{x}(T)\|$, where the histograms for selected values of μ and σ are plotted and compared with the corresponding normal density approximations. The simulated moment Lyapunov exponents using the algorithm in Section 2.3 and the old algorithm in Section 2.1, which uses the direct sample average of norm as the estimation of moment, are compared in Figure 2.12, with the same values of μ and σ used in Figure 2.11.

It can be seen that, for $\mu = 1$ and $\sigma = 5$, the variance of $\log\|\mathbf{x}(T)\|$ is small and the values of $\|\mathbf{x}(T)\|$ are also small, since $\|\mathbf{x}(T)\| = \exp\{\log\|\mathbf{x}(T)\|\}$, thus direct sample average of

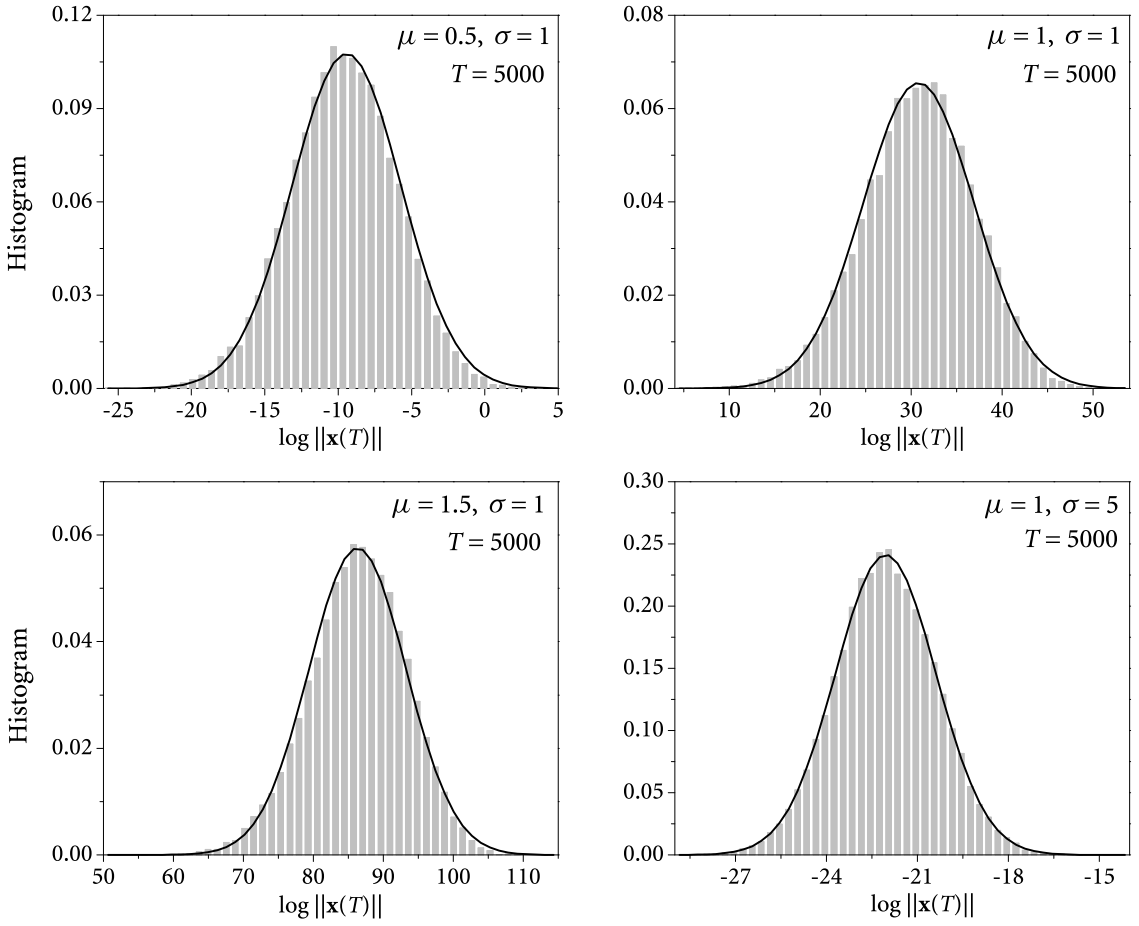

Figure 2.11 Histograms of logarithm of norm compared with normal density approximations under bounded noise excitation

pth norm gives a good estimation of pth moment. As a result, the moment Lyapunov exponents from both algorithms are almost the same in a wide range of p.

When $\mu = 0.5$ and $\sigma = 1$, most samples of $\log\|\mathbf{x}(T)\|$ are negative, this implies that the variance of $\|\mathbf{x}(T)\|$ is small, thus theoretically the sample average of pth norm should be a good estimator of pth moment. However, Figure 2.11 shows that the variance of $\log\|\mathbf{x}(T)\|$ is rather large. Note that the estimated pth moment through the sample average of pth norm is given by

$$\mathrm{E}\Big[\|\mathbf{x}(T)\|^p\Big] = \frac{1}{N}\sum_{s=1}^{N}\|\mathbf{x}^s(T)\|^p = \frac{1}{N}\sum_{s=1}^{N}\exp\Big\{p\log\|\mathbf{x}^s(T)\|\Big\},$$

when different samples of $\|\mathbf{x}^s(T)\|^p$ are summed up, the truncated error due to the finite lengths of floating-point representations will be significant, especially for large $|p|$, just as described in Section 2.1. This effect can be observed clearly from the difference of moment Lyapunov exponents for large $|p|$ in Figure 2.12.

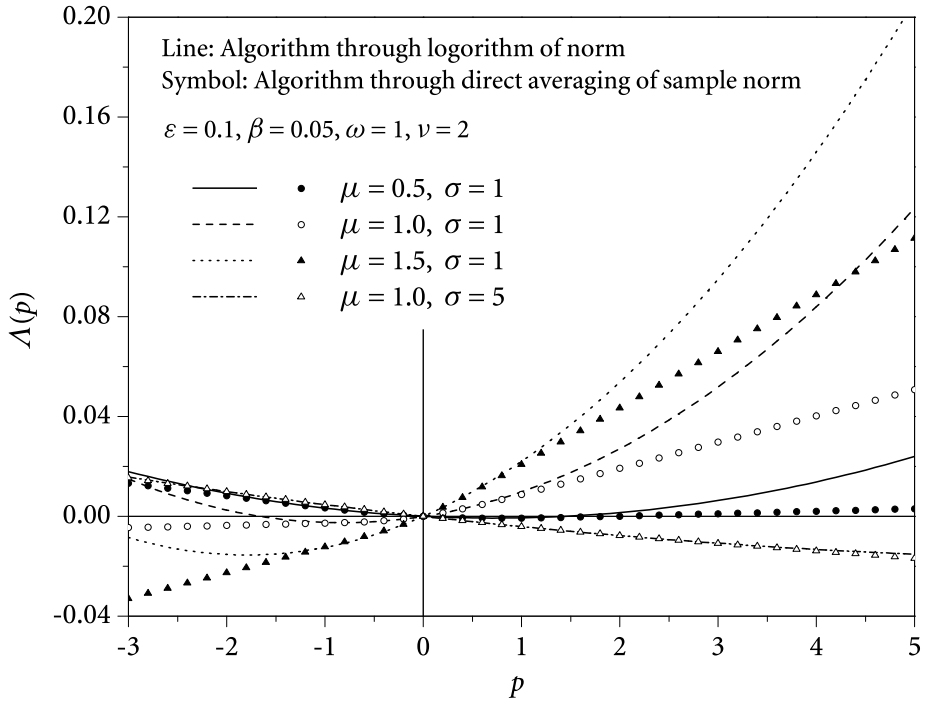

Figure 2.12 Comparison of algorithms for simulation of moment Lyapunov exponents

In the other two cases, i.e. $\mu = 1$, $\mu = 1.5$, and $\sigma = 1$, it is obvious that the values and the variances of $\|\mathbf{x}(T)\|$ are all extremely large, therefore the estimation of pth moment of $\|\mathbf{x}(T)\|$ in the old algorithm is not accurate for large p, and correspondingly the simulated moment Lyapunov exponents can only be trusted for small values of p.

2.5 Summary

Contrary to intuition, Monte Carlo simulation of moment Lyapunov exponents of stochastic dynamical systems is a very challenging topic. Because the solution of a system grows

exponentially when it is unstable and decays exponentially when it is stable, float-point overflow or underflow renders "brute-force" approaches inapplicable. Furthermore, because the variance of the solution may grow with time, it is very challenging to obtain an accurate estimation of the moments with finite sample size.

For linear homogeneous stochastic dynamical systems satisfying some conditions, the limit distribution of the logarithm of norm of the solution is normal. The mean value and variance of the logarithm of norm, combined with normalization of the solution, can be used to reduce the possible large variance of the solution so that the pth moment can be estimated. Numerical examples illustrated in Section 2.4 show that this approach gives a better numerical approximation than the previous method [118], which uses the direct sample average of norm as the estimation of expectation.

CHAPTER 3

Stochastic Stability of SDOF Linear Viscoelastic Systems

As shown in Section 1.4, the general equations of motion for linear viscoelastic systems are integro-partial differential equations, which are generally difficult to solve, and the stability of their solutions are not easy to determine. In applications, it may be possible to derive a simpler form of equations, say integro-ordinary differential equations, when considering the boundary conditions. In this way, studying the stability properties of the solutions may be easier.

3.1 An Example of SDOF Linear Viscoelastic System

Consider an elastic beam under dynamical axial compressive load $P(t)$. It is known that the equation of motion is given by

$$\rho A \frac{\partial^2 v}{\partial t^2} + \beta_0 \frac{\partial v}{\partial t} + EI \frac{\partial^4 v}{\partial x^4} + P(t) \frac{\partial^2 v}{\partial x^2} = 0,$$

where $v(x,t)$ is the transverse deflection of the beam, x the axial coordinate, ρA the mass per unit length of the beam, β_0 the damping constant, and EI the flexural rigidity of the beam.

Since the term including EI is associated with the constitutive relation, the equation of motion for the viscoelastic case becomes, using equation (1.4.3),

$$\rho A\frac{\partial^2 v}{\partial t^2}+\beta_0\frac{\partial v}{\partial t}+EI(1-\mathscr{H})\frac{\partial^4 v}{\partial x^4}+P(t)\frac{\partial^2 v}{\partial x^2}=0, \tag{3.1.1}$$

where the material relaxation operator $\mathscr{H}$ is taken as

$$\mathscr{H}\{u(t)\}=\int_0^t H(t-s)\,u(s)\,\mathrm{d}s, \tag{3.1.2}$$

in which $H(t)$ is the relaxation function describing the property of viscoelasticity.

If the beam is simply supported, the transverse deflection can be expressed as

$$v(x,t)=\sum_{n=1}^{\infty}q_n(t)\sin\frac{n\pi x}{L}. \tag{3.1.3}$$

Substituting equation (3.1.3) into (3.1.1) leads to the equations of motion

$$\ddot{q}_n(t)+2\beta\dot{q}_n(t)+\omega_n^2\left[1-\frac{P(t)}{P_n}-\mathscr{H}\right]q_n(t)=0,\quad n=1,\,2,\,\ldots, \tag{3.1.4}$$

where

$$\beta=\frac{\beta_0}{2\rho A},\quad \omega_n^2=\frac{EI}{\rho A}\left(\frac{n\pi}{L}\right)^4,\quad P_n=EI\left(\frac{n\pi}{L}\right)^2.$$

If only the nth mode is considered, and the damping, viscoelastic effect, and the amplitude of load are all small, the equation of motion of a single degree-of-freedom (SDOF) system can be written as, by introducing a small parameter ε,

$$\ddot{q}(t)+2\varepsilon\beta\dot{q}(t)+\omega^2\left\{\left[1+\varepsilon^{1/2}\xi(t)\right]q(t)-\varepsilon\int_0^t H(t-s)q(s)\mathrm{d}s\right\}=0. \tag{3.1.5}$$

The presence of small parameter ε is reasonable since damping and noise perturbation are small in many engineering applications. Moreover, the memory effect of many materials used in structural engineering is not too strong, therefore the viscoelasticity is also considered to be weak.

The almost-sure stability of viscoelastic systems has been investigated by some researchers. For example, Ariaratnam [1] studied the almost-sure stability of a SDOF linear viscoelastic system subjected to random fluctuation in the stiffness parameter by evaluating the largest Lyapunov exponent using the method of stochastic averaging for integro-differential equations due to Larionov [69]. Potapov [90] studied the almost-sure stability of

a viscoelastic column under the excitation of a random wide-band stationary process using Lyapunov's direct method. Potapov [91] described the behaviour of stochastic viscoelastic systems by numerical evaluation of Lyapunov exponents of linear integro-differential equations.

However, as described in Chapter 1, almost-sure stability cannot assure moment stability for non-autonomous systems. Therefore it is important to study the moment stability of SDOF linear viscoelastic systems (3.1.5) in terms of moment Lyapunov exponents.

For small ε such that $\omega^2-\varepsilon^2\beta^2>0$, letting

$$q(t) = x(t)\mathrm{e}^{-\varepsilon\beta t}, \tag{3.1.6}$$

the damping term in equation (3.1.5) can be removed to yield

$$\ddot{x}(t) + \tilde{\omega}^2\left\{\left[1+\varepsilon^{1/2}\tilde{\xi}(t)\right]x(t) - \varepsilon\int_0^t \tilde{H}(t-s)x(s)\,\mathrm{d}s\right\} = 0, \tag{3.1.7}$$

where

$$\tilde{\omega}^2 = \omega^2-\varepsilon^2\beta^2, \quad \tilde{\xi}(t) = \frac{\omega^2}{\omega^2-\varepsilon^2\beta^2}\xi(t), \quad \tilde{H}(t) = \frac{\omega^2}{\omega^2-\varepsilon^2\beta^2}\mathrm{e}^{-\varepsilon\beta t}h(t).$$

It is easy to verify that the moment Lyapunov exponents of systems (3.1.5) and (3.1.7) are related as

$$\Lambda_{q(t)}(p) = -\varepsilon p\beta + \Lambda_{x(t)}(p). \tag{3.1.8}$$

Therefore, without loss of generality, the stochastic stability of the SDOF viscoelastic system

$$\ddot{q}(t) + \omega^2\left\{\left[1+\varepsilon^{1/2}\xi(t)\right]q(t) - \varepsilon\int_0^t H(t-s)q(s)\,\mathrm{d}s\right\} = 0 \tag{3.1.9}$$

may be considered by determining its pth moment Lyapunov exponent.

3.2 Stability under Wide-band Noise Excitation

Consider the case that $\xi(t)$ in equation (3.1.9) is a wide-band stationary noise with zero mean. In this section, the method of averaging, both first-order and second-order, will be applied to obtain the differential equations governing the pth moment. The moment stability of viscoelastic system (3.1.9) can then be determined by solving the averaged equations.

As stated in Section 1.2, the solution of the averaged system (1.2.13) converges weakly to the solution of the original system (1.2.11) only in time scale of order $1/\varepsilon^2$ as $\varepsilon \to 0$. The definition of moment Lyapunov exponents requires to consider the moments of solutions as time approaches infinity, in this sense the results from the averaging method may not be close to the true results. Although this limitation exists, the averaging method still provides a way to simplify the generally more complicated systems and to obtain the corresponding properties as an approximation. Moreover, considering that the integral operator $\mathscr{H}$ has the low-pass property, i.e. it has the effect of depressing the fast-varying components, one can expect that the averaging method leads to a good approximation in the stability analysis of viscoelastic systems. On the other hand, numerical approaches for the original systems may also be applied. Combining the results from the averaging method and numerical approaches, it is possible to understand the behaviour of original systems.

3.2.1 First-Order Stochastic Averaging

In order to use the method of stochastic averaging to investigate system (3.1.9), the following transformation is applied

$$q(t) = a(t)\cos\Phi(t), \quad \dot{q}(t) = -\omega a(t)\sin\Phi(t), \quad \Phi(t) = \omega t + \varphi(t). \tag{3.2.1}$$

From the first two equations of (3.2.1), one has

$$\dot{a}(t)\cos\Phi(t) - a(t)\dot{\varphi}(t)\sin\Phi(t) = 0. \tag{3.2.2}$$

Substituting (3.2.1) into system (3.1.9) yields

$$\begin{aligned}&\dot{a}(t)\sin\Phi(t) + a(t)\dot{\varphi}(t)\cos\Phi(t)\\ &\qquad = -\varepsilon^{1/2}\omega\xi(t)a(t)\cos\Phi(t) - \varepsilon\omega\int_0^t H(t-s)a(s)\cos\Phi(s)\,\mathrm{d}s.\end{aligned} \tag{3.2.3}$$

Letting $P = a^p$, it is easy to see that P is the pth norm of system (3.1.9). Thus from equations (3.2.2) and (3.2.3), $P(t)$ and $\varphi(t)$ can be solved as

$$\begin{Bmatrix}\dot{P}(t)\\ \dot{\varphi}(t)\end{Bmatrix} = \varepsilon\mathbf{F}^{(1)}(P,\varphi,t) + \varepsilon^{1/2}\mathbf{F}^{(0)}(P,\varphi,\xi,t), \tag{3.2.4}$$

where

$$\mathbf{F}^{(1)}(P,\varphi,t)=\begin{Bmatrix}-\omega pI_h P(t)\sin\Phi(t)\\ -\omega I_h\cos\Phi(t)\end{Bmatrix}=\begin{Bmatrix}F_1^{(1)}(P,\varphi,t)\\ F_2^{(1)}(P,\varphi,t)\end{Bmatrix},$$

$$\mathbf{F}^{(0)}(P,\varphi,\xi,t)=\begin{Bmatrix}\frac{1}{2}\omega pP(t)\xi(t)\sin 2\Phi(t)\\ \frac{1}{2}\omega\xi(t)\big[1+\cos 2\Phi(t)\big]\end{Bmatrix}=\begin{Bmatrix}F_1^{(0)}(P,\varphi,\xi,t)\\ F_2^{(0)}(P,\varphi,\xi,t)\end{Bmatrix},$$

$$I_h=\int_0^t H(t-s)\left[\frac{P(s)}{P(t)}\right]^{1/p}\cos\Phi(s)\,\mathrm{d}s.$$

Then system (3.2.4) can be approximated by the following averaged equations

$$\mathrm{d}\begin{Bmatrix}\bar{P}(t)\\ \bar{\varphi}(t)\end{Bmatrix}=\varepsilon\begin{Bmatrix}\bar{m}_P\\ \bar{m}_\varphi\end{Bmatrix}\mathrm{d}t+\varepsilon^{1/2}\bar{\boldsymbol{\sigma}}\,\mathrm{d}\mathbf{W}(t),\tag{3.2.5}$$

where

$$\bar{m}_P=\underset{t}{\mathscr{M}}\left\{F_1^{(1)}(P,\varphi,t)+\int_{-\infty}^0\mathrm{E}\left[\frac{\partial F_1^{(0)}}{\partial P}F_{1\tau}^{(0)}+\frac{\partial F_1^{(0)}}{\partial\varphi}F_{2\tau}^{(0)}\right]\mathrm{d}\tau\right\},$$

$$\bar{m}_\varphi=\underset{t}{\mathscr{M}}\left\{F_2^{(1)}(P,\varphi,t)+\int_{-\infty}^0\mathrm{E}\left[\frac{\partial F_2^{(0)}}{\partial P}F_{1\tau}^{(0)}+\frac{\partial F_2^{(0)}}{\partial\varphi}F_{2\tau}^{(0)}\right]\mathrm{d}\tau\right\},$$

$$\left[\bar{\boldsymbol{\sigma}}\bar{\boldsymbol{\sigma}}^T\right]_{ij}=\underset{t}{\mathscr{M}}\left\{\int_{-\infty}^{\infty}\mathrm{E}\left[F_i^{(0)}F_{j\tau}^{(0)}\right]\mathrm{d}\tau\right\},\quad i,j=1,2,$$

$$\underset{t}{\mathscr{M}}\{\cdot\}=\lim_{T\to\infty}\frac{1}{T}\int_0^T\{\cdot\}\,\mathrm{d}t,$$

$$F_{j\tau}^{(0)}=F_j^{(0)}\big(P,\varphi,\xi(t+\tau),t+\tau\big),\quad j=1,2.$$

Noting that equations (3.2.4) are integro-differential equations, the averaging method for integro-differential equations [69] should also be applied. That is to say, in order to simplify the system, the method of stochastic averaging due to Khasminskii is used to obtain the approximate Itô stochastic differential equations, and the averaging method for integro-differential equations due to Larionov is used to obtain the approximate drift terms in the Itô equations in which the viscoelastic terms are involved.

When applying the averaging operation, $P(t)$ and $\varphi(t)$ are treated as unchanged, i.e. they are replaced by $\bar{P}$ and $\bar{\varphi}$ directly. Now consider $\bar{m}_P$ first. By substituting in the corresponding terms one has

$$\bar{m}_P = -\omega p\bar{P}\underset{t}{\mathscr{M}}\left\{I_h^{\mathrm{sc}}\right\} + \frac{1}{4}\omega^2 p\bar{P}\underset{t}{\mathscr{M}}\left\{J_1\right\},$$

where

$$I_h^{\mathrm{sc}} = \sin\Phi(t)\int_0^t H(t-s)\cos\Phi(s)\,\mathrm{d}s,$$

$$J_1 = \int_{-\infty}^0 R(\tau)\Big\{p\sin 2\Phi(t)\sin 2\Phi(t+\tau) + 2\cos 2\Phi(t)\big[1+\cos 2\Phi(t+\tau)\big]\Big\}\,\mathrm{d}\tau,$$

and $R(\tau)=\mathrm{E}\big[\xi(t)\xi(t+\tau)\big]$ is the correlation function of the wide-band noise $\xi(t)$.

Observing that conditions (1.4.4) are required, i.e. $H(t)$ and $t\cdot H(t)$ are integrable over $[0,\infty)$, then applying the transformation $s=t-\tau$ and changing the order of integration lead to

$$\begin{aligned}
\underset{t}{\mathscr{M}}\left\{I_h^{\mathrm{sc}}\right\} &= \lim_{T\to\infty}\frac{1}{T}\int_{t=0}^T\int_{s=0}^t H(t-s)\cos\Phi(s)\sin\Phi(t)\,\mathrm{d}s\,\mathrm{d}t\\
&= \lim_{T\to\infty}\frac{1}{T}\int_{t=0}^T\int_{\tau=0}^t H(\tau)\sin\Phi(t)\cos\Phi(t-\tau)\,\mathrm{d}\tau\,\mathrm{d}t\\
&= \lim_{T\to\infty}\frac{1}{2T}\int_{\tau=0}^T\int_{t=\tau}^T H(\tau)\big[\sin(2\omega t-\omega\tau+2\bar{\varphi})+\sin\omega\tau\big]\,\mathrm{d}t\,\mathrm{d}\tau\\
&= \frac{1}{2}\int_0^\infty H(\tau)\sin\omega\tau\,\mathrm{d}\tau = \frac{1}{2}\mathscr{H}^s(\omega).
\end{aligned}$$

Similarly, it can be shown that

$$\underset{t}{\mathscr{M}}\left\{\cos\Phi(t)\int_0^t H(t-s)\cos\Phi(s)\,\mathrm{d}s\right\} = \frac{1}{2}\mathscr{H}^c(\omega),$$

where

$$\mathscr{H}^s(\omega) = \int_0^\infty H(\tau)\sin\omega\tau\,\mathrm{d}\tau \qquad \text{and} \qquad \mathscr{H}^c(\omega) = \int_0^\infty H(\tau)\cos\omega\tau\,\mathrm{d}\tau \tag{3.2.6}$$

are the sine and cosine transformations of the viscoelastic kernel function $H(t)$.

On the other hand,

$$\begin{aligned}\underset{t}{\mathscr{M}}\{J_1\} &= \lim_{T\to\infty}\frac{p+2}{2T}\int_{t=0}^{T}\int_{\tau=-\infty}^{0} R(\tau)\cos 2\omega\tau\,\mathrm{d}\tau\,\mathrm{d}t \\ &\quad + \lim_{T\to\infty}\frac{1}{T}\int_{t=0}^{T}\int_{\tau=-\infty}^{0} R(\tau)\Big[\frac{2-p}{2}\cos(4\omega t+2\omega\tau+4\bar{\varphi}) \\ &\qquad\qquad + 2\cos(2\omega t+2\bar{\varphi})\Big]\mathrm{d}\tau\,\mathrm{d}t \\ &= \frac{p+2}{2}\int_{\tau=-\infty}^{0} R(\tau)\cos 2\omega\tau\,\mathrm{d}\tau = \frac{p+2}{4}S(2\omega),\end{aligned}$$

where the cosine and sine power spectral density functions of noise $\xi(t)$ are given by

$$\begin{aligned}S(\omega) &= \int_{-\infty}^{\infty} R(\tau)\cos\omega\tau\,\mathrm{d}\tau = 2\int_{0}^{\infty} R(\tau)\cos\omega\tau\,\mathrm{d}\tau = 2\int_{-\infty}^{0} R(\tau)\cos\omega\tau\,\mathrm{d}\tau, \\ \Psi(\omega) &= 2\int_{0}^{\infty} R(\tau)\sin\omega\tau\,\mathrm{d}\tau = -2\int_{-\infty}^{0} R(\tau)\sin\omega\tau\,\mathrm{d}\tau.\end{aligned} \tag{3.2.7}$$

Similarly, $\bar{m}_\varphi$ and $\left[\bar{\boldsymbol{\sigma}}\bar{\boldsymbol{\sigma}}^T\right]_{ij}$ can be evaluated to yield

$$\begin{aligned}&\bar{m}_P = \omega p\bar{P}\left[-\frac{1}{2}\mathcal{H}^s(\omega)+\frac{p+2}{16}\omega S(2\omega)\right], \qquad \bar{m}_\varphi = -\omega\left[\frac{1}{2}\mathcal{H}^c(\omega)+\frac{1}{8}\omega\Psi(2\omega)\right], \\ &\left[\bar{\boldsymbol{\sigma}}\bar{\boldsymbol{\sigma}}^T\right]_{11} = b_{11} = \frac{1}{8}\omega^2p^2\bar{P}^2S(2\omega), \qquad \left[\bar{\boldsymbol{\sigma}}\bar{\boldsymbol{\sigma}}^T\right]_{12} = \left[\bar{\boldsymbol{\sigma}}\bar{\boldsymbol{\sigma}}^T\right]_{21} = 0, \\ &\left[\bar{\boldsymbol{\sigma}}\bar{\boldsymbol{\sigma}}^T\right]_{22} = b_{22} = \frac{1}{8}\omega^2\big[2S(0)+S(2\omega)\big].\end{aligned} \tag{3.2.8}$$

Noting that the transition probability density function for the solution of the averaged equation is the solution of the Fokker-Planck equation, which depends on the diffusion matrix $\bar{\boldsymbol{\sigma}}\bar{\boldsymbol{\sigma}}^T$ but not every single element $\bar{\sigma}_{ij}$, thus one can take

$$\bar{\sigma}_{12} = \bar{\sigma}_{21} = 0, \quad \bar{\sigma}_{11} = \sqrt{b_{11}} = \omega p\bar{P}\sqrt{\frac{S(2\omega)}{8}}, \quad \bar{\sigma}_{22} = \sqrt{b_{22}} = \omega\sqrt{\frac{2S(0)+S(2\omega)}{8}}. \tag{3.2.9}$$

Finally the averaged Itô differential equations are

$$\mathrm{d}\bar{P} = \varepsilon\omega p\bar{P}\left[-\frac{1}{2}\mathcal{H}^s(\omega) + \frac{p+2}{16}\omega S(2\omega)\right]\mathrm{d}t + \varepsilon^{1/2}\omega p\bar{P}\sqrt{\frac{S(2\omega)}{8}}\mathrm{d}W_1(t), \tag{3.2.10}$$

$$\mathrm{d}\bar{\varphi} = -\varepsilon\omega\left[\frac{1}{2}\mathcal{H}^c(\omega) + \frac{1}{8}\omega\Psi(2\omega)\right]\mathrm{d}t + \varepsilon^{1/2}\omega\sqrt{\frac{2S(0)+S(2\omega)}{8}}\mathrm{d}W_2(t). \tag{3.2.11}$$

It can be seen that $\bar{P}(t)$ does not depend on $\bar{\varphi}(t)$; therefore it can be solved independently. The property of independent increment of Wiener process indicates that the expectation of the second term in equation (3.2.10) is zero. Therefore taking the expected value on both sides of eqation (3.2.10) yields

$$\mathrm{dE}\big[\bar{P}\big] = \varepsilon\omega p\left[-\frac{1}{2}\mathcal{H}^s(\omega) + \frac{p+2}{16}\omega S(2\omega)\right]\mathrm{E}\big[\bar{P}\big]\mathrm{d}t. \tag{3.2.12}$$

From equation (3.2.12) it is easy to obtain the moment Lyapunov exponents for the averaged system by

$$\Lambda(p) = \lim_{t\to\infty}\frac{\log \mathrm{E}\left[\bar{P}\right]}{t} = \varepsilon\omega p\left[-\frac{1}{2}\mathcal{H}^s(\omega) + \frac{p+2}{16}\omega S(2\omega)\right], \tag{3.2.13}$$

and the Lyapunov exponent is given by

$$\lambda = \Lambda'(0) = \varepsilon\omega\left[-\frac{1}{2}\mathcal{H}^s(\omega) + \frac{1}{8}\omega S(2\omega)\right]. \tag{3.2.14}$$

From equations (3.2.13) and (3.2.14) it is clear that the viscoelasticity helps to stabilize the system, whereas noises destabilize the system. The stronger the noise, the more unstable the system. The boundaries for almost-sure stability and pth moment stability are determined by $\lambda = 0$ and $\Lambda(p) = 0$, respectively.

Equations (3.2.13) and (3.2.14) show that, in the first-order approximation, the stability of the averaged system (3.2.5) is determined by the power spectral density of the wide-band random excitation at 2ω. Using equations (1.3.1) and (1.3.3), the pth moment Lyapunov exponent for *Gaussian white noise* model is reduced to

$$\Lambda(p) = \varepsilon\omega p\left[-\frac{1}{2}\mathcal{H}^s(\omega) + \frac{p+2}{16}\omega\sigma^2\right], \tag{3.2.15}$$

and that for *real noise* model becomes

$$\Lambda(p) = \varepsilon\omega p\left[-\frac{1}{2}\mathcal{H}^s(\omega) + \frac{p+2}{16}\frac{\omega\sigma^2}{\alpha^2+4\omega^2}\right]. \tag{3.2.16}$$

A general choice of viscoelastic kernel function is, according to equation (1.4.6) of generalized Maxwell model,

$$H(t) = \sum_{j=1}^{M} \gamma_j \mathrm{e}^{-\kappa_j t}. \tag{3.2.17}$$

Its sine and cosine transformations are given by

$$\mathcal{H}^s(\omega) = \sum_{j=1}^{M} \frac{\omega\gamma_j}{\kappa_j^2 + \omega^2}, \qquad \mathcal{H}^c(\omega) = \sum_{j=1}^{M} \frac{\gamma_j\kappa_j}{\kappa_j^2 + \omega^2}. \tag{3.2.18}$$

Thus, from equations (3.2.13) and (3.2.14), when

$$S(2\omega) < \sum_{j=1}^{M} \frac{4\gamma_j}{\kappa_j^2 + \omega^2},$$

system (3.2.5) is asymptotically stable almost-surely. When

$$S(2\omega) < \sum_{j=1}^{M} \frac{8\gamma_j}{(p+2)(\kappa_j^2+\omega^2)},$$

the pth moment of system (3.2.5) is asymptotically stable. These results indicate that the stronger the viscoelastic effect (i.e. larger γ), the wider the stability region; the larger the relaxation time (i.e. smaller κ), the wider the stability region.

3.2.2 Second-Order Stochastic Averaging

The first-order stochastic averaging may not be adequate in some applications. Similar to deterministic systems, higher-order averaging may be applied to obtain better approximations. Hijawi *et al.* [48] studied the dynamic response of nonlinear elastic structure under random load using both the first-order and the second-order stochastic averaging methods. Lin and Cai [74] also presented several examples where some terms in equations may not be small enough. In this section, a second-order averaging method is applied and the results are compared with those obtained using the first-order averaging.

Rewrite equations (3.2.4) as

$$\begin{Bmatrix} \dot{P}(t) \\ \dot{\varphi}(t) \end{Bmatrix} = \varepsilon \begin{Bmatrix} f_1 \\ f_2 \end{Bmatrix} + \varepsilon^{1/2} \begin{Bmatrix} g_1 \\ g_2 \end{Bmatrix}, \tag{3.2.19}$$

where

$$f_1 = -\omega pP \int_0^t H(t-s) \left[\frac{P(s)}{P(t)}\right]^{1/p} \sin(\omega t+\varphi)\cos(\omega s+\varphi)\,\mathrm{d}s,$$

$$f_2 = -\omega \int_0^t H(t-s) \left[\frac{P(s)}{P(t)}\right]^{1/p} \cos(\omega t+\varphi)\cos(\omega s+\varphi)\,\mathrm{d}s,$$

$$g_1 = \frac{1}{2}\omega pP\xi(t)\sin(2\omega t+2\varphi),$$

$$g_2 = \frac{1}{2}\omega\xi(t)\big[1+\cos(2\omega t+2\varphi)\big].$$

Let

$$P(t) = \bar{P}(t) + \varepsilon P_1(\bar{P},\bar{\varphi},t), \qquad \varphi(t) = \bar{\varphi}(t) + \varepsilon\varphi_1(\bar{P},\bar{\varphi},t), \tag{3.2.20}$$

where $\bar{P}(t)$ and $\bar{\varphi}(t)$, as will be shown, are the results of the first-order averaging and will be determined later. Differentiating equations (3.2.20) with respect to time t yields

$$\begin{Bmatrix} \dot{P} \\ \dot{\varphi} \end{Bmatrix} = \mathbf{A} \begin{Bmatrix} \dot{\bar{P}} \\ \dot{\bar{\varphi}} \end{Bmatrix} + \varepsilon \begin{Bmatrix} \dfrac{\partial P_1}{\partial t} \\ \dfrac{\partial \varphi_1}{\partial t} \end{Bmatrix}, \tag{3.2.21}$$

where

$$\mathbf{A} = \begin{bmatrix} 1+\varepsilon\dfrac{\partial P_1}{\partial \bar{P}} & \varepsilon\dfrac{\partial P_1}{\partial \bar{\varphi}} \\ \varepsilon\dfrac{\partial \varphi_1}{\partial \bar{P}} & 1+\varepsilon\dfrac{\partial \varphi_1}{\partial \bar{\varphi}} \end{bmatrix}.$$

It is easy to check that

$$\mathbf{A}^{-1} = \begin{bmatrix} 1-\varepsilon\dfrac{\partial P_1}{\partial \bar{P}} & -\varepsilon\dfrac{\partial P_1}{\partial \bar{\varphi}} \\ -\varepsilon\dfrac{\partial \varphi_1}{\partial \bar{P}} & 1-\varepsilon\dfrac{\partial \varphi_1}{\partial \bar{\varphi}} \end{bmatrix} + o(\varepsilon). \tag{3.2.22}$$

Substituting equations (3.2.21) and (3.2.22) into equation (3.2.19) yields

$$\begin{aligned}\begin{Bmatrix}\dot{\bar{P}}\\ \dot{\bar{\varphi}}\end{Bmatrix} &= \varepsilon\mathbf{A}^{-1}\begin{Bmatrix}f_1-\dfrac{\partial P_1}{\partial t}\\ f_2-\dfrac{\partial \varphi_1}{\partial t}\end{Bmatrix}+\varepsilon^{1/2}\mathbf{A}^{-1}\begin{Bmatrix}g_1\\ g_2\end{Bmatrix}\\ &= \varepsilon\begin{Bmatrix}f_1-\dfrac{\partial P_1}{\partial t}\\ f_2-\dfrac{\partial \varphi_1}{\partial t}\end{Bmatrix}+\varepsilon^2\begin{Bmatrix}-\dfrac{\partial P_1}{\partial \bar{P}}\Big(f_1-\dfrac{\partial P_1}{\partial t}\Big)-\dfrac{\partial P_1}{\partial \bar{\varphi}}\Big(f_2-\dfrac{\partial \varphi_1}{\partial t}\Big)\\ -\dfrac{\partial \varphi_1}{\partial \bar{P}}\Big(f_1-\dfrac{\partial P_1}{\partial t}\Big)-\dfrac{\partial \varphi_1}{\partial \bar{\varphi}}\Big(f_2-\dfrac{\partial \varphi_1}{\partial t}\Big)\end{Bmatrix}\\ &\quad+\varepsilon^{1/2}\begin{Bmatrix}g_1\\ g_2\end{Bmatrix}+\varepsilon^{3/2}\begin{Bmatrix}-\dfrac{\partial P_1}{\partial \bar{P}}g_1-\dfrac{\partial P_1}{\partial \bar{\varphi}}g_2\\ -\dfrac{\partial \varphi_1}{\partial \bar{P}}g_1-\dfrac{\partial \varphi_1}{\partial \bar{\varphi}}g_2\end{Bmatrix}+o\big(\varepsilon^2\big).\end{aligned}\tag{3.2.23}$$

Expanding f_1, f_2, g_1 and g_2 at $\bar{P}$ and $\bar{\varphi}$ leads to

$$\begin{aligned}f_1 &= -\omega p\left[\bar{P}I^{sc}+\varepsilon P_1 I^{sc}+\varepsilon\bar{P}\varphi_1(I^{cc}-I^{ss})\right]-\varepsilon\omega\bar{P}J^{sc}+o(\varepsilon),\\ f_2 &= -\omega\left[I^{cc}-\varepsilon\varphi_1(I^{cs}+I^{sc})\right]-\varepsilon\frac{\omega}{p}J^{cc}+o(\varepsilon),\\ g_1 &= \frac{1}{2}\omega p\bar{P}\xi(t)\sin(2\omega t+2\bar{\varphi})\\ &\quad+\varepsilon\omega p\xi(t)\left[\frac{P_1}{2}\sin(2\omega t+2\bar{\varphi})+\bar{P}\varphi_1\cos(2\omega t+2\bar{\varphi})\right]+o(\varepsilon),\\ g_2 &= \frac{1}{2}\omega\xi(t)\big[1+\cos(2\omega t+2\bar{\varphi})\big]-\varepsilon\omega\varphi_1\xi(t)\sin(2\omega t+2\bar{\varphi})+o(\varepsilon),\end{aligned}$$

where

$$\begin{aligned}I^{cc} &= \int_0^t H(t-s)\left[\frac{\bar{P}(s)}{\bar{P}(t)}\right]^{1/p}\cos(\omega t+\bar{\varphi})\cos(\omega s+\bar{\varphi})\,\mathrm{d}s,\\ I^{ss} &= \int_0^t H(t-s)\left[\frac{\bar{P}(s)}{\bar{P}(t)}\right]^{1/p}\sin(\omega t+\bar{\varphi})\sin(\omega s+\bar{\varphi})\,\mathrm{d}s,\\ I^{cs} &= \int_0^t H(t-s)\left[\frac{\bar{P}(s)}{\bar{P}(t)}\right]^{1/p}\cos(\omega t+\bar{\varphi})\sin(\omega s+\bar{\varphi})\,\mathrm{d}s,\\ I^{sc} &= \int_0^t H(t-s)\left[\frac{\bar{P}(s)}{\bar{P}(t)}\right]^{1/p}\sin(\omega t+\bar{\varphi})\cos(\omega s+\bar{\varphi})\,\mathrm{d}s,\end{aligned}$$

$$J^{cc} = \int_0^t H(t-s)\left[\frac{\bar{P}(s)}{\bar{P}(t)}\right]^{1/p}\left[\frac{P_1}{\bar{P}(s)} - \frac{P_1}{\bar{P}(t)}\right]\cos(\omega t+\bar{\varphi})\cos(\omega s+\bar{\varphi})\,\mathrm{d}s,$$

$$J^{sc} = \int_0^t H(t-s)\left[\frac{\bar{P}(s)}{\bar{P}(t)}\right]^{1/p}\left[\frac{P_1}{\bar{P}(s)} - \frac{P_1}{\bar{P}(t)}\right]\sin(\omega t+\bar{\varphi})\cos(\omega s+\bar{\varphi})\,\mathrm{d}s.$$

Thus equation (3.2.23) can be written as

$$\begin{Bmatrix}\dot{\bar{P}}\\ \dot{\bar{\varphi}}\end{Bmatrix} = \varepsilon\begin{Bmatrix}f_1^*\\ f_2^*\end{Bmatrix} + \varepsilon^2\begin{Bmatrix}f_1^{**}\\ f_2^{**}\end{Bmatrix} + \varepsilon^{1/2}\begin{Bmatrix}g_1^*\\ g_2^*\end{Bmatrix} + \varepsilon^{3/2}\begin{Bmatrix}g_1^{**}\\ g_2^{**}\end{Bmatrix} + o\big(\varepsilon^2\big), \tag{3.2.24}$$

where

$$\begin{aligned}
f_1^* &= -\omega p\bar{P}I^{sc} - \frac{\partial P_1}{\partial t}, \qquad f_2^* = -\omega I^{cc} - \frac{\partial \varphi_1}{\partial t},\\
g_1^* &= \frac{1}{2}\omega p\bar{P}\xi(t)\sin(2\omega t+2\bar{\varphi}), \qquad g_2^* = \frac{1}{2}\omega\xi(t)\big[1+\cos(2\omega t+2\bar{\varphi})\big],\\
f_1^{**} &= -\frac{\partial P_1}{\partial \bar{P}}f_1^* - \frac{\partial P_1}{\partial \bar{\varphi}}f_2^* - \omega\left[pP_1I^{sc} + p\bar{P}\varphi_1(I^{cc}-I^{ss}) + \bar{P}J^{sc}\right],\\
f_2^{**} &= -\frac{\partial \varphi_1}{\partial \bar{P}}f_1^* - \frac{\partial \varphi_1}{\partial \bar{\varphi}}f_2^* + \omega\left[\varphi_1(I^{cs}+I^{sc}) - \frac{1}{p}J^{cc}\right],\\
g_1^{**} &= -\frac{\partial P_1}{\partial \bar{P}}g_1^* - \frac{\partial P_1}{\partial \bar{\varphi}}g_2^* + \omega p\xi(t)\left[\frac{P_1}{2}\sin(2\omega t+2\bar{\varphi}) + \bar{P}\varphi_1\cos(2\omega t+2\bar{\varphi})\right],\\
g_2^{**} &= -\frac{\partial \varphi_1}{\partial \bar{P}}g_1^* - \frac{\partial \varphi_1}{\partial \bar{\varphi}}g_2^* - \omega\varphi_1\xi(t)\sin(2\omega t+2\bar{\varphi}).
\end{aligned} \tag{3.2.25}$$

From Section 3.2.1, it is known that

$$\underset{t}{\mathscr{M}}\left\{I^{sc}\right\} = \frac{1}{2}\mathcal{H}^s(\omega),$$

in which $\bar{P}$ is treated as a constant under the averaging operation. The first-order term in the $\bar{P}$ equation of (3.2.24) is given by f_1^*, which, after averaging, should be the same as the result of the first-order averaging. Setting f_1^* to the averaged result of the deterministic term in the P equation of (3.2.4), i.e. $\underset{t}{\mathscr{M}}\left\{F_1^{(1)}\right\}$ in $\bar{m}_P$ of equation (3.2.5), one obtains

$$\frac{\partial P_1}{\partial t} = -\omega p\bar{P}\left[I^{sc} - \frac{1}{2}\mathcal{H}^s(\omega)\right].$$

When $\bar{P}$ is treated as a constant in I^{sc}, it can be seen that

$$\begin{aligned} I^{sc} - \frac{1}{2}\mathcal{H}^s(\omega) &= \int_0^t H(t-s)\sin(\omega t+\bar{\varphi})\cos(\omega s+\bar{\varphi})\,\mathrm{d}s - \frac{1}{2}\int_0^\infty H(\tau)\sin\omega\tau\,\mathrm{d}\tau \\ &= \int_0^t H(\tau)\sin(\omega t+\bar{\varphi})\cos(\omega t-\omega\tau+\bar{\varphi})\,\mathrm{d}\tau - \frac{1}{2}\int_0^\infty H(\tau)\sin\omega\tau\,\mathrm{d}\tau \\ &= \frac{1}{2}\int_0^\infty H(\tau)\sin(2\omega t-\omega\tau+2\bar{\varphi})\,\mathrm{d}\tau - \int_t^\infty H(\tau)\sin(\omega t+\bar{\varphi})\cos(\omega t-\omega\tau+\bar{\varphi})\,\mathrm{d}\tau, \end{aligned} \tag{3.2.26}$$

and

$$\left|\int_t^\infty H(\tau)\sin(\omega t+\bar{\varphi})\cos(\omega t-\omega\tau+\bar{\varphi})\,\mathrm{d}\tau\right| \leqslant \int_t^\infty \left|H(\tau)\right|\mathrm{d}\tau.$$

From conditions (1.4.4), $H(t)$ is absolutely integrable over $[0,\infty)$, this means the second integral in equation (3.2.26) tends to zero as t approaches to infinity. Therefore one can choose approximately

$$\begin{aligned} \frac{\partial P_1}{\partial t} &= -\frac{1}{2}\omega p\bar{P}\int_0^\infty H(\tau)\sin(2\omega t-\omega\tau+2\bar{\varphi})\big|\,\mathrm{d}\tau \\ &= -\frac{1}{2}\omega p\bar{P}\left[\mathcal{H}^c(\omega)\sin(2\omega t+2\bar{\varphi}) - \mathcal{H}^s(\omega)\cos(2\omega t+2\bar{\varphi})\right], \end{aligned}$$

i.e.

$$P_1 = \frac{1}{4}p\bar{P}\left[\mathcal{H}^c(\omega)\cos(2\omega t+2\bar{\varphi}) + \mathcal{H}^s(\omega)\sin(2\omega t+2\bar{\varphi})\right]. \tag{3.2.27}$$

Similarly, noticing that

$$\frac{\partial\varphi_1}{\partial t} = -\omega\left[I^{cc} - \frac{1}{2}\mathcal{H}^c(\omega)\right],$$

it can be set approximately

$$\frac{\partial\varphi_1}{\partial t} = -\frac{1}{2}\omega\left[\mathcal{H}^c(\omega)\cos(2\omega t+2\bar{\varphi}) + \mathcal{H}^s(\omega)\sin(2\omega t+2\bar{\varphi})\right],$$

or

$$\varphi_1 = \frac{1}{4}\left[\mathcal{H}^s(\omega)\cos(2\omega t+2\bar{\varphi}) - \mathcal{H}^c(\omega)\sin(2\omega t+2\bar{\varphi})\right]. \tag{3.2.28}$$

Since P_1 and φ_1 have been determined, equation (3.2.24) can be simplified by substituting equations (3.2.27) and (3.2.28) into equations (3.2.25), and then the stochastic averaging

method can be performed for equation (3.2.24) as in Section 3.2.1. Thus following the same procedure as the first-order averaging, after some tedious deduction, the averaged version of equations (3.2.24) is given by, still denoted by $\bar{P}$ and $\bar{\varphi}$,

$$\begin{aligned} \mathrm{d}\bar{P} &= \bar{m}_P^* \,\mathrm{d}t + \bar{\sigma}_{11}^* \,\mathrm{d}W_1 + \bar{\sigma}_{12}^* \,\mathrm{d}W_2, \\ \mathrm{d}\bar{\varphi} &= \bar{m}_\varphi^* \,\mathrm{d}t + \bar{\sigma}_{21}^* \,\mathrm{d}W_1 + \bar{\sigma}_{22}^* \,\mathrm{d}W_2, \end{aligned} \tag{3.2.29}$$

where higher-order terms have been neglected, and

$$\bar{m}_P^* = \varepsilon\omega p\bar{P}\left[-\frac{1}{2}\mathcal{H}^s(\omega) + \frac{p+2}{16}\omega S(2\omega)\right] + \varepsilon^2\frac{p\,(p+2)}{16}\omega^2\bar{P}\mathcal{H}^c(\omega)S(2\omega),$$

$$\bar{m}_\varphi^* = \varepsilon\omega\left[-\frac{1}{2}\mathcal{H}^c(\omega) - \frac{1}{8}\omega\Psi(2\omega)\right] + \varepsilon^2\frac{1}{8}\omega\left\{-\left[\mathcal{H}^c(\omega)\right]^2 - \left[\mathcal{H}^s(\omega)\right]^2 - \omega\mathcal{H}^c(\omega)\Psi(2\omega)\right\},$$

$$b_{11}^* = \left[\bar{\boldsymbol{\sigma}}^*\bar{\boldsymbol{\sigma}}^{*T}\right]_{11} = \frac{1}{8}\omega^2 p^2\bar{P}^2 S(2\omega)\left[\varepsilon + \varepsilon^2\mathcal{H}^c(\omega)\right],$$

$$b_{12}^* = \left[\bar{\boldsymbol{\sigma}}^*\bar{\boldsymbol{\sigma}}^{*T}\right]_{12} = b_{21}^* = \left[\bar{\boldsymbol{\sigma}}^*\bar{\boldsymbol{\sigma}}^{*T}\right]_{21} = 0,$$

$$b_{22}^* = \left[\bar{\boldsymbol{\sigma}}^*\bar{\boldsymbol{\sigma}}^{*T}\right]_{22} = \frac{1}{8}\omega^2\left[S(2\omega) + 2S(0)\right]\left[\varepsilon + \varepsilon^2\mathcal{H}^c(\omega)\right].$$

Similar to the first-order averaging, it can be set that $\bar{\sigma}_{12}^* = \bar{\sigma}_{21}^* = 0$ and thus

$$\bar{\sigma}_{11}^* = \sqrt{b_{11}^*} = \omega p\bar{P}\sqrt{\frac{1}{8}S(2\omega)\left[\varepsilon + \varepsilon^2\mathcal{H}^c(\omega)\right]},$$

$$\bar{\sigma}_{22}^* = \sqrt{b_{22}^*} = \omega\sqrt{\frac{1}{8}\left[S(2\omega) + 2S(0)\right]\left[\varepsilon + \varepsilon^2\mathcal{H}^c(\omega)\right]}.$$

Therefore by taking the expectation on both sides of the Itô differential equation for $\bar{P}$ in (3.2.29) one has

$$\mathrm{d}\mathrm{E}\left[\bar{P}\right] = \left\{\varepsilon\omega p\left[-\frac{1}{2}\mathcal{H}^s(\omega) + \frac{p+2}{16}\omega S(2\omega)\right] + \varepsilon^2\frac{p(p+2)}{16}\omega^2\mathcal{H}^c(\omega)S(2\omega)\right\}\mathrm{E}\left[\bar{P}\right]\mathrm{d}t,$$

and the pth moment Lyapunov exponent, including the second-order term, is

$$\Lambda(p) = \varepsilon\omega p\left[-\frac{1}{2}\mathcal{H}^s(\omega) + \frac{p+2}{16}\omega S(2\omega)\right] + \varepsilon^2\frac{p(p+2)}{16}\omega^2\mathcal{H}^c(\omega)S(2\omega). \tag{3.2.30}$$

Obviously, the largest Lyapunov exponent from the second-order averaging is given by

$$\lambda = \varepsilon\omega\left[-\frac{1}{2}\mathcal{H}^s(\omega) + \frac{1}{8}\omega S(2\omega)\right] + \varepsilon^2\frac{1}{8}\omega^2\mathcal{H}^c(\omega)S(2\omega). \tag{3.2.31}$$

3.2.3 Numerical Results and Discussion

In order to check the accuracy of the approximate results obtained by the method of stochastic averaging, Monte Carlo simulation is applied to compute the moment Lyapunov exponents.

In the Monte Carlo simulation, the viscoelastic kernel function takes the form of equation (1.4.6), i.e.

$$H(t) = \sum_{j=1}^{M} \gamma_j \mathrm{e}^{-\kappa_j t}.$$

Two different models of wide-band noise approximation, i.e. Gaussian white noise and real noise, will be discussed separately.

Case I: The wide-band noise is taken as the simplest model, i.e. Gaussian white noise (1.3.1).

Letting

$$x_1(t) = q(t), \quad x_2(t) = \dot{q}(t), \quad x_{j+2}(t) = \int_0^t \gamma_j \mathrm{e}^{-\kappa_j(t-s)} q(s)\,\mathrm{d}s, \quad j = 1, 2, \cdots, M, \tag{3.2.32}$$

equation (3.1.5) can be written as an $(M+2)$ degrees-of-freedom system of Itô differential equations

$$\mathrm{d}\begin{Bmatrix} x_1 \\ x_2 \\ x_3 \\ \vdots \\ x_{M+2} \end{Bmatrix} = \begin{bmatrix} 0 & 1 & 0 & 0 & 0 \\ -\omega^2 & -2\varepsilon\beta & \varepsilon\omega^2 & \cdots & \varepsilon\omega^2 \\ \gamma_1 & 0 & -\kappa_1 & 0 & 0 \\ \vdots & 0 & 0 & \ddots & 0 \\ \gamma_M & 0 & 0 & 0 & -\kappa_M \end{bmatrix} \begin{Bmatrix} x_1 \\ x_2 \\ x_3 \\ \vdots \\ x_{M+2} \end{Bmatrix} \mathrm{d}t + \begin{Bmatrix} 0 \\ -\varepsilon^{1/2}\sigma\omega^2 x_1 \\ 0 \\ \vdots \\ 0 \end{Bmatrix} \mathrm{d}W(t). \tag{3.2.33}$$

Equation (3.2.33) is linear homogeneous. It can be verified that the algorithm introduced in Section 2.3 can be applied to simulate the moment Lyapunov exponents. The norm for evaluating the moment Lyapunov exponents is $\|\mathbf{x}(t)\| = \sqrt{x_1^2 + x_2^2 + \cdots + x_{M+2}^2}$. The

iteration equations are given by, using the explicit Euler scheme,

$$
\begin{aligned}
x_1^{k+1} &= x_1^k + x_2^k \cdot h, \\
x_2^{k+1} &= x_2^k + \Big(-\omega^2 x_1^k - 2\varepsilon\beta x_2^k + \varepsilon\omega^2 \sum_{j=1}^{M} x_{j+2}^k \Big) h - \varepsilon^{1/2}\sigma\omega^2 x_1^k \cdot \Delta W^k, \\
x_j^{k+1} &= x_j^k + \big(\gamma_j x_1^k - \kappa_j x_{j+2}^k\big) h, \qquad j = 1, 2, \cdots, M.
\end{aligned}
\tag{3.2.34}
$$

with h being the time step and k denoting the kth iteration.

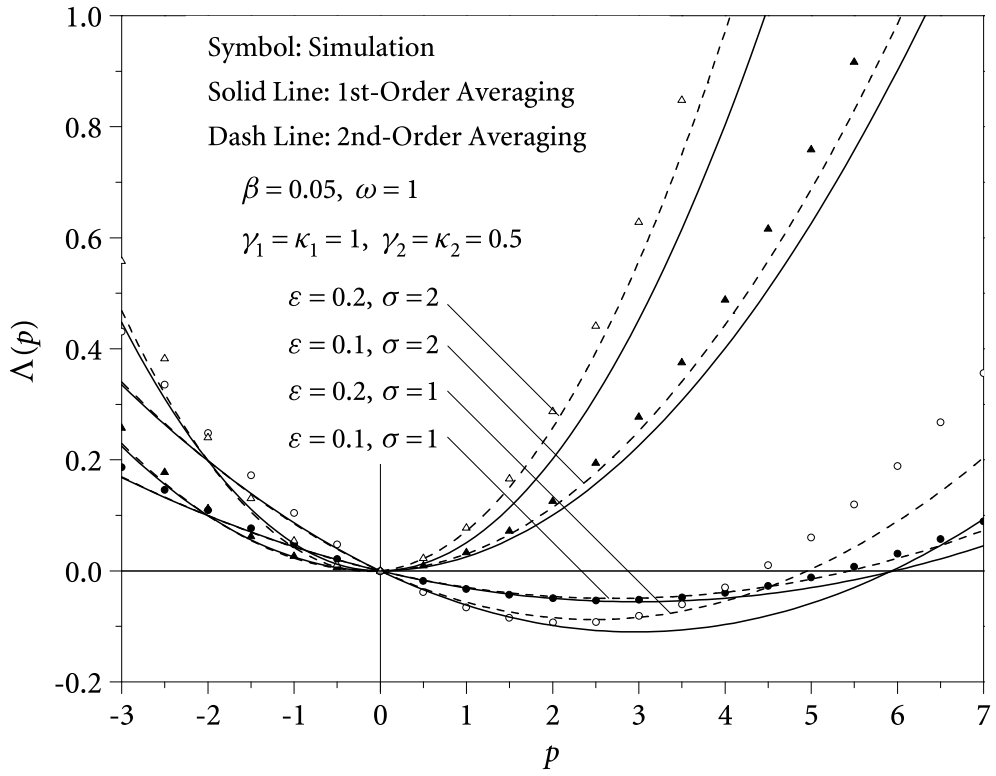

Figure 3.1 Moment Lyapunov exponents under white noise excitation for different ε and σ

Figure 3.1 shows typical results of the moment Lyapunov exponents for different values of ε and σ, where the parameters are taken as $\beta = 0.05, M = 2, \gamma_1 = \kappa_1 = 1, \gamma_2 = \kappa_2 = 0.5, \omega = 1$. The analytical results from the first-order and the second-order averaging are also included in the figure. In Monte Carlo simulation, the sample size for estimating the expected value

is $N=5000$, time step is $h=0.0001$, and the total length of time for simulation is $T=5000$, i.e. the number of iteration is 5×10^7.

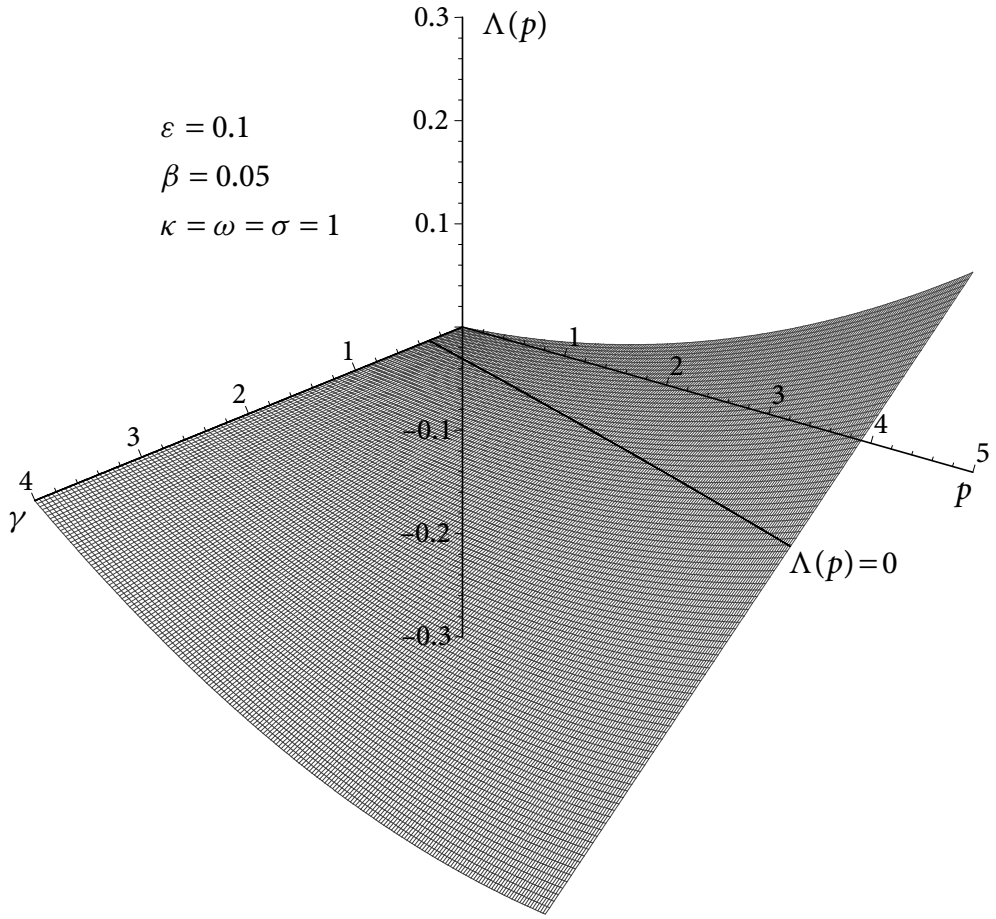

Figure 3.2 Moment Lyapunov exponents under white noise excitation

It can be seen that the first-order averaging results agree with the simulation results very well when ε and σ are small, i.e. the intensity of noise is weak. The second-order averaging does give a better approximation. As shown in equations (3.2.14) and (3.2.15), when the intensity of noise σ increases, the system becomes more and more unstable in the sense that the largest Lyapunov exponents and moment Lyapunov exponents (for $p>0$) increase.

Figures 3.2 and 3.3 illustrate the variation of moment Lyapunov exponents from second-order averaging with respect to the viscoelastic characteristic parameters γ and κ. The curves $\Lambda(p)=0$ give the boundaries of the moment stability. The pth moments for $p>0$

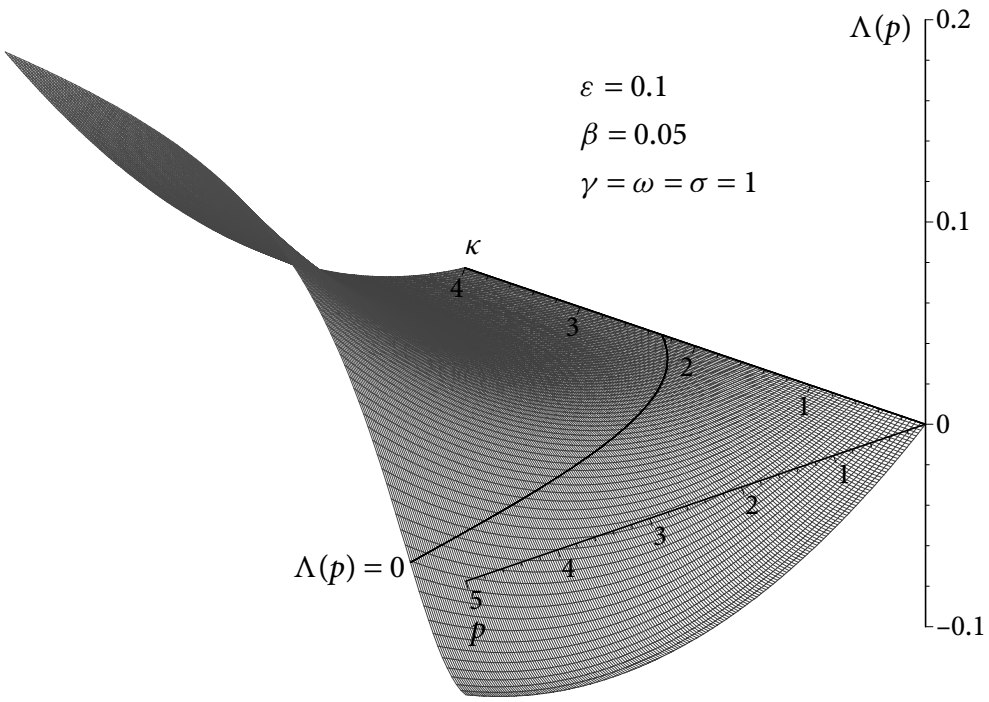

Figure 3.3 Moment Lyapunov exponents under white noise excitation

are of interest in application. As the figures show, with the increase of viscoelastic intensity γ, the stability region for $p>0$ becomes wider, which indicates that the viscoelasticity helps to stabilize the system. Moreover, when κ increases, i.e. when the relaxation time of viscoelasticity decreases, the stability region for $p>0$ becomes narrower, implying that larger relaxation time helps to stabilize the system.

Case II: The wide-band noise is approximated by a real noise, the Ornstein-Uhlenbeck process, given by equation (1.3.2).

Denoting

$$x_1(t)=q(t),\quad x_2(t)=\dot{q}(t),\quad x_{j+2}(t)=\int_0^t \gamma_j \mathrm{e}^{-\kappa_j(t-s)}q(s)\,\mathrm{d}s,\quad j=1,2,\cdots,M,$$
$$x_{M+3}(t)=\xi(t), \tag{3.2.35}$$

equation (3.1.5) is converted to the Itô differential equations

$$\mathrm{d}\begin{Bmatrix} x_1 \\ x_2 \\ x_3 \\ \vdots \\ x_{M+2} \\ x_{M+3} \end{Bmatrix} = \begin{bmatrix} 0 & 1 & 0 & 0 & 0 & 0 \\ -\omega^2 & -2\varepsilon\beta & \varepsilon\omega^2 & \cdots & \varepsilon\omega^2 & -\varepsilon^{1/2}\omega^2 x_1 \\ \gamma_1 & 0 & -\kappa_1 & 0 & 0 & 0 \\ \vdots & 0 & 0 & \ddots & 0 & 0 \\ \gamma_M & 0 & 0 & 0 & -\kappa_M & 0 \\ 0 & 0 & 0 & 0 & 0 & -\alpha \end{bmatrix} \begin{Bmatrix} x_1 \\ x_2 \\ x_3 \\ \vdots \\ x_{M+2} \\ x_{M+3} \end{Bmatrix} \mathrm{d}t + \begin{Bmatrix} 0 \\ 0 \\ 0 \\ 0 \\ 0 \\ \sigma \end{Bmatrix} \mathrm{d}W(t). \tag{3.2.36}$$

Thus the discretized equations using explicit Euler scheme are

$$\begin{aligned} x_1^{k+1} &= x_1^k + x_2^k \cdot h, \\ x_2^{k+1} &= x_2^k + \Big(-\omega^2 x_1^k - 2\varepsilon\beta x_2^k + \varepsilon\omega^2 \sum_{j=1}^{M} x_{j+2}^k - \varepsilon^{1/2}\omega^2 x_1^k x_{M+3}^k\Big) \cdot h, \\ x_{j+2}^{k+1} &= x_{j+2}^k + \big(\gamma_j x_1^k - \kappa_j x_{j+2}^k\big) \cdot h, \qquad j = 1, 2, \cdots, M, \\ x_{M+3}^{k+1} &= x_{M+3}^k + \big(-\alpha x_{M+3}^k\big) \cdot h + \sigma \cdot \Delta W^k. \end{aligned} \tag{3.2.37}$$

The norm for evaluating the moment Lyapunov exponents is $\|\mathbf{x}(t)\| = \sqrt{x_1^2 + x_2^2 + \cdots + x_{M+2}^2}$, and the algorithm presented in Section 2.3 is applied to simulate the moment Lyapunov exponents.

The moment Lyapunov exponents for different values of viscoelastic parameters are plotted in Figures 3.4 and 3.5, with $\varepsilon = 0.1$, $\beta = 0.05$, $\omega = \alpha = \sigma = 1$, and $M = 2$. Other parameters for numerical iterations are the same as for the case of Gaussian white noise. Figure 3.4 shows that the stronger the viscoelasticity (i.e. larger γ_j), the more stable the system, and larger relaxation times (i.e. smaller κ_j) make the system more stable as shown in Figure 3.5. These conclusions are indicated by equation (3.2.16) and are the same as the case of Gaussian white noise excitation.

Figures 3.4 and 3.5 also indicate that the second-order averaging method does not improve the accuracy of approximation significantly. Therefore the approximate results from the first-order averaging are acceptable in engineering applications.

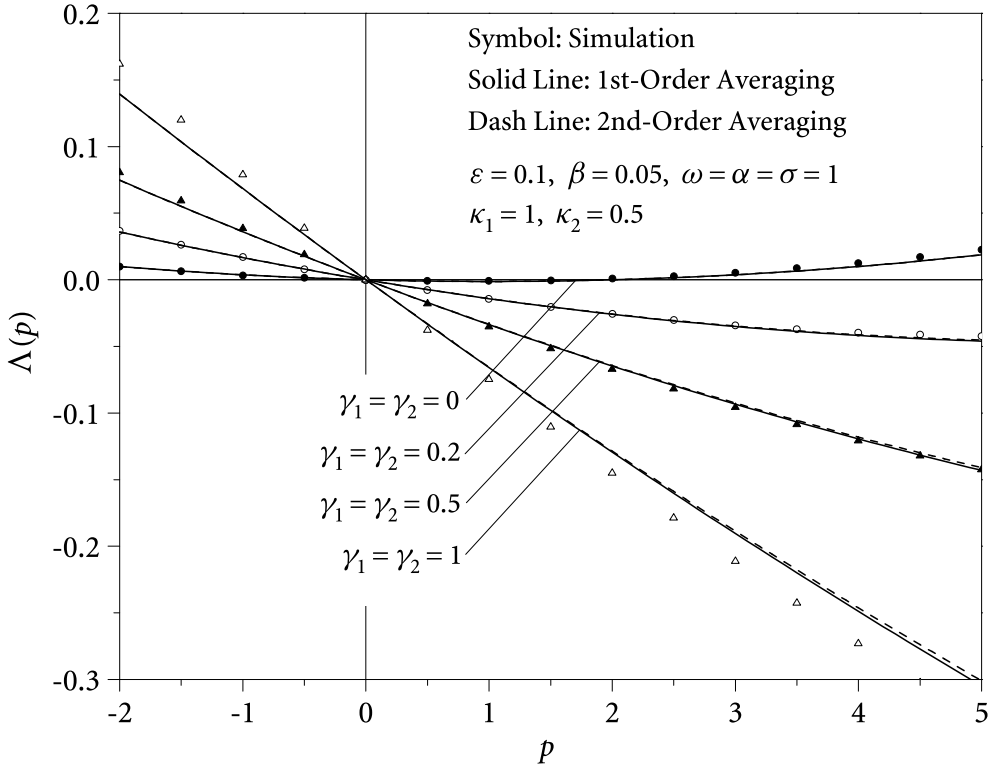

Figure 3.4 Moment Lyapunov exponents under real noise excitation for different γ

Figure 3.6 shows the comparison of moment Lyapunov exponents for different values of α, with $\varepsilon = 0.1, \beta = 0.05, M = 2, \gamma_1 = 1, \kappa_1 = 2, \gamma_2 = \kappa_2 = \omega = 1, \sigma = 2$. As discussed in Section 1.3.1, the power spectral density of real noise is flatter for larger values of α and thus a real noise can be approximated as a wide-band noise. The simulation results show that, when α is large but still of the same order as σ, this approximation is acceptable.

It should also be mentioned that, for Euler scheme in the Monte Carlo simulation of stochastic differential equations, the error of discrete approximation for moments is of the order of h. Since the numerical estimation of moment Lyapunov exponents requires large time T for simulation, the number of iteration must be extremely large to make the time step h be small enough, this increases the numerical error during computation. Therefore the discrepancy between the simulation results and averaging results is partly contributed by the round-off error in the iterative computation.

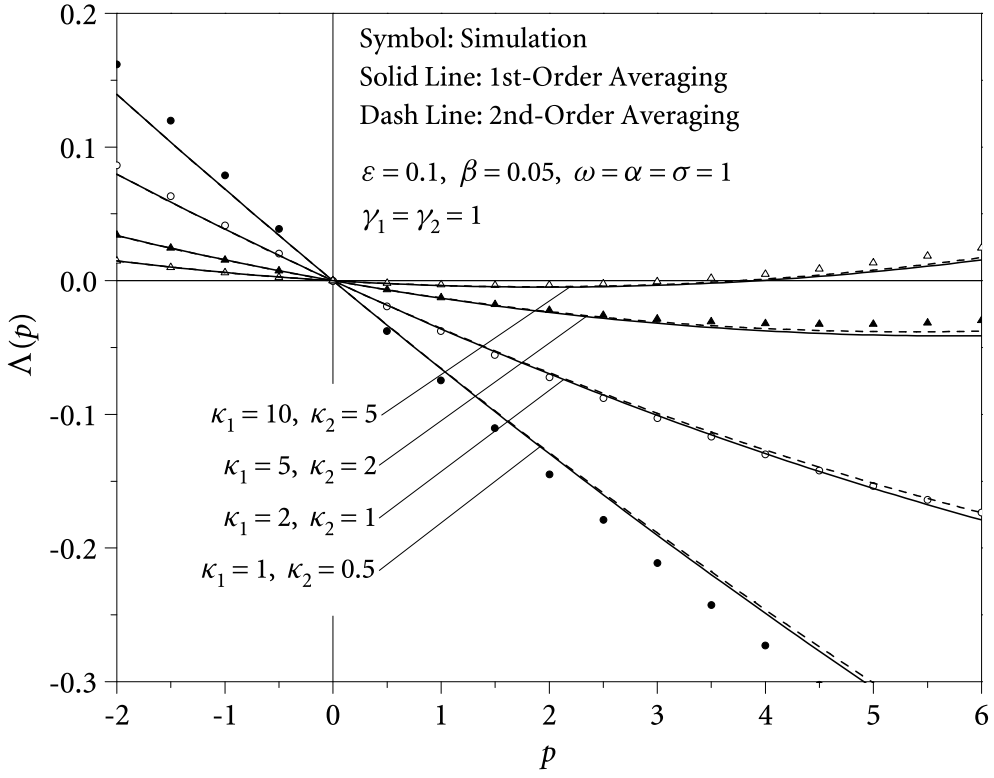

Figure 3.5 Moment Lyapunov exponents under real noise excitation for different κ

Figures 3.7 and 3.8 show the variation of moment Lyapunov exponents from second-order averaging with respect to the parameters of real noise. From Figure 3.7, it can be seen that the larger the noise parameter α, the wider the stability region for $p>0$, i.e. the more stable the system. According to equation (1.3.3), larger α means that the power of noise spreads over a wider frequency band, which reduces the power of the noise in the neighbourhood of resonance. Figure 3.8 shows that with the increase of noise intensity σ, the stability region of the pth moment (for $p>0$) dwindles away as expected.

3.3 Stability under Narow-band Noise Excitation

It is often the case that the noise perturbation in equation (3.1.5) is not wide-band. A general model of narrow-band noise is bounded noise, as described in Section 1.3.1. Ariaratnam [2] determined the largest Lyapunov exponent of a linear viscoelastic system parametrically

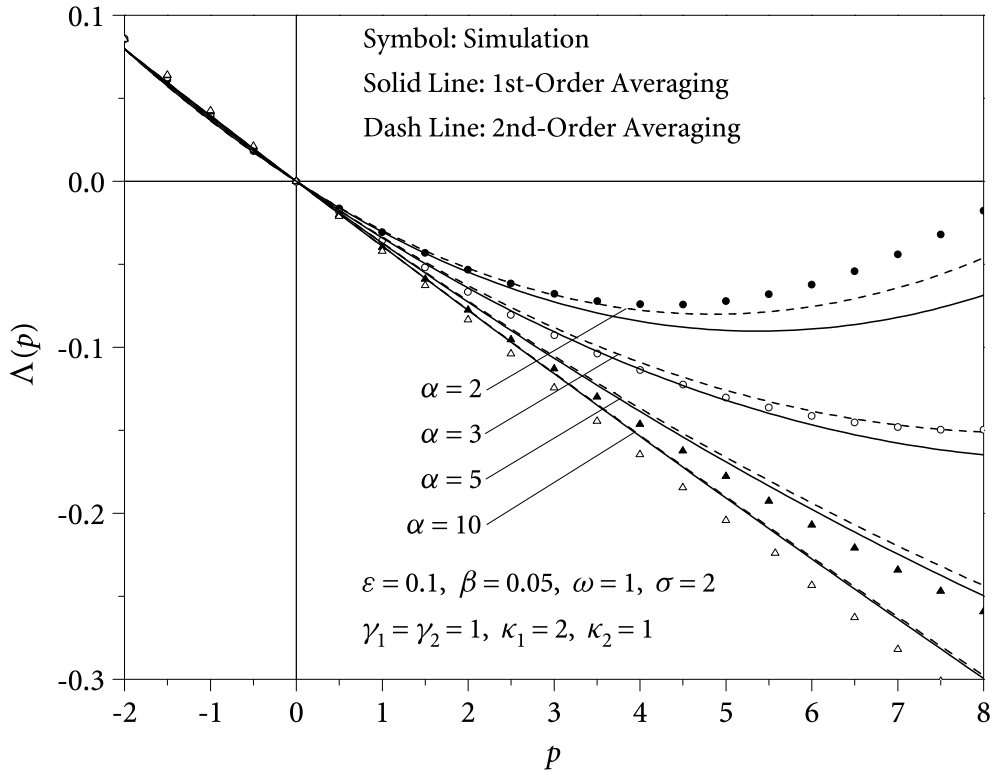

Figure 3.6 Moment Lyapunov exponents under real noise excitation for different α

excited by a bounded noise using the averaging method. Xie [119] obtained the largest Lyapunov exponent of a linear viscoelastic system excited by a bounded noise, which was a revised version to that of Ariaratnam [2]. In this section, the method of stochastic averaging, both first-order and second-order, will be used again to obtain the eigenvalue problem governing the pth moment Lyapunov exponent. The moment Lyapunov exponents of the system can then be determined by solving the eigenvalue problem.

In order to apply the averaging method for integro-differential equation, the SDOF viscoelastic system (3.1.5) is rewritten as

$$\ddot{q}(t) + 2\varepsilon\beta\dot{q}(t) + \omega^2\left\{\big[1 - \varepsilon\xi(t)\big]q(t) - \varepsilon\int_0^t H(t-s)q(s)\,\mathrm{d}s\right\} = 0, \tag{3.3.1}$$

where the excitation takes the form of bounded noise

$$\xi(t) = \mu\cos[\nu t + \varepsilon^{1/2}\sigma W(t) + \theta]. \tag{3.3.2}$$

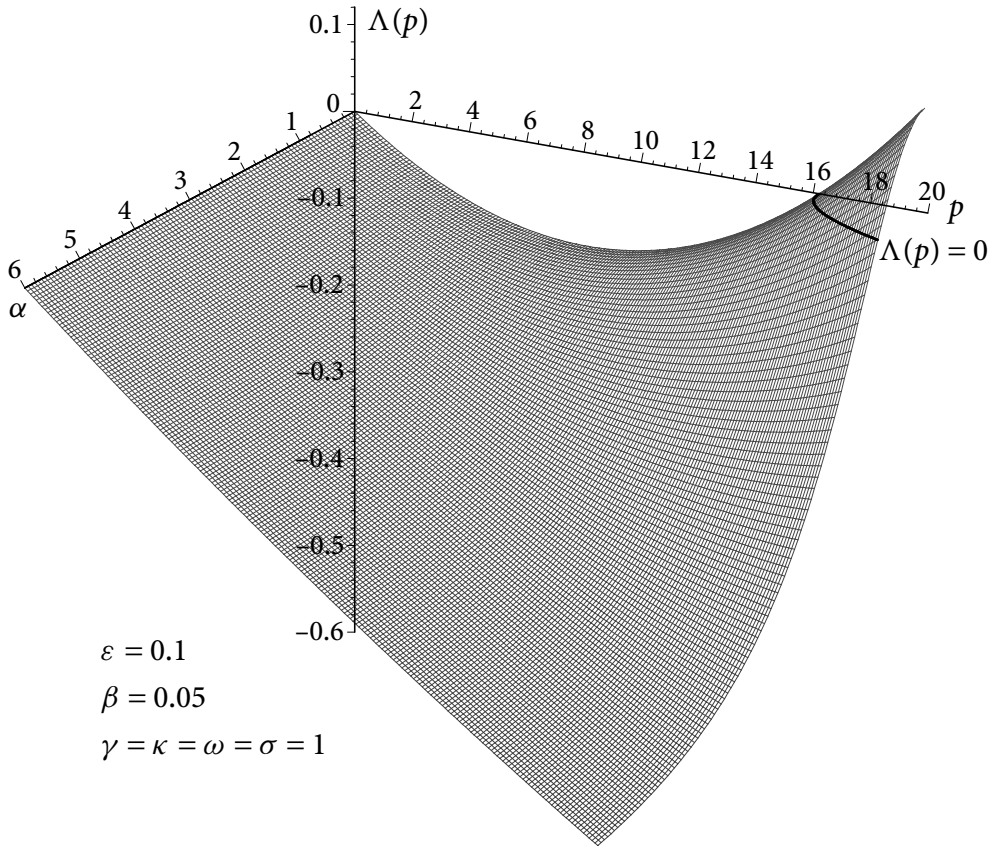

Figure 3.7 Moment Lyapunov exponents under real noise excitation

3.3.1 First-Order Stochastic Averaging

Applying the transformation

$$
\begin{aligned}
&q(t) = a(t)\cos\Phi(t), \qquad \dot{q}(t) = -\omega a(t)\sin\Phi(t),\\
&\Phi(t) = \frac{1}{2}\nu t + \varphi(t), \qquad P(t) = a(t)^p,\\
&\psi = \varepsilon^{1/2}\sigma W(t) + \theta,
\end{aligned}
\tag{3.3.3}
$$

and taking

$$
\varepsilon\Delta = \omega - \frac{1}{2}\nu \tag{3.3.4}
$$

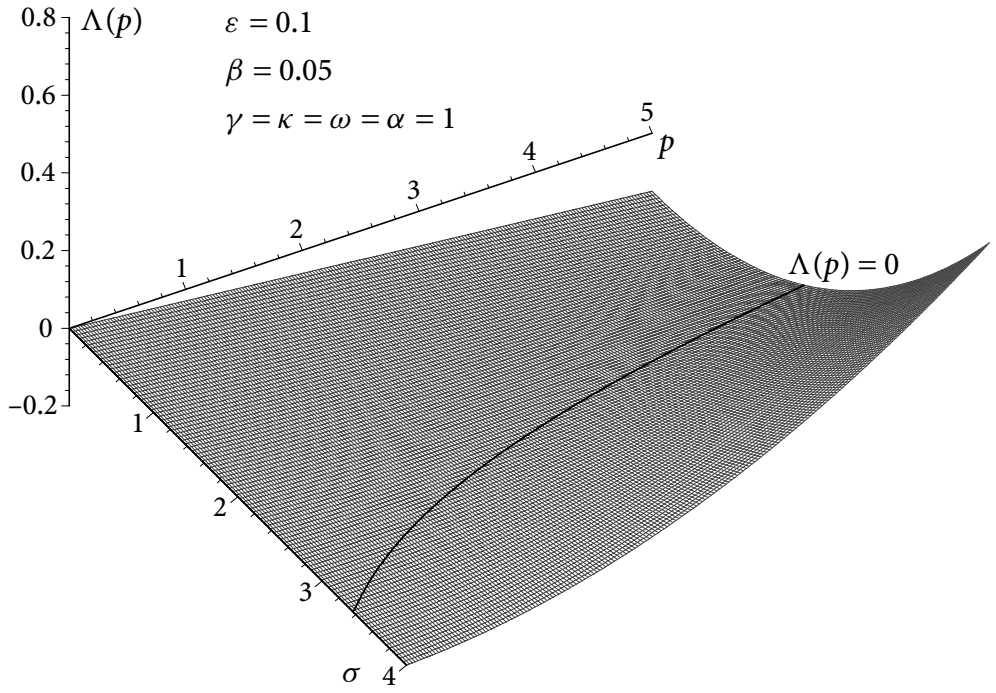

Figure 3.8 Moment Lyapunov exponents under real noise excitation

lead to the equations for $P(t)$ and $\varphi(t)$

$$\begin{aligned}
\dot{P}(t) &= \varepsilon pP\left\{\beta\left[\cos 2\Phi(t)-1\right]+\frac{\mu\omega}{2}\cos(\nu t+\psi)\sin 2\Phi(t)\right\}-\varepsilon\omega pPU_c\sin\Phi(t),\\
\dot{\varphi}(t) &= \varepsilon\left\{\Delta-\beta\sin 2\Phi(t)+\frac{\mu\omega}{2}\cos(\nu t+\psi)\left[1+\cos 2\Phi(t)\right]\right\}-\varepsilon\omega U_c\cos\Phi(t),\\
\mathrm{d}\psi(t) &= \varepsilon^{1/2}\sigma\,\mathrm{d}W(t),
\end{aligned}\tag{3.3.5}$$

where

$$U_c=\int_0^t H(t-s)\left[\frac{P(s)}{P(t)}\right]^{\frac{1}{p}}\cos\Phi(s)\,\mathrm{d}s.$$

Obviously, $P(t)$ is the pth norm of the state vector for system (3.3.1).

When applying the averaging operation, $P(t)$ and $\varphi(t)$ are treated as unchanged, i.e. they are replaced by the corresponding averaged variables directly.

Using the results in Section 3.2, it can be seen that

$$\underset{t}{\mathscr{M}}\{U_c \sin \Phi(t)\} = \frac{1}{2}H^s\left(\tfrac{1}{2}\nu\right),$$
$$\underset{t}{\mathscr{M}}\{U_c \cos \Phi(t)\} = \frac{1}{2}H^c\left(\tfrac{1}{2}\nu\right).$$

Thus the averaged equations for $P(t)$ and $\varphi(t)$ are given by, still denoted by $P(t)$ and $\varphi(t)$,

$$\begin{aligned}\dot{P}(t) &= \varepsilon pP\left[-\beta + \frac{\mu\omega}{4}\sin(2\varphi-\psi) - \frac{1}{2}\omega H^s\left(\tfrac{1}{2}\nu\right)\right],\\ \dot{\varphi}(t) &= \varepsilon\left[\Delta + \frac{\mu\omega}{4}\cos(2\varphi-\psi) - \frac{1}{2}\omega H^c\left(\tfrac{1}{2}\nu\right)\right].\end{aligned} \tag{3.3.6}$$

Denote

$$\hat{\beta} = \beta + \frac{1}{2}\omega H^s\left(\tfrac{1}{2}\nu\right), \quad \Delta_0 = \Delta - \frac{1}{2}\omega H^c\left(\tfrac{1}{2}\nu\right). \tag{3.3.7}$$

Applying the transformation

$$\Theta = \varphi(t) - \frac{1}{2}\psi(t), \tag{3.3.8}$$

and using the Itô's Lemma lead to the Itô differential equations

$$\begin{aligned}\mathrm{d}P(t) &= m_P P\,\mathrm{d}t,\\ \mathrm{d}\Theta(t) &= m_\Theta\,\mathrm{d}t - \varepsilon^{1/2}\frac{\sigma}{2}\mathrm{d}W(t),\\ \mathrm{d}\psi(t) &= \varepsilon^{1/2}\sigma\,\mathrm{d}W(t),\end{aligned} \tag{3.3.9}$$

where

$$m_P = \varepsilon p\left(\frac{1}{4}\mu\omega\sin 2\Theta - \hat{\beta}\right), \quad m_\Theta = \varepsilon\left(\Delta_0 + \frac{1}{4}\mu\omega\cos 2\Theta\right). \tag{3.3.10}$$

Solving the probability distribution of $P(t)$ from equations (3.3.9) is rather difficult since these equations are coupled. It is easier to obtain the eigenvalue problem governing the pth moment Lyapunov exponent. By taking a linear stochastic transformation

$$S = T(\Theta)P, \qquad 0 \leqslant \Theta \leqslant \pi, \tag{3.3.11}$$

where Θ takes the value in $[0,\pi]$ because the coefficients in equations (3.3.9) are periodic functions in Θ of period π, the Itô equation for the transformed pth norm process S is

$$\begin{aligned}\mathrm{d}S &= \left(m_P T + m_\Theta T' + \frac{\varepsilon\sigma^2}{8}T''\right)P\,\mathrm{d}t - \frac{\varepsilon^{1/2}\sigma}{2}T'P\,\mathrm{d}W(t)\\ &= \frac{1}{T}\left(m_P T + m_\Theta T' + \frac{\varepsilon\sigma^2}{8}T''\right)S\,\mathrm{d}t - \frac{\varepsilon^{1/2}\sigma}{2}\frac{T'}{T}S\,\mathrm{d}W(t).\end{aligned} \tag{3.3.12}$$

$T(\Theta)$ is chosen as a bounded and non-singular transformation such that processes P and S have the same stability behaviour [111]. Hence it is required that the drift term of the Itô equation (3.3.12) be independent of Θ, i.e.

$$\frac{1}{T}\Big(m_P T + m_\Theta T' + \frac{\varepsilon\sigma^2}{8}T''\Big) = \Lambda,$$

so that

$$\mathrm{d}S = \Lambda S\,\mathrm{d}t + \sigma_S\,\mathrm{d}W(t). \tag{3.3.13}$$

Taking the expected value of equation (3.3.13) leads to $\mathrm{dE}[S] = \Lambda\,\mathrm{E}[S]\,\mathrm{d}t$. According to the definition of the moment Lyapunov exponent, Λ is the moment Lyapunov exponent of the averaged system (3.3.9). Comparing the drift terms in equations (3.3.12) and (3.3.13) results in the eigenvalue problem governing the pth moment Lyapunov exponent

$$\frac{\sigma^2}{8}T'' + \Big(\Delta_0 + \frac{\mu\omega}{4}\cos 2\Theta\Big)T' + p\Big(-\hat{\beta} + \frac{\mu\omega}{4}\sin 2\Theta\Big)T = \hat{\Lambda}T, \tag{3.3.14}$$

with $\Lambda_{q(t)}(p) = \Lambda(p) = \varepsilon\hat{\Lambda}(p)$.

For the special case $\sigma = 0$, i.e. the bounded noise reduces to harmonic excitation, the problem becomes deterministic, and it is not necessary to solve the eigenvalue problem (3.3.14) to determine the stability property. In this case, the averaged equations (3.3.6) reduce to, by taking $p = 1$ to restore to variable $a(t)$,

$$\begin{aligned}\dot{a}(t) &= \varepsilon a\left[-\hat{\beta} + \frac{1}{4}\mu\omega\sin(2\varphi-\theta)\right],\\ \dot{\varphi}(t) &= \varepsilon\left[\Delta_0 + \frac{1}{4}\mu\omega\cos(2\varphi-\theta)\right].\end{aligned} \tag{3.3.15}$$

Since equations (3.3.15) are not stochastic differential equations, the method for deterministic systems can be used to study this system. Applying the transformations

$$x(t) = a(t)\cos\varphi(t), \qquad y(t) = a(t)\sin\varphi(t),$$

leads to

$$\begin{Bmatrix}\dot{x}\\ \dot{y}\end{Bmatrix} = \begin{bmatrix} -\varepsilon\hat{\beta} - \frac{1}{4}\varepsilon\mu\omega\sin\theta & -\varepsilon\Delta_0 + \frac{1}{4}\varepsilon\mu\omega\cos\theta \\ \varepsilon\Delta_0 + \frac{1}{4}\varepsilon\mu\omega\cos\theta & -\varepsilon\hat{\beta} + \frac{1}{4}\varepsilon\mu\omega\sin\theta \end{bmatrix}\begin{Bmatrix}x\\ y\end{Bmatrix}.$$

The characteristic equation is given by

$$(\rho+\varepsilon\hat{\beta})^2+\varepsilon^2\left(\Delta_0^2-\frac{1}{16}\mu^2\omega^2\right)=0.$$

It is obvious that the roots of the characteristic equation are not affected by θ, and they are given by

$$\rho_{1,2}=\begin{cases}\varepsilon\Big(-\hat{\beta}\pm\frac{1}{4}\sqrt{\mu^2\omega^2-16\Delta_0^2}\Big), & \mu\omega\geqslant 4\Delta_0,\\ \varepsilon\Big(-\hat{\beta}\pm \mathrm{i}\,\frac{1}{4}\sqrt{16\Delta_0^2-\mu^2\omega^2}\Big), & \mu\omega<4\Delta_0.\end{cases}\tag{3.3.16}$$

Since the solution $a(t)$ can be written in the form of $a(t)=c_1\exp(\rho_1 t)+c_2\exp(\rho_2 t)$, the stability of system (3.3.6) under the case $\sigma=0$ is determined from equation (3.3.16) by the Lyapunov exponents

$$\lambda_{1,2}=\begin{cases}\varepsilon\Big(-\hat{\beta}\pm\frac{1}{4}\sqrt{\mu^2\omega^2-16\Delta_0^2}\Big), & \mu\omega\geqslant 4\Delta_0,\\ -\varepsilon\hat{\beta}, & \mu\omega<4\Delta_0.\end{cases}\tag{3.3.17}$$

From equation (3.3.17) it can be seen that, when $\mu\omega<4\Delta_0$, system (3.3.6) is always stable. However, if $\mu\omega\geqslant 4\Delta_0$, and $\sqrt{\mu^2\omega^2-16\Delta_0^2}>4\hat{\beta}$, system (3.3.6) becomes unstable.

3.3.2 Second-Order Stochastic Averaging

The second-order averaging operation may be applied to improve the accuracy of moment Lyapunov exponents. Similar to the case of wide-band noise excitation, the transformations (3.2.20), i.e.

$$P(t)=\bar{P}(t)+\varepsilon P_1(\bar{P},\bar{\varphi},t),\quad \varphi(t)=\bar{\varphi}(t)+\varepsilon\varphi_1(\bar{P},\bar{\varphi},t),$$

are applied again with $\bar{P}(t)$ and $\bar{\varphi}(t)$ being determined later. Substituting equations (3.2.20) into equations (3.3.5) yields

$$\begin{Bmatrix}\dot{P}\\ \dot{\varphi}\end{Bmatrix}=\varepsilon\begin{Bmatrix}p\bar{P}f_1\\ f_2\end{Bmatrix}+\varepsilon^2\begin{Bmatrix}p(\bar{P}g_1+P_1f_1)\\ g_2\end{Bmatrix}+o(\varepsilon^2),\tag{3.3.18}$$

where

$$\bar{\Phi}(t) = \frac{1}{2}\nu t + \bar{\varphi}(t),$$

$$f_1 = \beta\left[\cos 2\bar{\Phi}(t) - 1\right] + \frac{\mu\omega}{2}\cos(\nu t+\psi)\sin 2\bar{\Phi}(t) - \omega\bar{U}_c \sin\bar{\Phi}(t),$$

$$f_2 = \Delta - \beta\sin 2\bar{\Phi}(t) + \frac{\mu\omega}{2}\cos(\nu t+\psi)\left[1+\cos 2\bar{\Phi}(t)\right] - \omega\bar{U}_c\cos\bar{\Phi}(t),$$

$$\begin{aligned} g_1 = {} & -2\beta\varphi_1\sin 2\bar{\Phi}(t) + \mu\omega\varphi_1\cos(\nu t+\psi)\cos 2\bar{\Phi}(t) \\ & - \omega\varphi_1\bar{U}_c\cos\bar{\Phi}(t) + \omega\varphi_1\bar{U}_s\sin\bar{\Phi}(t) - \frac{\omega}{p}U_c^*\sin\bar{\Phi}(t), \end{aligned}$$

$$\begin{aligned} g_2 = {} & -2\beta\varphi_1\cos 2\bar{\Phi}(t) - \mu\omega\varphi_1\cos(\nu t+\psi)\sin 2\bar{\Phi}(t) \\ & + \omega\varphi_1\bar{U}_c\sin\bar{\Phi}(t) + \omega\varphi_1\bar{U}_s\cos\bar{\Phi}(t) - \frac{\omega}{p}U_c^*\cos\bar{\Phi}(t), \end{aligned}$$

$$\bar{U}_c = \int_0^t H(t-s)\left[\frac{\bar{P}(s)}{\bar{P}(t)}\right]^{\frac{1}{p}}\cos\bar{\Phi}(s)\,\mathrm{d}s,$$

$$\bar{U}_s = \int_0^t H(t-s)\left[\frac{\bar{P}(s)}{\bar{P}(t)}\right]^{\frac{1}{p}}\sin\bar{\Phi}(s)\,\mathrm{d}s,$$

$$U_c^* = \int_0^t H(t-s)\left[\frac{\bar{P}(s)}{\bar{P}(t)}\right]^{\frac{1}{p}}\left[\frac{P_1(s)}{\bar{P}(s)} - \frac{P_1(t)}{\bar{P}(t)}\right]\cos\bar{\Phi}(s)\,\mathrm{d}s.$$

Using equations (3.2.21) and (3.2.22), and neglecting the third- and higher-order terms of ε, equations (3.3.18) are converted to a dynamical system in variables $\bar{P}$ and $\bar{\varphi}$

$$\begin{aligned} \begin{Bmatrix} \dot{\bar{P}} \\ \dot{\bar{\varphi}} \end{Bmatrix} = {} & \varepsilon\begin{Bmatrix} p\bar{P}f_1 - \dfrac{\partial P_1}{\partial t} \\ f_2 - \dfrac{\partial\varphi_1}{\partial t} \end{Bmatrix} + \varepsilon^2\begin{Bmatrix} p(\bar{P}g_1 + P_1 f_1) \\ g_2 \end{Bmatrix} \\ & + \varepsilon^2\begin{Bmatrix} -(p\bar{P}f_1 - \dfrac{\partial P_1}{\partial t})\dfrac{\partial P_1}{\partial\bar{P}} - (f_2 - \dfrac{\partial\varphi_1}{\partial t})\dfrac{\partial P_1}{\partial\bar{\varphi}} \\ -(p\bar{P}f_1 - \dfrac{\partial P_1}{\partial t})\dfrac{\partial\varphi_1}{\partial\bar{P}} - (f_2 - \dfrac{\partial\varphi_1}{\partial t})\dfrac{\partial\varphi_1}{\partial\bar{\varphi}} \end{Bmatrix}. \end{aligned} \tag{3.3.19}$$

Noticing that f_1 and f_2 yield the same results as those of the first-order averaging after they are averaged, $\partial P_1/\partial t$ and $\partial\varphi_1/\partial t$ can be taken as the fast oscillation terms to avoid the complexity of solving the integro-differential equations, i.e. the terms which vanish after the

averaging operation,

$$\begin{aligned}\frac{\partial P_1}{\partial t} &= p\bar{P}\left[\beta\cos(\nu t+2\bar{\varphi})+\frac{\mu\omega\sin(2\nu t+2\bar{\varphi}+\psi)}{4}\right],\\ \frac{\partial \varphi_1}{\partial t} &= -\beta\sin(\nu t+2\bar{\varphi})+\frac{\mu\omega\cos(\nu t+\psi)}{2}+\frac{\mu\omega\cos(2\nu t+2\bar{\varphi}+\psi)}{4}.\end{aligned} \tag{3.3.20}$$

Solving P_1 and φ_1 from equations (3.3.20) leads to

$$\begin{aligned}P_1 &= p\bar{P}\left[\frac{\beta\sin(\nu t+2\bar{\varphi})}{\nu}-\frac{\mu\omega\cos(2\nu t+2\bar{\varphi}+\psi)}{8\nu}\right],\\ \varphi_1 &= \frac{\beta\cos(\nu t+2\bar{\varphi})}{\nu}+\frac{\mu\omega\sin(\nu t+\psi)}{2\nu}+\frac{\mu\omega\sin(2\nu t+2\bar{\varphi}+\psi)}{8\nu}.\end{aligned} \tag{3.3.21}$$

After P_1 and φ_1 are known, the averaging operation can be performed over equations (3.3.19). In the process of averaging, $\bar{P}$ and $\bar{\varphi}$ are still treated as constants. Based on the results in Section 3.2, it is easy to obtain that

$$\begin{aligned}\mathscr{M}_t\{\bar{U}_c\sin\bar{\Phi}(t)\} &= \frac{1}{2}H^s\left(\tfrac{1}{2}\nu\right), \qquad \mathscr{M}_t\{\bar{U}_c\cos\bar{\Phi}(t)\} = \frac{1}{2}H^c\left(\tfrac{1}{2}\nu\right),\\ \mathscr{M}_t\{\bar{U}_s\sin\bar{\Phi}(t)\} &= \frac{1}{2}H^c\left(\tfrac{1}{2}\nu\right), \qquad \mathscr{M}_t\{\bar{U}_s\cos\bar{\Phi}(t)\} = -\frac{1}{2}H^s\left(\tfrac{1}{2}\nu\right).\end{aligned}$$

Hence the second-order averaged equations are

$$\begin{aligned}\mathrm{d}\begin{Bmatrix}\bar{P}\\ \bar{\varphi}\end{Bmatrix} &= \varepsilon\begin{Bmatrix}p\left(\frac{1}{4}\mu\omega\sin 2\bar{\Theta}-\hat{\beta}\right)\bar{P}\\ \Delta_0+\frac{1}{4}\mu\omega\cos 2\bar{\Theta}\end{Bmatrix}\mathrm{d}t+\varepsilon^2\frac{1}{2\nu}\begin{Bmatrix}\mu\omega p\left(-\hat{\beta}\cos 2\bar{\Theta}+\hat{\alpha}\sin 2\bar{\Theta}\right)\bar{P}\\ \hat{\delta}+\mu\omega\left(\hat{\beta}\sin 2\bar{\Theta}+\hat{\alpha}\cos 2\bar{\Theta}\right)\end{Bmatrix}\mathrm{d}t\\ &\quad+\varepsilon^{1/2}\begin{Bmatrix}0\\ -\frac{1}{2}\sigma\end{Bmatrix}\mathrm{d}W(t),\end{aligned} \tag{3.3.22}$$

where

$$\bar{\Theta}=\bar{\varphi}(t)-\frac{1}{2}\psi(t),\quad \hat{\alpha}=\frac{1}{2}\omega H^c\left(\tfrac{1}{2}\nu\right),\quad \hat{\delta}=2\beta(\beta-2\hat{\beta})-\frac{1}{16}\mu^2\omega^2. \tag{3.3.23}$$

Similar to the first-order averaging, taking the transformation $\bar{S}=\bar{T}(\bar{\Theta})\bar{P}, 0\leqslant\bar{\Theta}\leqslant\pi$, and using the Itô's Lemma lead to the eigenvalue problem

$$\begin{aligned}&\varepsilon\left[\frac{\sigma^2}{8}T''+\left(\Delta_0+\frac{\mu\omega}{4}\cos 2\Theta\right)T'+p\left(-\hat{\beta}+\frac{\mu\omega}{4}\sin 2\Theta\right)T\right]\\ &\quad+\varepsilon^2\frac{1}{2\nu}\left[\hat{\delta}+\mu\omega\left(\hat{\beta}\sin 2\Theta+\hat{\alpha}\cos 2\Theta\right)\right]T'+\varepsilon^2\frac{\mu\omega p}{2\nu}\left(\hat{\alpha}\sin 2\Theta-\hat{\beta}\cos 2\Theta\right)T=\Lambda T,\end{aligned} \tag{3.3.24}$$

in which, for simplicity of presentation, the overbar has been dropped.

3.3.3 Solving the Eigenvalue Problems

It is still not easy to find the analytical solutions to eigenvalue problems (3.3.14) and (3.3.24). Noticing that the coefficients in equations (3.3.14) and (3.3.24) are periodic in Θ with period π, thus eigenfunctions $T(\Theta)$ can be expanded to a Fourier series in the form

$$T(\Theta) = C_0 + \sum_{k=1}^{\infty}(C_k \cos 2k\Theta + S_k \sin 2k\Theta). \tag{3.3.25}$$

Substituting the expansion into eigenvalue problem (3.3.14) or (3.3.24) yields a set of homogeneous linear algebraic equations with infinitely many equations for the unknown coefficients C_0, C_k and S_k, $k=1,2,\ldots$. In particular, for the first order eigenvalue problem (3.3.14), one has

$$\begin{aligned}
-(c_0+\hat{\Lambda})C_0 + b_0 S_1 &= 0,\\
-(c_1+\hat{\Lambda})C_1 + d_1 S_1 + b_1 S_2 &= 0,\\
2a_1 C_0 + d_1 C_1 + (c_1+\hat{\Lambda})S_1 + b_1 C_2 &= 0,\\
a_k S_{k-1} - (c_k+\hat{\Lambda})C_k + d_k S_k + b_k S_{k+1} &= 0,\\
a_k C_{k-1} + d_k C_k + (c_k+\hat{\Lambda})S_k + b_k C_{k+1} &= 0, \quad k=2,3,\ldots,
\end{aligned} \tag{3.3.26}$$

where

$$\begin{aligned}
a_n &= \frac{1}{8}\mu\omega(2n-2-p), \quad b_n = \frac{1}{8}\mu\omega(2n+2+p),\\
c_n &= \frac{1}{2}\sigma^2 n^2 + p\hat{\beta}, \quad d_n = 2\Delta_0 n, \quad n=0,1,2,\ldots.
\end{aligned}$$

In principle, infinite terms of coefficients C_k and S_k are required to obtain the exact solutions of the eigenvalue problems. However it is difficult to do so in practice. Therefore, only a finite number of terms are considered to obtain an approximate solution. If the expansion is truncated to order K, i.e.

$$T(\Theta) = C_0 + \sum_{k=1}^{K}(C_k \cos 2k\Theta + S_k \sin 2k\Theta), \tag{3.3.27}$$

the system of equations, e.g. (3.3.26), reduces to a generalized linear algebraic eigenvalue problem of the form

$$\left[\mathbf{A} - \hat{\Lambda}^{(K)}\mathbf{B}\right]\mathbf{Y} = \mathbf{0}, \tag{3.3.28}$$

where $\mathbf{Y} = \{C_0, C_1, S_1, \ldots, C_K, S_K\}^T$, $\mathbf{A}$ and bB are $(2K+1)\times(2K+1)$ matrices including the coefficients a_n, b_n, c_n, d_n.

Equation (3.3.28) has non-trivial solutions only if the determinant $\left|\mathbf{A} - \hat{\Lambda}^{(K)}\mathbf{B}\right| = 0$, which leads to a polynomial equation for $\hat{\Lambda}^{(K)}$ of degree $2K+1$. Solving the polynomial equation for the largest root leads to the approximate moment Lyapunov exponents. Generally there is no analytical solution for this polynomial equation of $\hat{\Lambda}^{(K)}$ when $K > 1$. Therefore numerical method has to be adopted.

3.3.4 Numerical Results and Discussion

In the Monte Carlo simulation, the Maxwell viscoelastic model is considered, i.e. the viscoelastic kernel function is taken as $H(t) = \gamma \mathrm{e}^{-\kappa t}$. Let

$$\begin{aligned} &x_1(t) = q(t), \quad x_2(t) = \dot{q}(t), \quad x_3(t) = \int_0^t H(t-s)q(s)\,\mathrm{d}s, \\ &x_4(t) = \nu t + \varepsilon^{1/2}\sigma W(t) + \theta. \end{aligned} \tag{3.3.29}$$

Equation (3.3.1) can be rewritten as Itô differential equations

$$\mathrm{d}\begin{Bmatrix} x_1 \\ x_2 \\ x_3 \\ x_4 \end{Bmatrix} = \begin{Bmatrix} x_2 \\ -2\varepsilon\beta x_2 - \omega^2(1+\varepsilon\mu\cos x_4)x_1 + \varepsilon\omega^2 x_3 \\ \gamma x_1 - \kappa x_3 \\ \nu \end{Bmatrix}\mathrm{d}t + \begin{Bmatrix} 0 \\ 0 \\ 0 \\ \varepsilon^{1/2}\sigma \end{Bmatrix}\mathrm{d}W(t). \tag{3.3.30}$$

The norm for evaluating the moment Lyapunov exponents is $\left\|\mathbf{x}(t)\right\| = \sqrt{x_1^2 + x_2^2 + x_3^2}$. The moment Lyapunov exponents are simulated using the algorithm in Section 2.3 with explicit

Euler scheme given by

$$
\begin{aligned}
x_1^{k+1} &= x_1^k + x_2^k \cdot h, \\
x_2^{k+1} &= x_2^k + \big(-\omega^2 x_1^k - 2\varepsilon\beta x_2^k + \varepsilon\omega^2 x_3^k - \varepsilon\mu\omega^2 x_1^k \cos x_4^k \big) h, \\
x_3^{k+1} &= x_3^k + \big(\gamma x_1^k - \kappa x_3^k \big) h, \\
x_4^{k+1} &= x_4^k + \nu \cdot h + \varepsilon^{1/2}\sigma \cdot \Delta W^k.
\end{aligned}
\tag{3.3.31}
$$

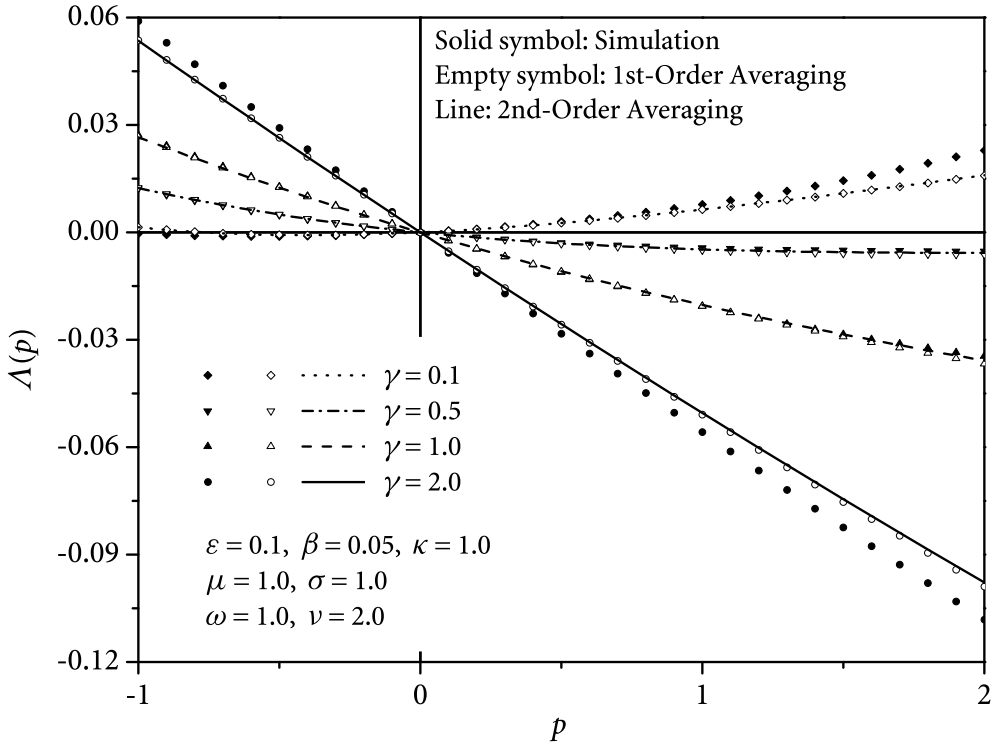

Figure 3.9 Moment Lyapunov exponents under bounded noise excitation for different γ

Different parameters are selected to compare the moment Lyapunov exponents obtained by the averaging method and Monte Carlo simulation. The Fourier series expansion for $T(\Theta)$ is truncated to the order 4, i.e. $K=4$, to obtain the approximate analytical result. The sample size for evaluating the ensemble average as the expected value is $N=5000$, time step $h=0.001$, and the number of iterations is 5×10^6. The following parameters are fixed as: $\varepsilon=0.1, \beta=0.05, \omega=1.0, \nu=2.0$, i.e. $\Delta=0$.

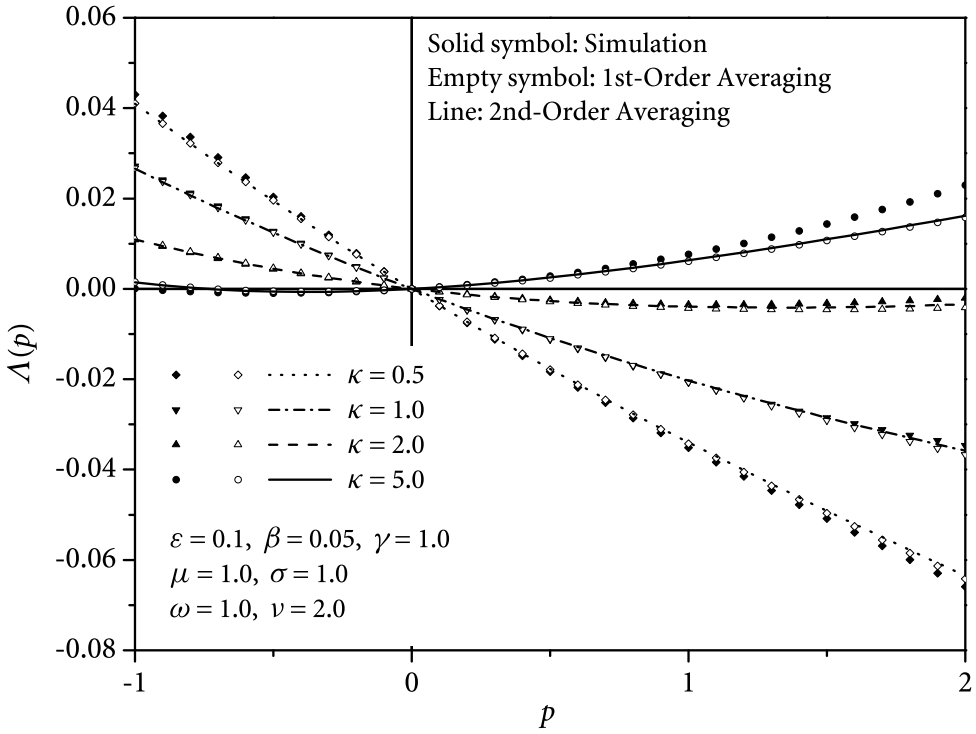

Figure 3.10 Moment Lyapunov exponents under bounded noise excitation for different κ

Figure 3.9 shows the moment Lyapunov exponents for different γ with $\kappa = \sigma = \mu = 1$. The simulation results and the approximate analytical results agree very well for small values of γ and $p > 0$. It can be seen that with the increase of the intensity of material relaxation, the moment Lyapunov exponents at $p > 0$ decrease. This observation implies that the material viscoelasticity helps to stabilize the system.

The moment Lyapunov exponents for different κ at $\gamma = \sigma = \mu = 1$ are plotted in Figure 3.10. It shows that the averaging method provides a good approximation of the moment Lyapunov exponents. It is obvious that, the smaller the value of κ, the smaller the moment Lyapunov exponents for $p > 0$. Since small κ means large relaxation time constant, this result indicates that longer relaxation time will also help to stabilize the system.

In Figure 3.11, the moment Lyapunov exponents for different values of σ and $\gamma = 0.5$, $\kappa = \mu = 1$ are presented. It is clearly seen that the stability of the system increases, when the noise intensity parameter σ increases, in the sense that the moment Lyapunov exponents

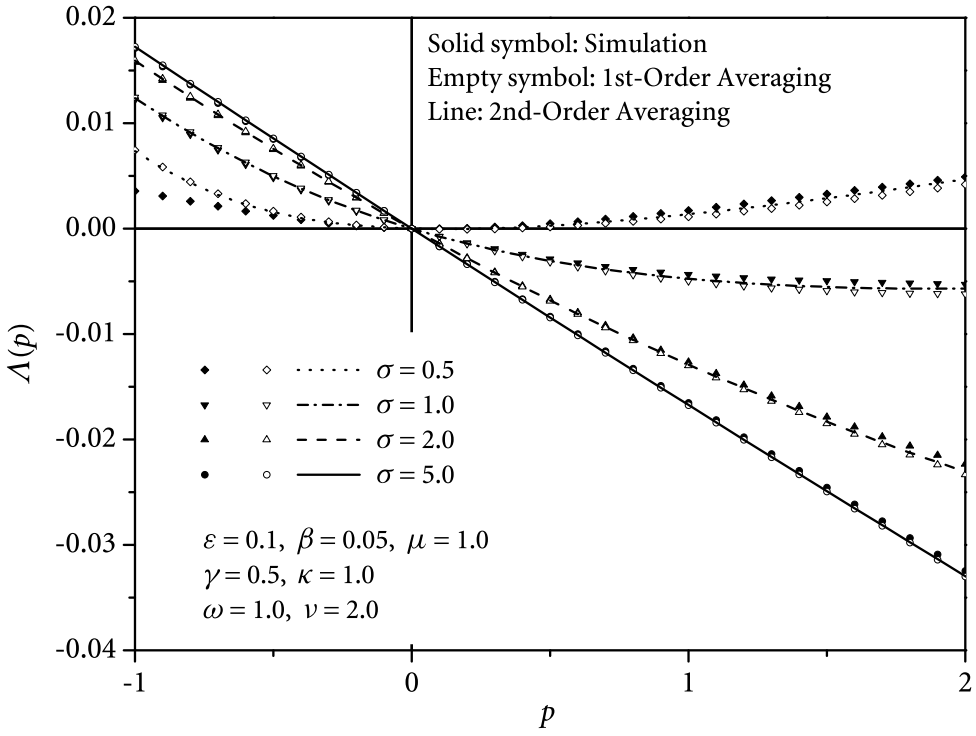

Figure 3.11 Moment Lyapunov exponents under bounded noise excitation for different σ

decrease for $p>0$. It is because that, the larger the value of σ, the wider the frequency band of the power spectral distribution. This means that the power of the noise will not be concentrated in the neighborhood of the central frequency ν, which reduces the effect of the primary parametric resonance. Also, increasing the noise parameter σ decreases the discrepancy between the simulation results and the approximate analytical results for $p>0$.

The moment Lyapunov exponents for various values of μ are showed in Figure 3.12, where $\gamma=0.5$, $\kappa=1$, $\sigma=2$. The result indicates that, as expected, increasing the noise amplitude μ makes the system unstable. Moreover, with the increase of amplitude μ, the difference between the simulation results and the approximate analytical results becomes more and more significant.

Figure 3.13 shows the asymptotic normality of $\log\|\mathbf{x}(T)\|$ for some selected parameters, where the histograms and the corresponding normal density approximations are compared. From the figure it can be seen that the sample size $N=5000$ may not be enough in simulation.

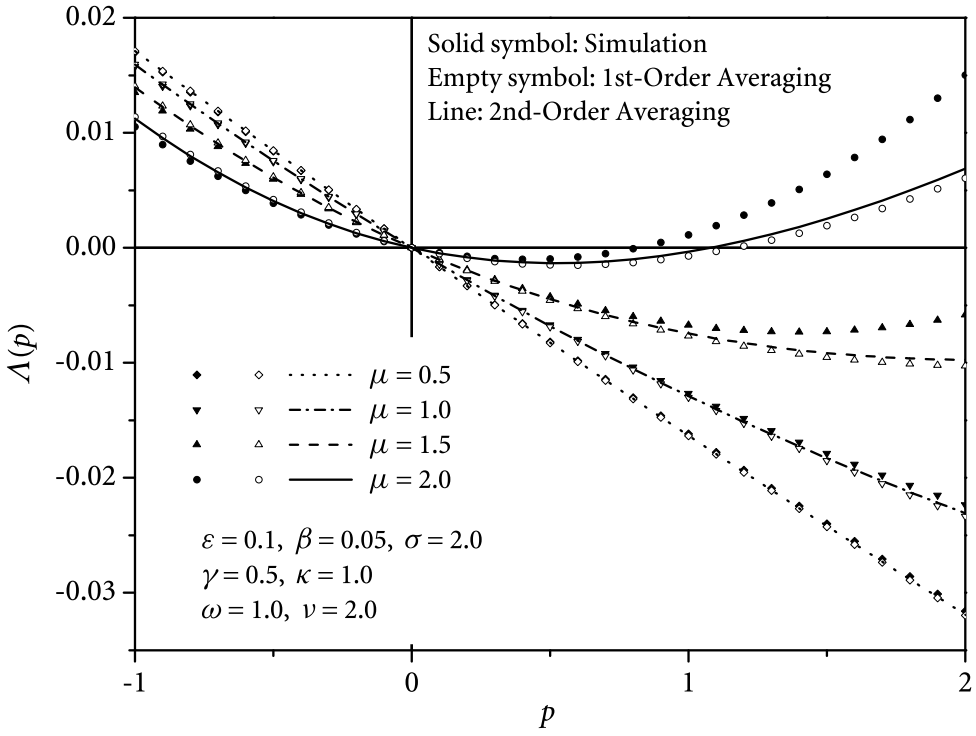

Figure 3.12 Moment Lyapunov exponents under bounded noise excitation for different μ

To improve the simulation results, larger sample size is required to obtain a better estimation of the mean and variance of $\log\|\mathbf{x}(T)\|$.

On the other hand, from Figure 3.9 to Figure 3.12, it can be observed that the second-order averaging does not improve the accuracy of analytical results too much. To illustrate this more, some typical numerical results of the moment Lyapunov exponents obtained from the eigenvalue problems are plotted in Figure 3.14. The Fourier series is expanded to the fourth order, i.e. $K = 4$. It is obvious that the results for the first-order and the second-order averaging have no significant difference provided that $0 < \varepsilon \ll 1$. This means that as far as the method of averaging is concerned, the first-order is enough to determine the stability of SDOF viscoelastic system with small parameter ε under bounded noise excitation.

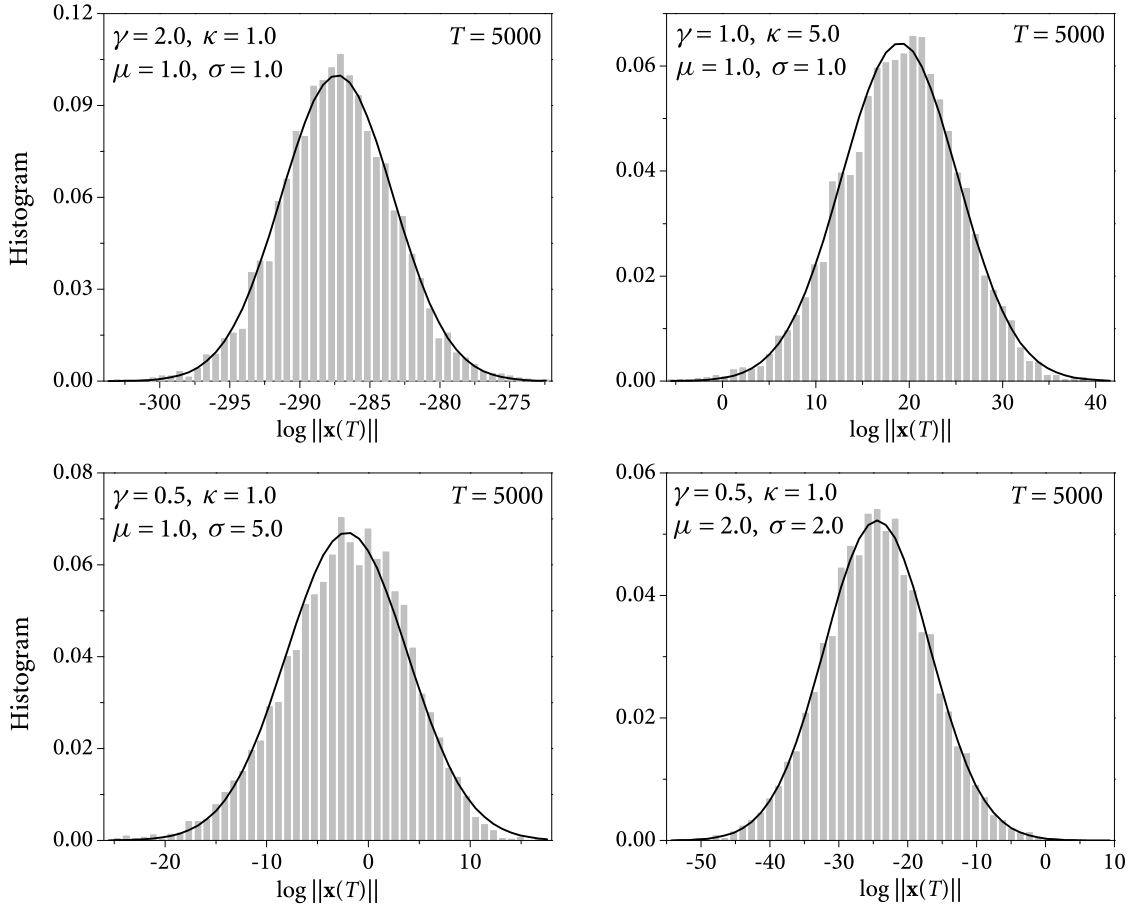

Figure 3.13 Histograms of logarithm of norm compared with normal density approximations under bounded noise excitation

3.4 Summary

SDOF viscoelastic systems under parametric perturbations of random loads, including wide-band noise and narrow-band noise, are studied in this chapter. As described in Section 1.3.1, Gaussian white noise and Ornstein-Uhlenbeck process are the models of wide-band noise, and bounded noise is treated as a narrow-band noise. Stochastic averaging method is applied to simplify the equations of motion, which are integro-differential equations. Then the stability of the averaged systems is determined in the sense of moment Lyapunov exponents. The algorithm presented in Section 2.3 is used to simulate the stability of the

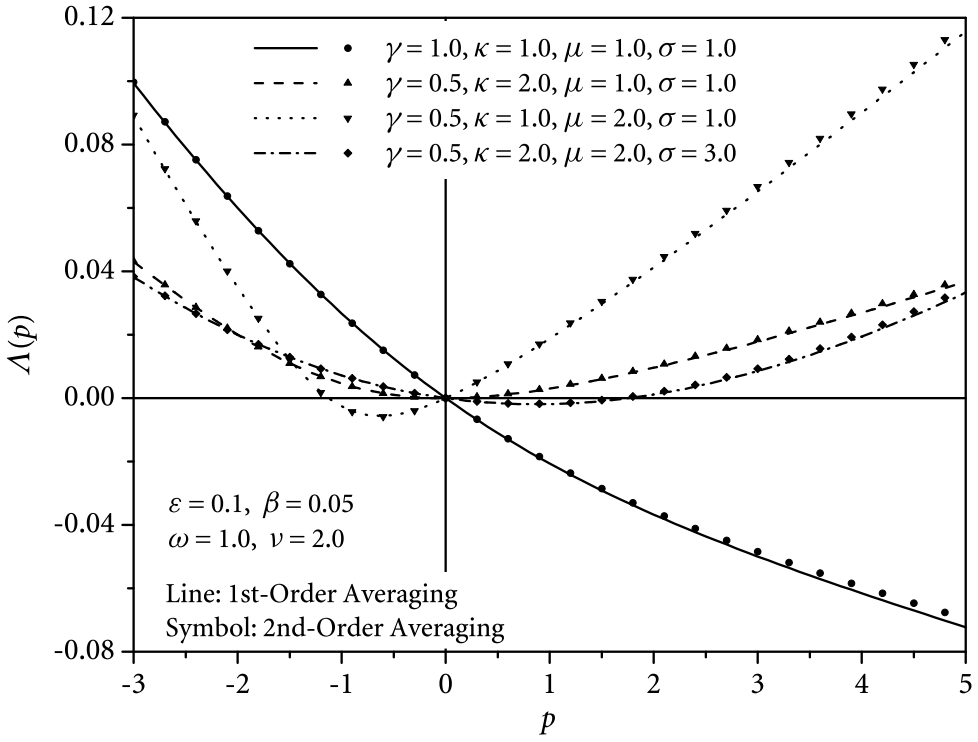

Figure 3.14 Comparison of moment Lyapunov exponents for the 1st-order and 2nd-order averaging

original SDOF viscoelastic systems. Comparing the approximate analytical results and the simulation results, it can be seen that averaging method provides a good approximation to the original SDOF viscoelastic systems in most cases. However, in the cases when the energy of noises concentrate in the neighborhood the primary parametric resonance frequency and their intensities are not small enough, the averaging method appears to be insufficient, as indicated by the results from bounded noise excitation. Moreover, higher-order averaging seems to provide no significant improvement for the analytical approximation; thus the first-order averaging is enough in determining the stability of viscoelastic systems.

From the approximate analytical results and the Monte Carlo simulation results of the moment Lyapunov exponents in Section 3.2 and 3.3, it is clear that increasing the intensity of viscoelasticity, material relaxation time, and decreasing the noise intensity help to stabilize the viscoelastic system. This result is useful in engineering applications.

C H A P T E R 4

Stochastic Stability of SDOF Nonlinear Viscoelastic Systems

Stochastic stability of SDOF linear viscoelastic systems has been discussed in Chapter 3 in the sense of moment Lyapunov exponents, where only the trivial solutions are considered. In engineering applications, the linear constitutive relation may not be sufficient for many materials. Therefore it is necessary to consider the situation where nonlinear viscoelasticity is exhibited.

4.1 An Example of SDOF Nonlinear Viscoelastic System

With the material relaxation operator $\mathscr{H}$ defined by equation (3.1.2), the linear viscoelastic constitutive relation for uniaxial stress $\sigma(t)$ and strain $\varepsilon(t)$ can be expressed as

$$\sigma(t) = E\Big[\varepsilon(t) - \int_0^t H(t-\tau)\varepsilon(\tau)\,\mathrm{d}\tau\Big] = E(1-\mathscr{H})\varepsilon(t), \tag{4.1.1}$$

where E is the Young's modulus.

The exploration of nonlinear theory has started its way many years ago since the behaviour of materials cannot always be described by the linear theory correctly. However, due to the complexity of modelling of materials, which is related to many other areas such as physics and chemistry, the study of nonlinear constitutive relations for viscoelastic materials has a long way to go.

In the common approach of Green-Rivlin theory, stress is expressed as a polynomial expansion in linear functionals of strain history. Thus the one-dimensional uniaxial constitutive relation has the form [25]

$$\sigma(t) = \int_0^t H_1(t-\tau)\frac{\mathrm{d}e(\tau)}{\mathrm{d}\tau}\,\mathrm{d}\tau + \int_0^t\int_0^t\int_0^t H_3(t-\tau_1, t-\tau_2, t-\tau_3)\frac{\mathrm{d}e(\tau_1)}{\mathrm{d}\tau_1}\frac{\mathrm{d}e(\tau_2)}{\mathrm{d}\tau_2}\frac{\mathrm{d}e(\tau_3)}{\mathrm{d}\tau_3}\,\mathrm{d}\tau_1\,\mathrm{d}\tau_2\,\mathrm{d}\tau_3 + \cdots, \tag{4.1.2}$$

where $e(\tau)$ is the nonlinear strain measure. In the case of one dimension, $e(\tau)$ is given by

$$e(\tau) = \frac{1}{2}\big\{[1+\varepsilon(\tau)]^2 - 1\big\}. \tag{4.1.3}$$

Equation (4.1.2) appears to be too complicated in practice. Therefore, there are many other different but simplier forms of constitutive relations related to the variety of materials. One possible constitutive relation is

$$\sigma(t) = E\Big[g(\varepsilon(t)) - \int_0^t H(t-\tau)g(\varepsilon(\tau))\,\mathrm{d}\tau\Big] = E(1-\mathscr{H})g(\varepsilon(t)), \tag{4.1.4}$$

where

$$g(\varepsilon) = \varepsilon\big(1+\delta_1\varepsilon+\delta_2\varepsilon^2\big), \tag{4.1.5}$$

and δ_1, δ_2 are small constants related to materials. Constitutive relation (4.1.4) was introduced by Leaderman [71]; it has been used to characterize the large deformation of rubberlike network polymers and textile fibers [70], [46].

Using equation (4.1.4) for nonlinear visoelastic materials, it is possible to derive the equations of motion, which are generally integro-partial differential equations and are difficult to solve as described in Section 1.4. As an example, consider a column under dynamical axial compressive load $P(t)$ as shown in Figure 4.1. The equation of motion is

$$\frac{\partial^2 M(x,t)}{\partial x^2} = \rho A\frac{\partial^2 v(x,t)}{\partial t^2} + \beta_0\frac{\partial v(x,t)}{\partial t} + P(t)\frac{\partial^2 v(x,t)}{\partial x^2}, \tag{4.1.6}$$

where ρ is the mass density per unit volumne of the column, A the cross-sectional area, $v(x,t)$ the transverse displacement of the central axis, β_0 the damping constant, $M(x,t)$ the moment at the cross-section x.

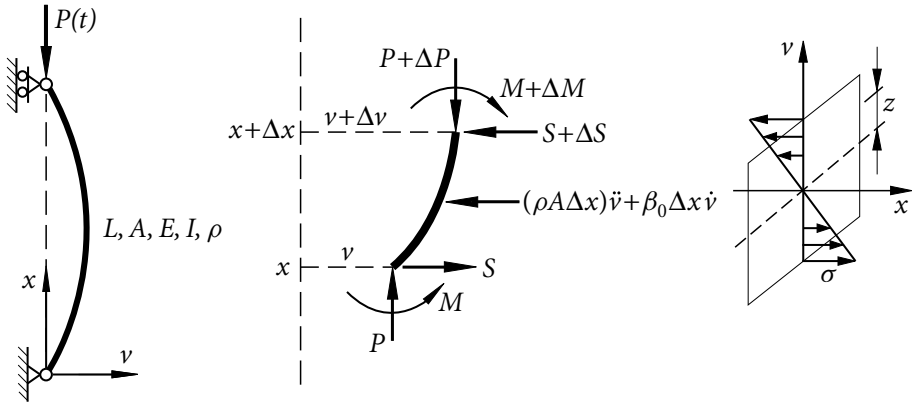

Figure 4.1 A column under axial compressive load

Noticing that the geometry relation

$$\varepsilon = -\frac{\partial^2 v}{\partial x^2} z = -v_{xx} z$$

holds, in which z is the distance from the central axis of a point in the cross-section. If the column is elastic, one obtains

$$M(x,t) = \int_A \sigma z \, \mathrm{d}A = -\int_A E v_{xx} z^2 \, \mathrm{d}A = -EI\, v_{xx},$$

where I is the moment inertia of the cross-section. If the column takes the nonlinear viscoelastic constitutive relation (4.1.4), and the cross-section is symmetry about the central axis, then

$$\begin{aligned} M(x,t) &= \int_A \sigma z \, \mathrm{d}A = \int_A E(1-\mathscr{H})g(\varepsilon) z \, \mathrm{d}A \\ &= -EI(1-\mathscr{H})v_{xx} - \delta_2 EJ(1-\mathscr{H})v_{xx}^3, \end{aligned} \tag{4.1.7}$$

where J is given by

$$J = \int_A z^4 \, \mathrm{d}A.$$

Substituting equation (4.1.7) into (4.1.6) leads to the equations of motion

$$\begin{aligned} &\rho A \frac{\partial^2 v}{\partial t^2} + \beta_0 \frac{\partial v}{\partial t} + P(t)\frac{\partial^2 v}{\partial x^2} + EI(1-\mathscr{H})\frac{\partial^4 v}{\partial x^4} \\ &\qquad + 3\delta_2 EJ(1-\mathscr{H})\Big[2\frac{\partial^2 v}{\partial x^2}\Big(\frac{\partial^3 v}{\partial x^3}\Big)^2 + \Big(\frac{\partial^2 v}{\partial x^2}\Big)^2 \frac{\partial^4 v}{\partial x^4}\Big] = 0. \end{aligned} \tag{4.1.8}$$

Further suppose the column is simply supported, then the boundary conditions are

$$v(0,t) = v(L,t) = v_{xx}(0,t) = v_{xx}(L,t) = 0, \tag{4.1.9}$$

where L is the length of the column.

It is not an easy task to solve the nonlinear equation (4.1.8) analytically. To simplify the problem, if the axial compressive force does not greatly exceed the Euler buckling load of linear elastic column, it is reasonable to assume that the transverse displacement can be approximated by the one-mode vibration [22], i.e. the Galerkin approximation in the form of

$$v(x,t) = q(t)\sin\frac{\pi x}{L}, \tag{4.1.10}$$

which satisfies the boundary conditions (4.1.9) automatically. Substituting equation (4.1.10) into (4.1.8) yields

$$\begin{aligned}\rho A\ddot{q} + \beta_0\dot{q} - \left(\frac{\pi}{L}\right)^2 P(t)q \\ + \left(\frac{\pi}{L}\right)^4 EI(1-\mathscr{H})q + \frac{3\delta_2 EJ}{4}\left(\frac{\pi}{L}\right)^8(1-\mathscr{H})q^3 = 0.\end{aligned} \tag{4.1.11}$$

Letting

$$\beta = \frac{\beta_0}{2\rho A}, \quad \omega^2 = \frac{EI}{\rho A}\left(\frac{\pi}{L}\right)^4, \quad \xi(t) = \frac{P(t)}{EI}\left(\frac{L}{\pi}\right)^2, \quad \delta = \frac{3\delta_2 J}{4I}\left(\frac{\pi}{L}\right)^4,$$

equation (4.1.11) becomes the following general single degree-of-freedom nonlinear viscoelastic system with cubic nonlinearity,

$$\ddot{q} + 2\beta\dot{q} + \omega^2\Big[(1-\mathscr{H})q - \xi(t)q + \delta(1-\mathscr{H})q^3\Big] = 0. \tag{4.1.12}$$

It can be seen that, when $\delta = 0$, equation (4.1.12) reduces to a SDOF linear viscoelastic system, whose stochastic stability properties have been studied in Chapter 3. The existence of cubic nonlinearity makes the behaviour of equation (4.1.12) different from that of the linear cases. As it will be shown, stochastic bifurcation phenomena, which never exist in linear systems, may occur.

4.2 Stability and Bifurcation under Wide-band Noise Excitation

There seems no previous study on the stochastic stability properties of nonlinear viscoelastic systems in the form of equation (4.1.12). Only a similar problem was discussed by Ariaratnam [3], where the nonlinearity appears in the damping term but not the stiffness term and viscoelastic term.

Consider the case that the excitation $\xi(t)$ in equation (4.1.12) is a wide-band noise with zero mean. Similar to the study in Chapter 3, the stochastic averaging method is applied to simplify equation (4.1.12) so that it is easier to investigate the properties of the averaged system.

4.2.1 Approximation by Stochastic Averaging

In order to use the averaging method, in the cases that the damping, viscoelastic effect, and the amplitude of excitation are all small, a small parameter $0<\varepsilon\ll 1$ is introduced such that equation (4.1.12) becomes

$$\ddot{q}(t)+2\varepsilon\beta\dot{q}(t)+\omega^2\Big\{\big[1-\varepsilon^{1/2}\xi(t)\big]q(t)-\varepsilon\int_0^t H(t-s)q(s)\,\mathrm{d}s\Big\} + \omega^2\delta\Big\{q^3(t)-\varepsilon\int_0^t H(t-s)q^3(s)\,\mathrm{d}s\Big\}=0. \tag{4.2.1}$$

After the same transformation as that in equations (3.2.1), i.e.

$$q(t)=a(t)\cos\Phi(t),\quad \dot{q}(t)=-\omega a(t)\sin\Phi(t),\quad \Phi(t)=\omega t+\varphi(t),$$

is applied, it is found that

$$\begin{aligned}\dot{a}(t)&=F_1^{(1)}(a,\varphi,t)+F_1^{(0)}(a,\varphi,\xi,t),\\ \dot{\varphi}(t)&=F_2^{(1)}(a,\varphi,t)+F_2^{(0)}(a,\varphi,\xi,t),\end{aligned} \tag{4.2.2}$$

where

$$
\begin{aligned}
F_1^{(1)}(a,\varphi,t) &= -\varepsilon\beta a(t)\big[1-\cos 2\Phi(t)\big] + \delta\frac{\omega}{8}a^3(t)\big[\sin 4\Phi(t) + 2\sin 2\Phi(t)\big] \\
&\quad - \varepsilon\omega\sin\Phi(t)I^c - \varepsilon\delta\omega\sin\Phi(t)J^c, \\
F_2^{(1)}(a,\varphi,t) &= -\varepsilon\beta a(t)\sin 2\Phi(t) + \delta\frac{\omega}{8}a^2(t)\big[\cos 4\Phi(t) + 4\cos 2\Phi(t) + 3\big] \\
&\quad - \varepsilon\frac{\omega}{a(t)}\cos\Phi(t)I^c - \varepsilon\delta\frac{\omega}{a(t)}\cos\Phi(t)J^c, \\
F_1^{(0)}(a,\varphi,\xi,t) &= -\frac{1}{2}\varepsilon^{1/2}\omega\xi(t)a(t)\sin 2\Phi(t), \\
F_2^{(0)}(a,\varphi,\xi,t) &= -\frac{1}{2}\varepsilon^{1/2}\omega\xi(t)a(t)\big[1+\cos 2\Phi(t)\big], \\
I^c &= \int_0^t H(t-s)a(s)\cos\Phi(s)\,\mathrm{d}s, \\
J^c &= \int_0^t H(t-s)a^3(s)\cos^3\Phi(s)\,\mathrm{d}s.
\end{aligned}
$$

Since $\xi(t)$ is a wide-band noise, δ is also a small constant, according to the method of stochastic averaging, equations (4.2.2) can be approximated by the following averaged equations

$$
\mathrm{d}\left\{\begin{array}{c}\bar{a}(t)\\ \bar{\varphi}(t)\end{array}\right\} = \left\{\begin{array}{c}\bar{m}_a\\ \bar{m}_\varphi\end{array}\right\}\mathrm{d}t + \bar{\boldsymbol{\sigma}}\,\mathrm{d}\mathbf{W}(t), \tag{4.2.3}
$$

where the coefficients are determined following the same procedure as that in Section 3.2,

$$
\begin{aligned}
\bar{m}_a &= \varepsilon\Big[-\beta - \frac{1}{2}\omega\mathcal{H}^s(\omega) + \frac{3}{16}\omega^2 S(2\omega) - \frac{3}{8}\delta\omega\mathcal{H}^s(\omega)\bar{a}^2\Big]\bar{a}, \\
\bar{m}_\varphi &= \varepsilon\Big[-\frac{1}{2}\omega\mathcal{H}^c(\omega) - \frac{1}{8}\omega^2\Psi(2\omega) - \delta\omega\frac{3}{8}\mathcal{H}^c(\omega)\bar{a}^2\Big] + \frac{3}{8}\delta\omega\bar{a}^2, \\
\big[\bar{\boldsymbol{\sigma}}\bar{\boldsymbol{\sigma}}^T\big]_{11} &= b_{11} = \frac{1}{8}\varepsilon\omega^2 S(2\omega)\bar{a}^2, \\
\big[\bar{\boldsymbol{\sigma}}\bar{\boldsymbol{\sigma}}^T\big]_{12} &= \big[\bar{\boldsymbol{\sigma}}\bar{\boldsymbol{\sigma}}^T\big]_{21} = 0, \\
\big[\bar{\boldsymbol{\sigma}}\bar{\boldsymbol{\sigma}}^T\big]_{22} &= b_{22} = \frac{1}{8}\varepsilon\omega^2\big[2S(0) + S(2\omega)\big].
\end{aligned} \tag{4.2.4}
$$

To make the variables $\bar{a}(t)$ and $\bar{\varphi}(t)$ decoupled, the elements of matrix $\bar{\boldsymbol{\sigma}}$ can be chosen as

$$\bar{\sigma}_{11} = \sqrt{b_{11}} = \varepsilon^{1/2}\omega\bar{a}\sqrt{\frac{S(2\omega)}{8}},$$

$$\bar{\sigma}_{22} = \sqrt{b_{22}} = \varepsilon^{1/2}\omega\sqrt{\frac{2S(0)+S(2\omega)}{8}},$$

$$\bar{\sigma}_{12} = \bar{\sigma}_{21} = 0.$$

Therefore, the Itô stochastic differential equation for $\bar{a}$ is given by

$$\mathrm{d}\bar{a} = \varepsilon\left(\eta_1\bar{a} - \eta_2\bar{a}^3\right)\mathrm{d}t + \varepsilon^{1/2}\eta_3\bar{a}\,\mathrm{d}W(t), \tag{4.2.5}$$

where

$$\eta_1 = -\beta - \frac{1}{2}\omega\mathcal{H}^s(\omega) + \frac{3}{16}\omega^2 S(2\omega), \quad \eta_2 = \frac{3}{8}\delta\omega\mathcal{H}^s(\omega), \quad \eta_3 = \omega\sqrt{\frac{S(2\omega)}{8}}. \tag{4.2.6}$$

Note that for a given initial condition, the transition density function of equations (4.2.3) determines the properties of the one-point motion, i.e. the motion of $\left(\bar{a}(t), \bar{\varphi}(t)\right)$ with the given $\left(\bar{a}(0), \bar{\varphi}(0)\right)$. This means the stationary response of equations (4.2.3) is completely described by the one-point motion. Since the selection of $\bar{\boldsymbol{\sigma}}$ which resulting in equation (4.2.5) does not change the form of Fokker-Plank equation associating with equations (4.2.3), the stability of amplitude of the one-point motion can be determined through equation (4.2.5), which is decoupled from $\bar{\varphi}(t)$ and is easier to solve.

However, if one is interested in the variation of invariant measure for the random dynamical system generated by equations (4.2.3), the n-point motion, i.e. the simultaneous motion of n pairs of $\left(\bar{a}(t), \bar{\varphi}(t)\right)$ with different initial conditions has to be considered. This implies that the system is studied in the view of stochastic flow [15]. There are many possible stochastic differential equations which have the same one-point motion as that of equations (4.2.3) [67], different choices of stochastic differential equations may have different invariant measures [15]. Since only the amplitude of motion of the original equation (4.2.1) is of interested in this chapter, and the study of stability is through the corresponding linearized system, it is an appropriate way to consider the stability of equation (4.2.5). For more details about the n-point motion and stochastic flow, one may refer to [67], and other articles such as [15], [14], [6], [98], [99], [16], and [17].

It is observed that the nonlinearity of stiffness term in system (4.2.1) does not contribute in the averaged equation (4.2.5). This is due to the transformation (3.2.1) in standard stochastic averaging method, which appears to neglect the contribution from the cubic nonlinear stiffness term. If the viscoelastic terms do not appear in equation (4.2.1), i.e. if system (4.2.1) reduces to an elastic nonlinear system, the standard stochastic averaging method leads to a linear averaged system, which makes it impossible to study stochastic bifurcation. Therefore standard averaging method is generally ineffective in investigating systems with strong nonlinearity in stiffness terms [95], [93]. If the nonlinearity in stiffness term can not be neglected, modified averaging method accounting the total system energy may be applied to certain autonomous systems whose stiffness terms are integrable [94].

However, the viscoelastic terms in equation (4.2.1) make the system being non-autonomous, thus it is not an easy task to proceed following the modified averaging method. Fortunately, the presence of viscoelasticity leads to an averaged equation including nonlinear effect as in equation (4.2.5), which is of great importance in stability analysis. Moreover, δ is small because both δ_1 and δ_2 are small constants for most materials characterized by equation (4.1.5). This means the contribution from nonlinear stiffness term may be neglected compared to the damping effect of viscoelasticity. Hence, the approximation from the standard stochastic averaging method in this section is easier to apply and may be acceptable in applications.

4.2.2 Stability and Bifurcation of the Averaged System

The Stratonovich form of equation (4.2.5) is

$$\mathrm{d}\bar{a} = \varepsilon\Big[\Big(\eta_1 - \frac{1}{2}\eta_3^2\Big)\bar{a} - \eta_2\bar{a}^3\Big]\mathrm{d}t + \varepsilon^{1/2}\eta_3\bar{a}\circ\mathrm{d}W(t), \tag{4.2.7}$$

which acts as a mathematical model of the deterministic system

$$\frac{\mathrm{d}\bar{a}}{\mathrm{d}t} = \varepsilon\Big[\Big(\eta_1 - \frac{1}{2}\eta_3^2\Big)\bar{a} - \eta_2\bar{a}^3\Big] \tag{4.2.8}$$

under parametric white noise perturbation.

Consider the deterministic nonlinear system (4.2.8). Note that $\bar{a}$ should be non-negative in transformation (3.2.1), thus, from the deterministic stability theory, it is known that there

are equilibrium points $a_0 = 0$ in all cases, and

$$a_1 = \sqrt{\frac{1}{\eta_2}\Big(\eta_1 - \frac{1}{2}\eta_3^2\Big)},$$

if $\eta_1 - \frac{1}{2}\eta_3^2$ and η_2 take the same signs. Linear stability analysis shows that the eigenvalue, i.e. the Lyapunov exponent associated with $a_0 = 0$, is

$$\lambda_0 = \varepsilon\Big(\eta_1 - \frac{1}{2}\eta_3^2\Big).$$

Therefore the trivial solution is stable if $\lambda_0 < 0$. Similarly, by linearizing equation (4.2.8) near a_1 as

$$\frac{\mathrm{d}u}{\mathrm{d}t} = \varepsilon\Big[\Big(\eta_1 - \frac{1}{2}\eta_3^2\Big) - 3\eta_2\bar{a}_1^2\Big]u,$$

where u denotes the variation of solution from a_1, it can be seen that the eigenvalue associated with a_1 is

$$\lambda_1 = \varepsilon\Big[\Big(\eta_1 - \frac{1}{2}\eta_3^2\Big) - 3\eta_2\bar{a}_1^2\Big] = -2\varepsilon\Big(\eta_1 - \frac{1}{2}\eta_3^2\Big),$$

which indicates that the non-trivial solution a_1 is stable when $\lambda_1 < 0$.

Clearly, noise in equation (4.2.5) or (4.2.7) is multiplicative with respect to the trivial solution, since $a_0 = 0$ is also the solution of the noise-disturbed system. On the other hand, is additive with respect to the non-trivial solution of the undisturbed system (4.2.8) because a_1 cannot solve equation (4.2.5) or (4.2.7) [10].

For the stochastic nonlinear system (4.2.5) or (4.2.7), it is obvious that $a_0 = 0$ is the trivial stationary solution. In order to find the the non-trivial stationary solution $a_s(t)$, i.e. the "stochastic attractor", one may follow the procedure in [3]. Letting $r_s(t) = \ln a_s(t)$ and applying Itô's Lemma lead to

$$\mathrm{d}r_s = \varepsilon\Big(\eta_1 - \frac{1}{2}\eta_3^2 - \eta_2 a_s^2\Big)\,\mathrm{d}t + \varepsilon^{1/2}\eta_3\,\mathrm{d}W(t). \tag{4.2.9}$$

Since $a_s(t)$ is stationary, so is $r_s(t)$, thus

$$\frac{\mathrm{dE}\big[r_s(t)\big]}{\mathrm{d}t} = 0.$$

Taking expectation on both sides of equation (4.2.9) yields

$$\eta_1 - \frac{1}{2}\eta_3^2 - \eta_2 \mathrm{E}\big[a_s^2\big] = 0. \tag{4.2.10}$$

Define η^* by

$$\eta^* \triangleq \frac{1}{\eta_2}\Big(\eta_1 - \frac{1}{2}\eta_3^2\Big). \tag{4.2.11}$$

It can be seen that, only when $\eta^* > 0$, $\mathrm{E}\left[a_s^2\right]$ can be solved from equation (4.2.10) as

$$\mathrm{E}\left[a_s^2\right] = \eta^* = \frac{1}{\eta_2}\Big(\eta_1 - \frac{1}{2}\eta_3^2\Big), \tag{4.2.12}$$

i.e. the non-trivial stationary solution only exists when $\eta^* > 0$.

The stationary probability density $p_s(a)$ for system (4.2.5) is determined by the Fokker-Planck equation

$$-\frac{\mathrm{d}\big[\varepsilon\big(\eta_1 a - \eta_2 a^3\big)p_s(a)\big]}{\mathrm{d}a} + \frac{1}{2}\frac{\mathrm{d}^2\big[\varepsilon\eta_3^2 a^2 p_s(a)\big]}{\mathrm{d}a^2} = 0. \tag{4.2.13}$$

Solving equation (4.2.13) yields, $p_s(a) = \delta(a)$ associated with the trivial solution in all cases, where $\delta(a)$ is the Dirac delta function; and when $\eta_1 - \frac{1}{2}\eta_3^2 > 0$,

$$p_s(a) = \begin{cases} Ca^{2\eta_1/\eta_3^2 - 2}\exp\Big(-\dfrac{\eta_2 a^2}{\eta_3^2}\Big), & a > 0, \\ 0 & a \leqslant 0, \end{cases} \tag{4.2.14}$$

where C is a normalization constant. The condition that $p_s(a)$ is a density function requires $\eta_2 > 0$, therefore $\eta^* > 0$ is satisfied and the existence of the non-trivial stationary solution is confirmed.

The stability of stochastic dynamical system in the form of equation (4.2.5) or (4.2.7) has been well-studied in many books and articles such as [10]. Since the Lyapunov exponents of a stochastic system can characterize its almost-sure stability, the largest Lyapunov exponent of equation (4.2.5) is solved below and then the stability of the trivial and non-trivial stationary solutions can be determined.

By linearizing equation (4.2.5) at the trivial solution $a_0 = 0$, the corresponding Lyapunov exponent is given by

$$\lambda_0 = \varepsilon\Big(\eta_1 - \frac{1}{2}\eta_3^2\Big) = \varepsilon\Big[-\beta - \frac{1}{2}\omega\mathcal{H}^s(\omega) + \frac{1}{8}\omega^2 S(2\omega)\Big]. \tag{4.2.15}$$

It can be seen that the nonlinearity in viscoelasticity has no contribution in λ_0, therefore it does not affect the almost-sure stability of the trivial solution.

Denote the variation of solution from the non-trivial stationary solution $a_s(t)$ by

$$u(t) = \bar{a}(t) - a_s(t).$$

Then $u(t)$ can be used to determine the stability of $a_s(t)$. Substituing $u(t)$ into equation (4.2.5) and considering the linear parts with respect to $u(t)$ lead to the linearized system

$$\mathrm{d}u = \varepsilon\left(\eta_1 - 3\eta_2 a_s^2\right)u\,\mathrm{d}t + \varepsilon^{1/2}\eta_3 u\,\mathrm{d}W(t). \tag{4.2.16}$$

Letting $r(t) = \ln\left|u(t)\right|$ and applying Itô's Lemma yield

$$\mathrm{d}r = \varepsilon\left(\eta_1 - \frac{1}{2}\eta_3^2 - 3\eta_2 a_s^2\right)\mathrm{d}t + \varepsilon^{1/2}\eta_3\,\mathrm{d}W(t),$$

i.e.

$$r(t) = r(0) + \varepsilon\int_0^t \left(\eta_1 - \frac{1}{2}\eta_3^2 - 3\eta_2 a_s^2\right)\mathrm{d}s + \int_0^t \varepsilon^{1/2}\eta_3\,\mathrm{d}W(s).$$

Since $a_s(t)$ is stationary and ergodic, from the ergodic theory it is known that

$$\lim_{t\to\infty}\frac{1}{t}\int_0^t a_s^2\mathrm{d}s = \mathrm{E}\left[a_s^2\right]. \tag{4.2.17}$$

Thus using the law of iterated logarithm for Wiener process, equations (4.2.17) and (4.2.12), the Lyapunov exponent for the non-trivial stationary solution is given by

$$\begin{aligned}\lambda_1 &= \lim_{t\to\infty}\frac{1}{t}\ln\left|u(t)\right| = \varepsilon\left(\eta_1 - \frac{1}{2}\eta_3^2 - 3\eta_2\mathrm{E}\left[a_s^2\right]\right)\\ &= -2\varepsilon\left(\eta_1 - \frac{1}{2}\eta_3^2\right) = 2\varepsilon\left[\beta + \frac{1}{2}\omega\mathcal{H}^s(\omega) - \frac{1}{8}\omega^2 S(2\omega)\right].\end{aligned} \tag{4.2.18}$$

When λ_1 is negative, $a_s(t)$ is stable w.p.1. Again, the nonlinearity in viscoelasticity does not affect the almost-sure stability of the non-trivial solution.

From equations (4.2.15) and (4.2.18), it can be seen that, when system parameters change such that λ_0 varies from negative to positive, the trivial solution will change its stability from stable to unstable with probability one. If $\eta^* > 0$ such that the non-trivial solution exists, because λ_1 takes the opposite sign as λ_0, λ_1 will change from positive to negative and thus the non-trivial solution will change from unstable state to stable state with probability one. This means the "jump" from a stationary solution to another stationary solution, and indicates that system (4.2.5) exhibits stochastic dynamic or D-bifurcation [10] at the point where $\eta_1 - \frac{1}{2}\eta_3^2 = 0$.

If the non-trivial solution exists with the stationary density function given by equation (4.2.14), one may describe the properties of $p_s(a)$ by its shape. The peak value of $p_s(a)$, if exists, locates at the point where $\dfrac{\mathrm{d}p_s(a)}{\mathrm{d}a}=0$. For $a>0$,

$$\frac{\mathrm{d}p_s(a)}{\mathrm{d}a}=2C\frac{\eta_1-\eta_3^2-\eta_2a^2}{\eta_3^2}a^{2\eta_1/\eta_3^2-3}\exp\Big(-\frac{\eta_2a^2}{\eta_3^2}\Big). \tag{4.2.19}$$

Since $\eta_2>0$, it can be seen that equation $\mathrm{d}p_s(a)/\mathrm{d}a=0$ has solution only when $\eta_1-\eta_3^2>0$. This indicates that when $\eta_1-\eta_3^2\le 0, p_s(a)$ has no peak; while $\eta_1-\eta_3^2>0, p_s(a)$ has one peak. Thus the shape of $p_s(a)$ has a qualitative change, i.e. the system exhibits phenomenological or P-bifurcation [10], at the point where $\eta_1-\eta_3^2=0$.

Define two variables b_D and b_P as

$$b_D\triangleq\eta_1-\frac{1}{2}\eta_3^2=-\beta-\frac{1}{2}\omega\mathcal{H}^s(\omega)+\frac{1}{8}\omega^2S(2\omega), \tag{4.2.20}$$

$$b_P\triangleq\eta_1-\eta_3^2=-\beta-\frac{1}{2}\omega\mathcal{H}^s(\omega)+\frac{1}{16}\omega^2S(2\omega). \tag{4.2.21}$$

Obviously $b_D>b_P$, $\lambda_0=\varepsilon b_D$, $\lambda_1=-2\varepsilon b_D$. The complete bifurcation scheme can be described as follow.

When $b_P<b_D<0$, one has $\lambda_0<0, \lambda_1>0$, thus only the trivial solution exists and is stable. If the system parameters change such that $b_P<0<b_D$, the Lyapunov exponents become $\lambda_0>0, \lambda_1<0$, therefore the trivial solution loses its stability, and the non-trivial stationary solution appears and is stable. This indicates that, phenomenally, the solution of the system "jumps" from the trivial solution to the non-trivial stationary solution. Furthermore, if system parameters continue changing such that $0<b_P<b_D$, the stability of the stationary solutions do not change, i.e. only the non-trivial stationary solution appears as stable. However, the shape of the stationary density function changes, from having no peak to having one peak.

The bifurcation phenomenon can be clearly described in Figure 4.2, with the power spectral density of the wide-band noise being the varied parameter. The D-bifurcation point is given by

$$S_D=\frac{8}{\omega^2}\Big[\beta+\frac{1}{2}\omega\mathcal{H}^s(\omega)\Big],$$

while the P-bifurcation point is

$$S_P = \frac{16}{\omega^2}\left[\beta + \frac{1}{2}\omega \mathcal{H}^s(\omega)\right].$$

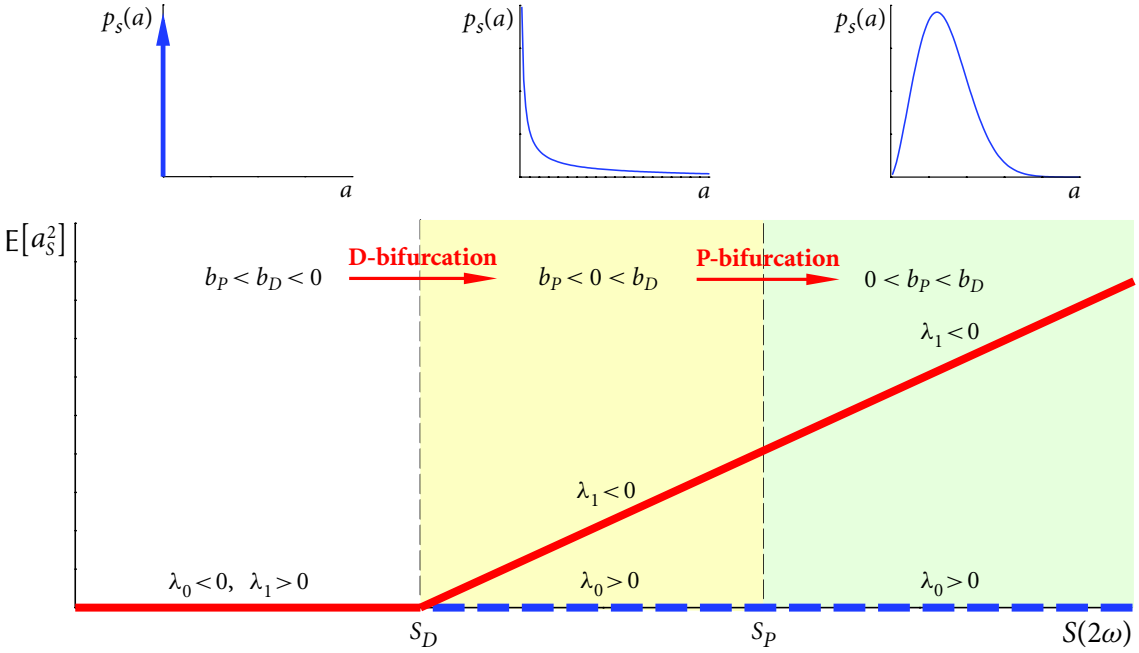

Figure 4.2 Illustration of D-bifurcation and P-bifurcation

4.2.3 Numerical Results and Discussion

In order to validate the approximate analytical results in the previous section, Monte Carlo simulation is applied to the original nonlinear viscoelastic system (4.2.1). The Maxwell viscoelastic model is considered, i.e. the viscoelastic kernel function is taken as $H(t) = \gamma e^{-\kappa t}$.

The wide-band excitation is taken as the Gaussian white noise with constant power spectral density σ^2. Let

$$x_1(t) = q(t), \quad x_2(t) = \dot{q}(t), \quad x_3(t) = \int_0^t H(t-s)\,q(s)\mathrm{d}s,$$

$$x_4(t) = \int_0^t H(t-s)q^3(s)\,\mathrm{d}s. \tag{4.2.22}$$

Equation (4.2.1) can be converted to Itô differential equations, which are the same as Stratonovich form,

$$\mathrm{d}\begin{Bmatrix} x_1 \\ x_2 \\ x_3 \\ x_4 \end{Bmatrix} = \begin{Bmatrix} x_2 \\ -2\varepsilon\beta x_2 - \omega^2 x_1 + \varepsilon\omega^2 x_3 - \delta\omega^2 x_1^3 + \varepsilon\delta\omega^2 x_4 \\ \gamma x_1 - \kappa x_3 \\ \gamma x_1^3 - \kappa x_4 \end{Bmatrix} \mathrm{d}t + \begin{Bmatrix} 0 \\ \varepsilon^{1/2}\omega^2\sigma x_1 \\ 0 \\ 0 \end{Bmatrix} \mathrm{d}W(t) \tag{4.2.23}$$

The explicit Euler scheme is applied to simulate the response of system (4.2.23), i.e.

$$\begin{aligned} x_1^{k+1} &= x_1^k + x_2^k \cdot h, \\ x_2^{k+1} &= x_2^k + \left[-\omega^2 x_1^k - 2\varepsilon\beta x_2^k + \varepsilon\omega^2 x_3^k + \varepsilon\delta\omega^2 x_4^k - \delta\omega^2\left(x_1^k\right)^3\right] \cdot h + \varepsilon^{1/2}\omega^2\sigma \cdot \Delta W^k, \\ x_3^{k+1} &= x_3^k + \left(\gamma x_1^k - \kappa x_3^k\right) \cdot h, \\ x_4^{k+1} &= x_3^k + \left[\gamma\left(x_1^k\right)^3 - \kappa x_4^k\right] \cdot h. \end{aligned}$$

The amplitude of response is taken as, corresponding to equation (3.2.1),

$$a(t) = \left[x_1^2 + \left(\frac{x_2}{\omega}\right)^2\right]^{1/2}. \tag{4.2.24}$$

In the simulation, time step is chosen as $h = 0.0005$. The following parameters are fixed as: $\varepsilon = 0.1, \omega = 1, \beta = 0.05$.

In order to illustrate the stationary solution and inspect the bifurcation phenomenon, different initial conditions should be used. A simple choice is to initialize the samples with the initial displacement and velocity $\left(x_1(0), x_2(0)\right)$ uniformly distributed in a region.

Figures 4.3 to 4.6 show the numerical solutions for $\sigma = 0.5$, $\sigma = 1.0$, and $\sigma = 1.5$, respectively, with $\gamma = 0.5, \kappa = 3, \delta = 0.01$ fixed. The sample size is taken up to $N = 50000$ to better illustrate the statistic properties. The histogram of $a(T)$ can be an approximation of the stationary probability density $p_s(a)$ when T is large enough.

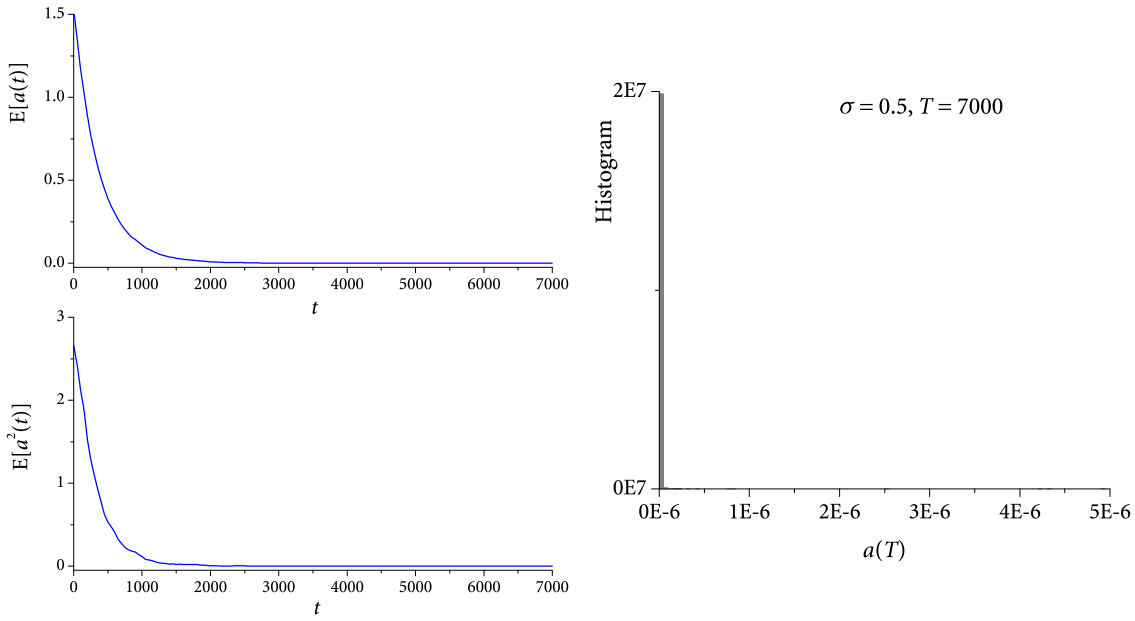

Figure 4.3 Stationary solution for $\delta = 0.01, \sigma = 0.5$

A simple calculation shows that, for $\sigma = 0.5$,

$$b_D = -\beta - \frac{1}{2}\omega H^s(\omega) + \frac{1}{8}\omega^2\sigma^2 = -0.04375 < 0,$$
$$b_P = -\beta - \frac{1}{2}\omega H^s(\omega) + \frac{1}{16}\omega^2\sigma^2 = -0.059375 < 0,$$
$$\lambda_0 = \varepsilon b_D = -0.004375 < 0, \quad \lambda_1 = -2\varepsilon b_D = 0.00875 > 0. \tag{4.2.25}$$

Obviously, approximate analytical results show that the trivial solution is a stable stationary solution. This is indicated in Figure 4.3, as the first- and second-order moment appear to be zero and have almost no change when simulation time $t > 2000$. The histogram of $a(T)$ at $T = 7000$ shows that the stationary density function approaches the Dirac function.

In the case $\sigma = 1.0$,

$$b_D = -\beta - \frac{1}{2}\omega H^s(\omega) + \frac{1}{8}\omega^2\sigma^2 = 0.05 > 0,$$
$$b_P = -\beta - \frac{1}{2}\omega H^s(\omega) + \frac{1}{16}\omega^2\sigma^2 = -0.0125 < 0,$$
$$\lambda_0 = \varepsilon b_D = 0.005 > 0, \quad \lambda_1 = -2\varepsilon b_D = -0.01 < 0. \tag{4.2.26}$$

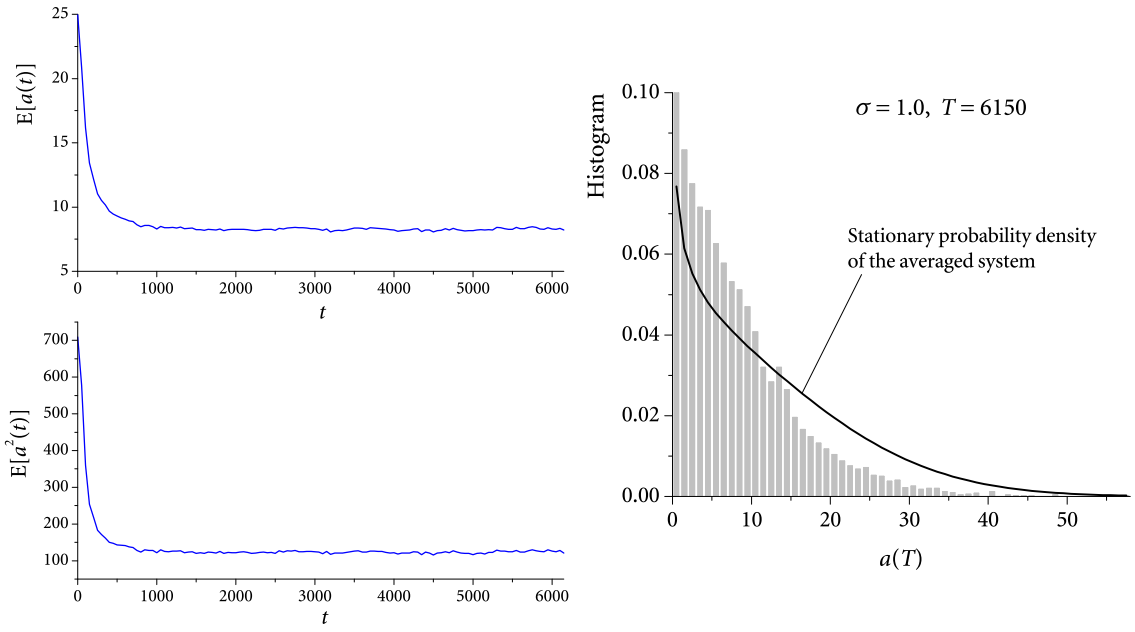

Figure 4.4 Stationary solution for $\delta = 0.01, \sigma = 1.0$

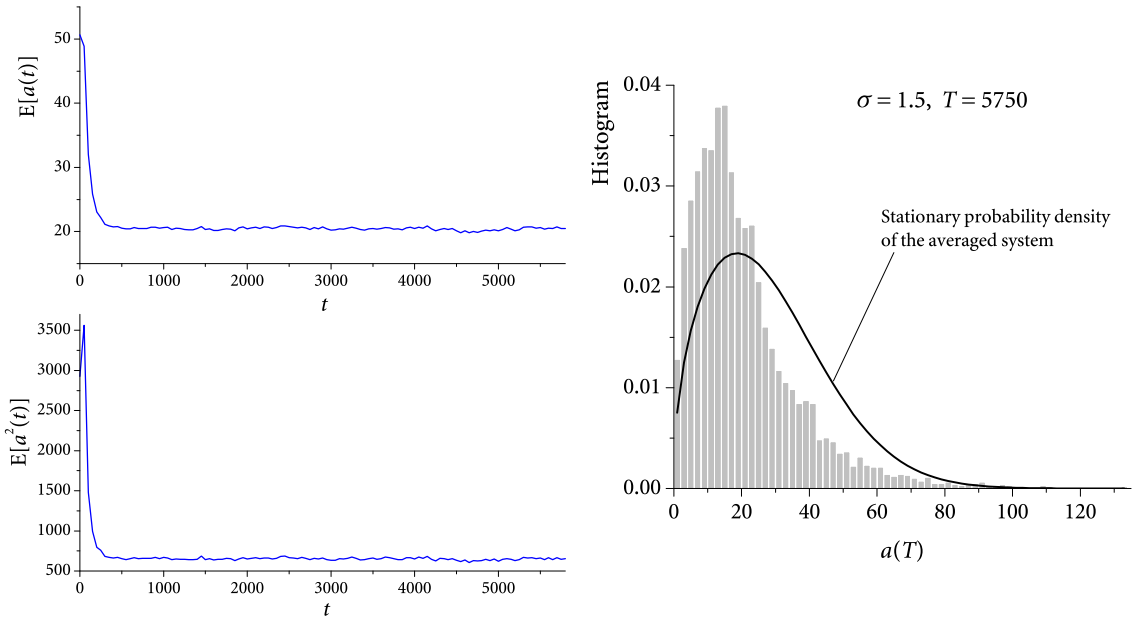

Figure 4.5 Stationary solution for $\delta = 0.01, \sigma = 1.5$

Since $b_P < 0 < b_D$, the trivial solution loses its stability property, and the solution should appear as a non-trivial solution, i.e. D-bifurcation has occurred. The trends of $\mathrm{E}[a_s]$ and

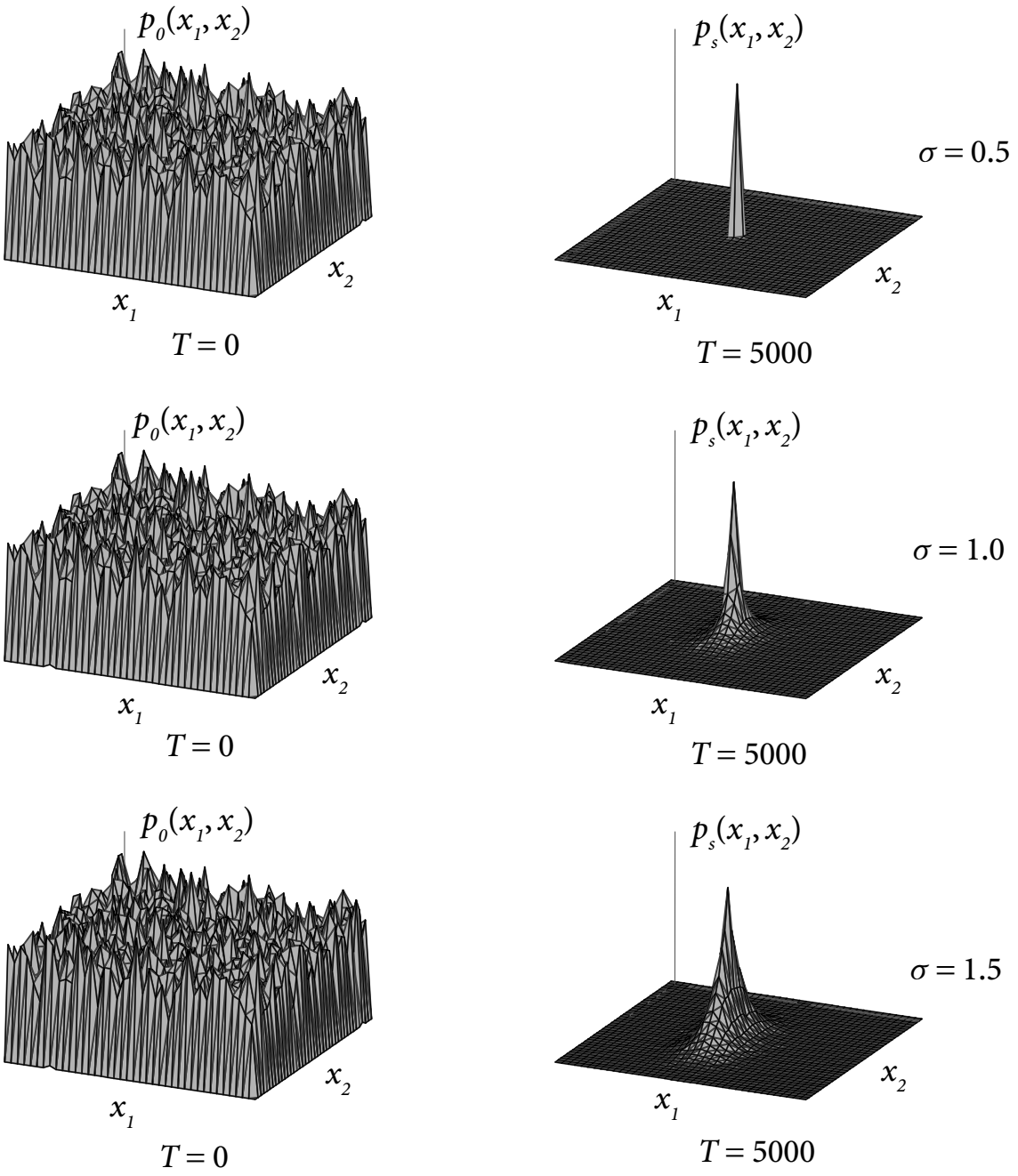

Figure 4.6 Joint histograms of stationary solutions for different values of σ ($\delta = 0.01$)

$\mathrm{E}\left[a_s^2\right]$ and their values for large t in Figure 4.4 show that it is true. Moreover, the histogram of $a(T)$ for large simulation time $T = 6150$ has no peak, just the same as what the approximate

analytical result predicts. This indicates that the attraction from the non-trivial stationary solution is not strong enough, thus most sample trajectories are still be attracted by the trivial solution. The stationary density function of the averaged system given by equation (4.2.14) is plotted and compared with the histogram of $a(T)$. It shows that the averaged system has some difference with the original system, although their stability properties are similar.

For $\sigma = 1.5$,

$$
\begin{aligned}
b_D &= -\beta - \frac{1}{2}\omega \mathcal{H}^s(\omega) + \frac{1}{8}\omega^2\sigma^2 = 0.20625 > 0, \\
b_P &= -\beta - \frac{1}{2}\omega \mathcal{H}^s(\omega) + \frac{1}{16}\omega^2\sigma^2 = 0.065625 > 0, \\
\lambda_0 &= \varepsilon b_D = 0.020625 > 0, \quad \lambda_1 = -2\varepsilon b_D = -0.04125 < 0.
\end{aligned} \tag{4.2.27}
$$

It is expected that the stability of non-trivial stationary solution should not change. This is also verified by Figure 4.5. One peak appears in the histogram of $a(T)$ at time $T = 5800$, which agrees with the approximate analytical result and shows that P-bifurcation has occurred. The difference of the stationary density function $p_s(a)$ and the histogram of $a(T)$ again shows that the averaged system can not thoroughly describe the behaviour of the original system.

Some joint density fuctions of the state variables x_1 and x_2, i.e. the displacement and velocity of the system, are shown in Figure 4.6. They can be approximated by the joint histograms of x_1 and x_2. The left column is the initial joint densities $p_0(x_1, x_2)$ at $t = 0$, which are set to be uniformly distributed in a rectangle region. The right column shows the stationary densities $p_s(x_1, x_2)$, which are approximated at large simulation time $T = 5000$. The differences of $p_s(x_1, x_2)$ can be seen in the figure.

In order to simulate the Lyapunov exponents, linearization near the stationary solution is required. For the Lyapunov exponent λ_0, which is related to the trivial solution, the

equations for simulation is

$$\mathrm{d}\begin{Bmatrix} u_1 \\ u_2 \\ u_3 \\ u_4 \end{Bmatrix} = \begin{Bmatrix} u_2 \\ -2\varepsilon\beta u_2 - \omega^2 u_1 + \varepsilon\omega^2 u_3 + \varepsilon\delta\omega^2 u_4 \\ \gamma u_1 - \kappa u_3 \\ -\kappa u_4 \end{Bmatrix} \mathrm{d}t + \begin{Bmatrix} 0 \\ \varepsilon^{1/2}\omega^2\sigma u_1 \\ 0 \\ 0 \end{Bmatrix} \mathrm{d}W(t). \tag{4.2.28}$$

While for the Lyapunov exponent λ_1 related to the non-trivial solution, the equations for simulation become

$$\mathrm{d}\begin{Bmatrix} u_1 \\ u_2 \\ u_3 \\ u_4 \end{Bmatrix} = \begin{Bmatrix} u_2 \\ -2\varepsilon\beta u_2 - \omega^2 u_1 + \varepsilon\omega^2 u_3 + \varepsilon\delta\omega^2 u_4 - 3\delta\omega^2 (x_1^{st})^2 u_1 \\ \gamma u_1 - \kappa u_3 \\ 3\gamma (x_1^{st})^2 u_1 - \kappa u_4 \end{Bmatrix} \mathrm{d}t$$

$$+ \begin{Bmatrix} 0 \\ \varepsilon^{1/2}\omega^2\sigma u_1 \\ 0 \\ 0 \end{Bmatrix} \mathrm{d}W(t), \tag{4.2.29}$$

where x_1^{st} is the stationary solution of equation (4.2.23), i.e. the simultion of λ_1 should start after the sample solutions of equation (4.2.23) have entered stationary state. This can be reached by running the iteration of equation (4.2.23) for a long enough period of time.

Figures 4.7 shows the simulated Lyapunov exponents for different values of σ with $\gamma = 0.5$, $\kappa = 3$. The results for two cases, $\delta = 0.01$ and $\delta = 0.1$, are plotted in the same figure. The analytical results given by equations (4.2.15) and (4.2.18) are also plotted in the figure for comparison. It can be seen that the approximate Lyapunov exponents related to the trivial solution λ_0 agree very well with the simulation results. However, the simulation results of λ_1 through equation (4.2.29) stand totally on the opposite side of the axis, although the simulation results in Figures 4.3 to 4.6 show that the non-trivial stationary solutions are stable. The reason may be due to the method of simulation, i.e. the linearized equation

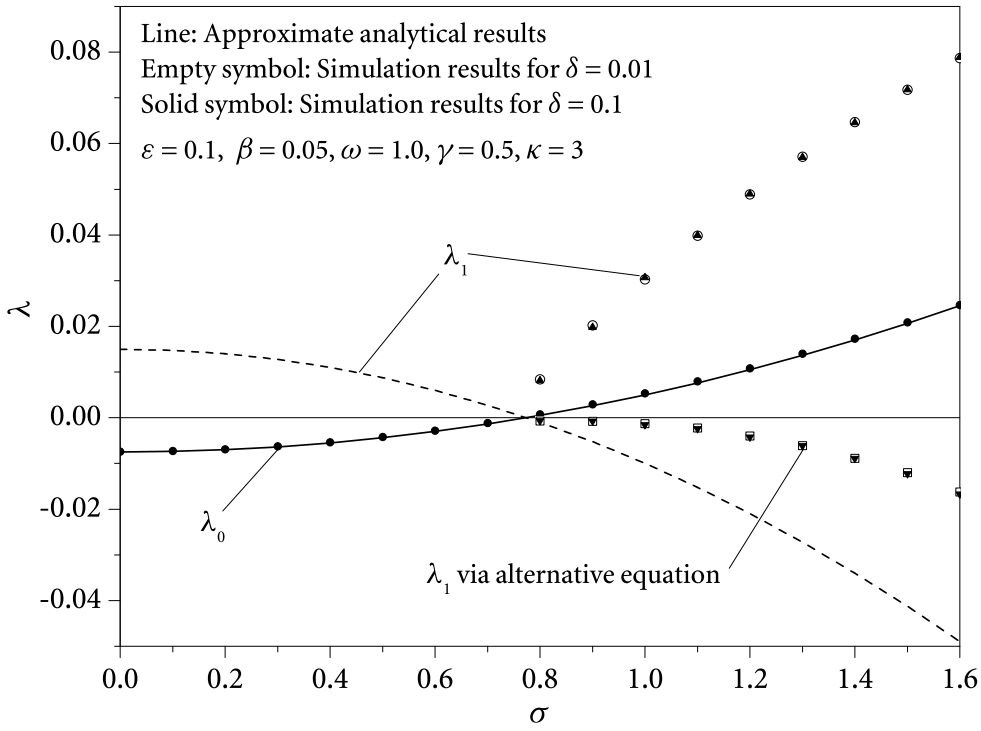

Figure 4.7 Lyapunov exponents for different values of σ

(4.2.29) near the non-trivial stationary solution may not be proper in numerical calculation of λ_1. Although the simulated stationary solutions have close probability properties with the true stationary solutions in the statistic sense, each single trajectory may have large changes or jumps during the simulation, which makes the estimation of variation between the staionary solution and the perturbed solution impossible.

An alternative way of simulation of λ_1 is through the equation

$$\mathrm{d}u = \varepsilon\Big[\eta_1 - 3\eta_2\big(a^{st}(t)\big)^2\Big]u\,\mathrm{d}t + \varepsilon^{1/2}\eta_3 u\,\mathrm{d}W(t), \tag{4.2.30}$$

which is the linearization of equation (4.2.5) near its non-trivial stationary solution, and $a^{st}(t)$ is the non-trivial staionary solution of the original system (4.2.1) and can be obtained by equation (4.2.24) using the stationary simulation results of (4.2.23). The simulated $a^{st}(t)$ is be better than $x_1^{st}(t)$ because it is the amplitude of motion and has much less variation than every single state variable. However, equation (4.2.5) is the averaged version of equation (4.2.1), thus it is still not sufficient to describe the stability properties of the true stationary

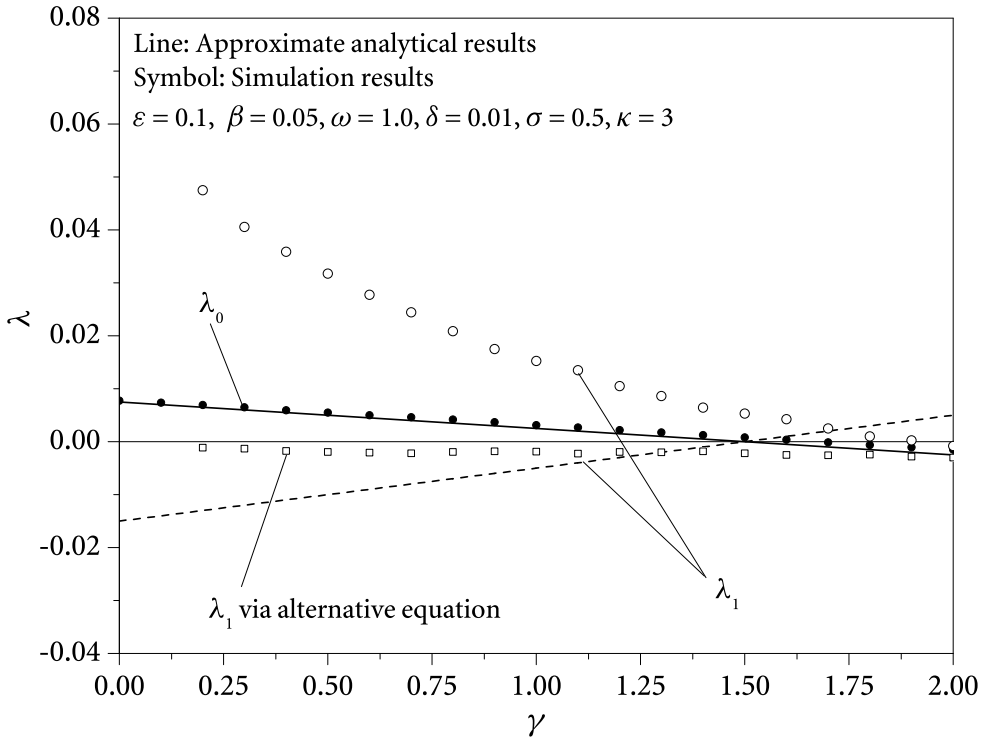

Figure 4.8 Lyapunov exponents for different values of γ

solution. The simulated Lyapunov exponents λ_1 through the alternative equation (4.2.30) are plotted in Figure 4.7. It can be seen that they correctly indicate that the true non-trivial stationary solution is stable, but the rates of decay may not be accurate.

All the simulated results of λ_1 in Figure 4.7 show that different values of δ have very little effect in the stability of the stationary solutions, provided that δ is small. This verifies the approximate ananlytical result obtained in Section 4.2.2, where it is stated that δ has no contribution to the Lyapunov exponents.

Figures 4.8 and 4.9 show the comparison of the Lyapunov exponents for different values of γ and κ, which illustrate the effect of viscoelasticity on the stability of stationary solutions. Both figures confirm that the analytical approximation through averaging agrees with the simulation of λ_0, i.e. the stability of trivial solution. It can be seen that, with the increase of viscoelastic intensity, the trivial solutions will change from unstable to stable. That is, viscoelasticity helps to reduce the amplitude of vibration. On the other hand, with the

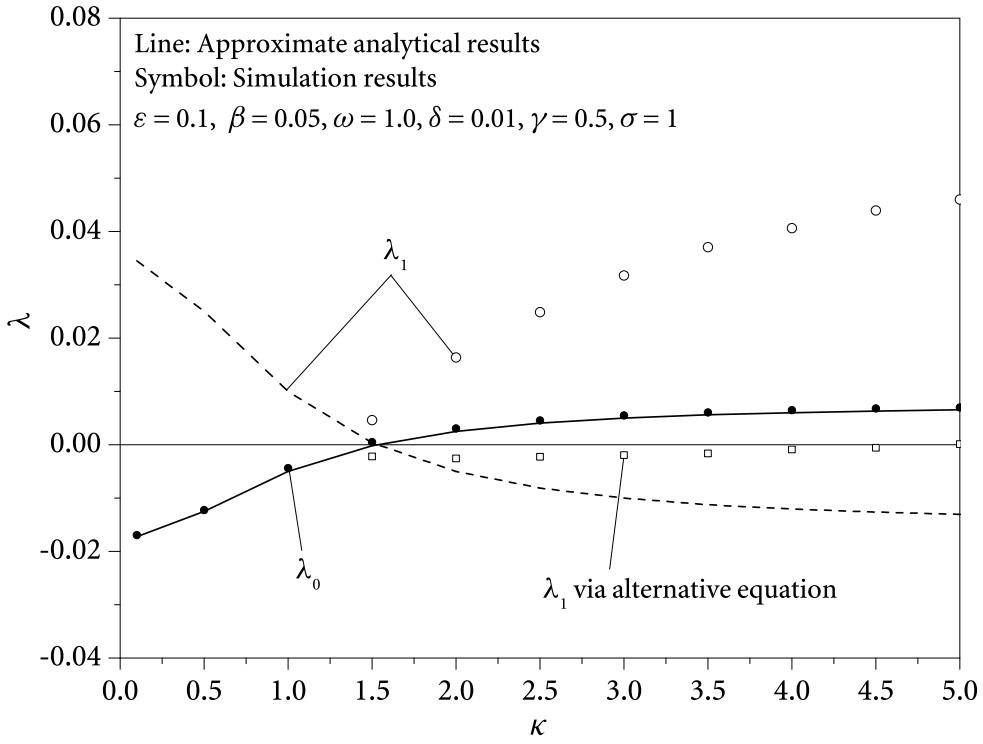

Figure 4.9 Lyapunov exponents for different values of κ

decrease of κ, or the increase of the relaxation time $1/\kappa$, the trivial solutions also become stable. Therefore materials with longer relaxation time help to stabilize the system to a lower level of vibration.

Figure 4.10 shows the approximated analytical results of the Lyapunov exponents obtained through stochastic averaging with the variation of γ and κ, for the case of $S(2\omega) = 1.5$, where both the boundaries of D-bifurcation and P-bifurcation are plotted. It can be seen that, under the excitation of wide-band noise with a certain intensity, the nonlinear viscoelastic system stays near the non-trivial staionary solution when γ is small. When γ increases, the system change to stay near the trivial staionary solution. The larger the value of γ, the wider the area where the system stays near zero.

4.3 Summary

The stochastic stability and bifurcation of a SDOF nonlinear viscoelastic system under the parametric excitation of wide-band noise are studied in Section 4.2. By applying the standard stochastic averaging method and the averaging method for integro-differential equations, the largest Lyapunov exponents associated with the trivial and non-trivial stationary solutions are obtained for the nonlinear averaged system.

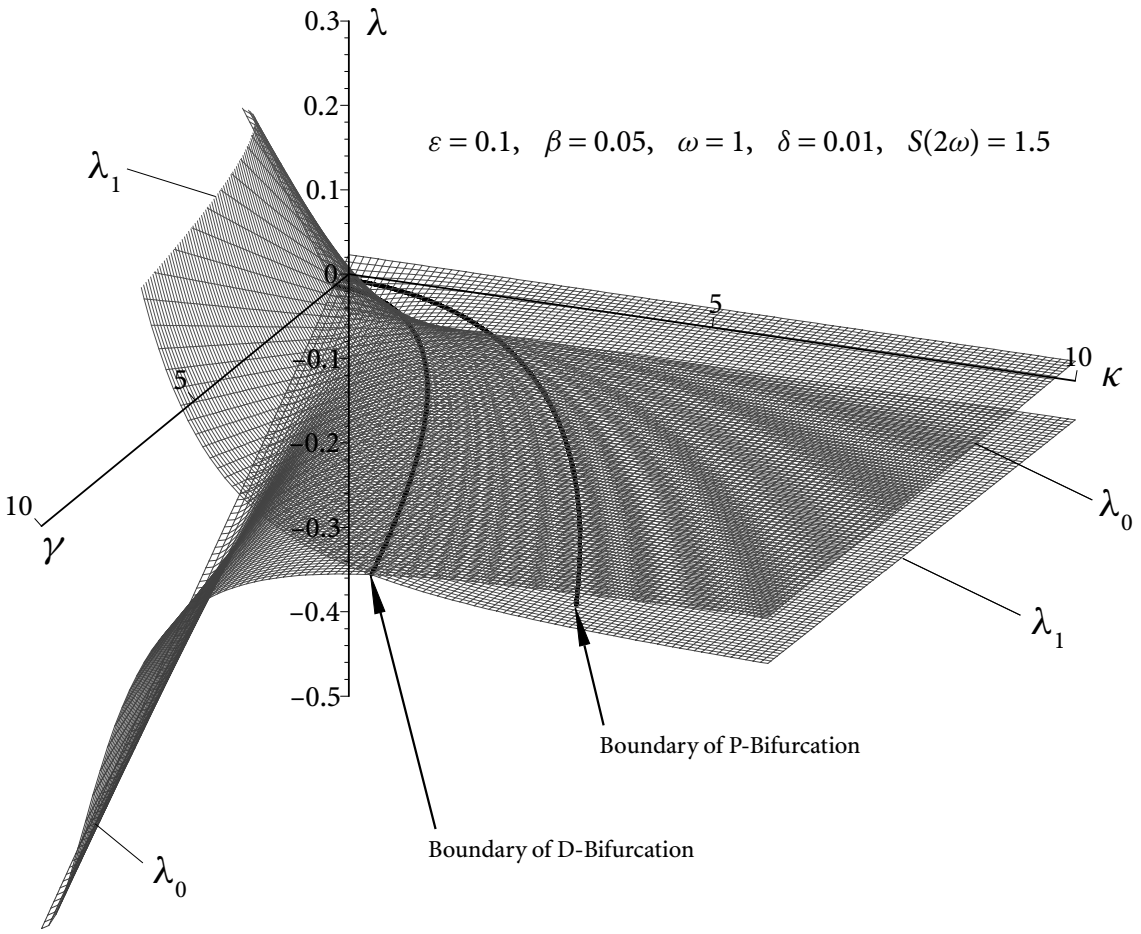

Figure 4.10 Lyapunov exponents and boundaries of bifurcations

The existence of nonlinearity induces stochastic bifurcation when the intensity of random excitation increases, which makes it different from the linear case. Combining the largest Lyapunov exponents and the stationary probability density, the existence of nonlinear

viscoelasticity indicates that, when the power spectral density of wide-band excitation increases, the system "jumps" from the trivial solution to the non-trivial stationary solution with probability one. When the intensity of excitation continues to increase, the stationary probability density $p_s(a)$ will change its form, from having no peak to having one peak.

The existence of viscoelasticity always help to stabilize the system to the static state in the sense that the largest Lyapunov exponents associated with the trivial solution are smaller and the energy of random excitation required to stimulate the stochastic bifurcation is larger. Unlike linear viscoelastic systems, with the increase of the intensity of excitation, the amplitude of vibration of a nonlinear viscoelastic system does not increase to infinity with probability one, but limit to a higher level of vibration with large probability. This is an important property in engineering applications of viscoelastic materials.

Monte Carlo simulation confirms the bifurcation phenomena. The simulated results show that the standard stochastic averaging method provides a good approximation for the nonlinear viscoelastic system when the nonlinear effect is small. The discrepancy of the largest Lyapunov exponents between simulation and analytical approximation appears after D-bifurcation occurs, this means an improvement of simulation methods should be considered.

CHAPTER 5

Conclusions and Future Research

5.1 Conclusions

The objective of this thesis is to study the stability properties of viscoelastic systems under stochastic excitations. The equations of motion of viscoelastic bodies appear to be integro-partial differential equations due to the time history dependence of viscoelastic constitutive relation. Therefore, it is impossible to solve the equations analytically in almost all the cases. Under certain boundary conditions, the general equations of motions may reduce to integro-differential equations, which are easier to be investigated, analytically or numerically. The Lyapunov exponents, which characterize the almost-sure stability, and the moment Lyapunov exponents, which describe the moment stability, may be obtained through different approximate methods. Since the equations of motion of a viscoelastic body includes the time history, they are non-autonomous. Hence, it is required to study the moment stability of such systems so that the complete behaviour of the responses can be determined.

Monte Carlo simulation is an important numerical approach to study the properties of stochastic dynamical systems. It may also be a referential criterion to determine how accurate the approximate analytical solution is. The simulated moment Lyapunov exponents may be evaluated through the sample average of norms. However, when a system is unstable, its solution may grow exponentially with large variance. This makes the estimation of

moments through sample average norms inaccurate. Therefore a good algorithm for the simulation of moment Lyapunov exponents is necessary.

An improved algorithm for simulating the moment Lyapunov exponents of linear homogenuous systems is presented in Chapter 2. The importance of linear homogenuous systems lies in the fact that studying the stability of a general stochastic dynamical system usually leads to the stability problem of a homogeneous system linearized near the stationary solution. Considering the asymptotic normality of the logarithm of norm, which is satisfied by most systems in applications, the estimation of moments is converted to the estimation of mean and variance of the logarithm of norm, which uses the results of sums of independent random variables by Komlós-Major-Tusnády. Numerical examples show that this approach works well for different cases in engineering applications.

The stability of a single degree-of-freedom linear viscoelastic system under the parametric excitation of wide-band noise and narrow-band noise is studied in Chapter 3, where the bounded noise is the model of narrow-band noise, and the Gaussian white noise and Ornstein-Uhlenbeck process are the models of wide-band noise in Monte Carlo simulation. The method of averaging, both first-order and second-order, is applied to simplify the integro-differential equations. Then the moment Lyapunov exponents are determined directly from the averaged equations for the cases of wide-band noise excitation, or are determined numerically by Fourier series expansion from the eigenvalue problems governing the moment Lyapunov exponents in the bounded noise case. The stability of the SDOF linear viscoelastic system is determined in the sense of the moment Lyapunov exponents. Numerical simulations using the algorithm presented in Chapter 2 show that the approximated analytical results from the averaged system agree well with the simulation results. This indicates that the method of stochastic averaging is an effective tool in analyzing the stability properties of viscoelastic systems.

The approximate analytical results and the Monte Carlo simulation results of the moment Lyapunov exponents in Chapter 3 show that, in order to stabilize the SDOF linear viscoelastic system, the intensity of viscoelasticity and the material relaxation time have to be increased, while the noise intensity has to be decreased.

Since nonlinearity exists everywhere, Chapter 4 investigates the stability of a SDOF viscoelastic system with cubic nonlinearity under the parametric excitation of wide-band noise. Stochastic averaging method is applied again to simplify the system. The existence of nonlinear viscoelasticity makes the nonlinear analysis possible because the averaged equation is nonlinear. The Lyapunov exponents of the averaged system are solved using the ergodic property of the stationary solutions. Monte Carlo simulation is also applied to obtain the Lyapunov exponents numerically. The results indicate that, when the trivial stationary solution loses its stability property under the change of some system parameters, the response does not always increase infinitely, but stays as the non-trivial stationary solution. This D-bifurcation phenomenon makes the behaviour of nonlinear viscoelastic systems different for that of linear viscoelastic systems. The nonlinear viscoelastic system may exhibit P-bifurcation under some conditions. However, P-bifurcation does not mean the change of stability of solutions, but the formal change of stationary probability density. In the case of weak nonlinearity, the averaging method provides a good approximation to the original SDOF nonlinear viscoelastic system.

From the results in this thesis, it can be concluded that viscoelasticity always help to stabilize the system, in the sense that the Lyapunov exponents and moment Lyapunov exponents decrease when the effect of viscoelasticity increases.

5.2 Future Research

It can be seen that the method of stochastic averaging plays an important role in the research of this thesis. As introduced in Chapter 1, the solution of the averaged system only converges weakly to the solution of the original system in a finite time scale. However, the evaluation of Lyapunov exponents and moment Lyapunov exponents requires the properties of the solutions at infinite time according to their definitions. Therfore, theoretically, the Lyapunov exponents and moment Lyapunov exponents obtained from the averaged systems are still not sufficient to totally describe the properties of the original systems. Although there is such limitation, as an effective approximation, the averaging method has widely used in physical sciences and engineering since it was developed, and it has provided many

important results in applications. If the averaging principle can be strengthened in the convergence properties or in wider time scale, it would be of great help. However, this seems to be a challenge work, and has to wait for the advances in mathematics.

The results in Chapter 4 advise that modified averaging methods need to be developed for the cases with strong nonlinearity. Even in the cases of weak nonlinearity, the standard averaging method needs to be improved if considering the difference of staionary density functions between the averaging approximation and the simulation. The simulation results of the Lyapunov exponents related to the non-trivial solution also require improvement in algorithm. It seems that simulation through the linearized equations of nonlinear systems is not an appropriate approach, especially for high-dimensional systems. One possible approach may be through the non-trivial solutions themselves, i.e. the Lyapunov exponents are found from the stationary time series [114], [50].

In the practical analysis of structural dynamics, a large structure is usually discretized by finite element method, which leads to a multiple degrees-of-freedom (MDOF) system. Therefore, studying the stability of MDOF viscoelastic systems under stochastic perturbations is of great importance. Some research have been found for coupled oscillators, i.e. the cases of two degrees-of-freedom elastic systems, where the polar coordinate transformation similar to the SDOF case was applied [83], [84], [85]. However, for systems with degrees-of-freedom higher than 2, even in the elastic cases, the analysis is not easy to proceed when considering the random perturbations.

The theory of stochastic dynamical systems are far from complete. There is a long way to go before a satisfactorily complete understanding can be obtained. However, the splendid world encourages everyone step deep into the research of this essentially random nature.

Bibliography

1. S.T. Ariaratnam. Stochastic stability of linear viscoelastic systems. *Probablistic Engineering Mechanics*, **8**, pp. 153–155, 1993.

2. S.T. Ariaratnam. Stochastic stability of viscoelastic systems under bounded noise excitation. In A. Naess and S. Krenk, editors, *IUTAM Symposium on Advances in Nonlinear Stochastic Mechanics*, pp. 11–18. Kluwer Academic Publishers, 1996.

3. S.T. Ariaratnam. Stochastic bifurcation in hereditary systems. In *Proceedings of the 8th ASCE Joint Specialty Conference on Probabilistic Mechanics and Structural Reliability*, University of Notre Dame, Notre Dame, Indiana, 2000. CD-ROM Proceedings (Kareem, Haldar, Spencer, and Johnson, eds.), paper PMC2000-163, 6 pages.

4. L. Arnold, M.M. Doyle, and N.S. Namachchivaya. Small noise expansion of moment Lyapunov exponents for two-dimensional systems. *Dynamics and Stability of Systems*, **12**(3), pp. 187–211, 1997.

5. L. Arnold, W. Kliemann, and E. Oeljeklaus. Lyapunov exponents of linear stochastic systems. In L. Arnold and V. Wihstutz, editors, *Lecture Notes in Mathematics*, vol. 1186, pp. 85–125, Berlin, 1986. Springer-Verlag. Proceedings of a Workshop, Bremen, Germany, 1984.

6. L. Arnold, N.S. Namachchivaya, and K. Schenk-Hoppé. Toward an understanding of the stochastic hopf bifurcation: a case study. *International Journal of Bifurcation and Chaos*, **6**(11), pp. 1947–1975, 1996.

7. L. Arnold, E. Oeljeklaus, and E. Pardoux. Almost sure and moment stability for linear Itô equations. In L. Arnold and V. Wihstutz, editors, *Lecture Notes in Mathematics*, vol. 1186, pp. 129–159, Berlin, 1986. Springer-Verlag. Proceedings of a Workshop, Bremen, Germany, 1984.

8. L. Arnold. *Stochastic Differential Equations : Theory and Applications*. John Wiley & Sons, Inc., New York, 1974.

9. L. Arnold. A formula connecting sample and moment stability of linear stochastic systems. *SIAM Journal of Applied Mathematics*, **44**(4), pp. 793–802, 1984.

10. L. Arnold. *Random Dynamical Systems*. Springer-Verlag, Berlin, 1998.

11. V.I. Arnold and A. Avez. *Ergodic Problems of Classical Mechanics*. Addisin-Wesley Publishing Company, Inc., Redwood City, California, 1968.

12. V.I. Arnold. *Ordinary Differential Equations*. The MIT Press, Cambridge, Massachusetts, 1973. Translated from the Russian by R.A. Silverman.

13. O.E. Barndorff-Nielsen and D.R. Cox. *Asymptotic Techniques for Use in Statistics*. Chapman and Hall, London, 1989.

14. P.H. Baxendale and D.W. Stroock. Large deviations and stochastic flows of diffeomorphisms. *Probability Theory and Related Fields*, **80**, pp. 169–215, 1988.

15. P.H. Baxendale. Asymptotic behavior of stochastic flows of diffeomorphisms. In K. Itô and T. Hida, editors, *Lecture Notes in Mathematics*, vol. 1203, pp. 1–19, Berlin, 1986. Springer-Verlag. Proceedings of the International Conference Held in Nagoya, 1985.

16. P.H. Baxendale. Stability along trajectories at a stochastic bifurcation point. In H. Crauel and M. Gundlach, editors, *Stochastic Dynamics*, pp. 1–25, New York, 1999. Springer-Verlag.

17. P.H. Baxendale. Stochastic averaging and asymptotic behavior of the stochastic Duffing-van der Pol equation. *Stochastic Processes and Their Applications*, **113**, pp. 235–272, 2004.

18. G.D. Birkhoff. *Dynamical Systems*. American Mathematical Society, Providence, Rhode Island, 1966.

19. F. Bloom. *Ill-Posed Problems for Integrodifferential Equations in Mechanics and Electromagnetic Theory*. Society for Industrial and Applied Mathematics, Philadelphia, 1981.

20. N. Bogoliubov and A. Mitropolskii. *Asymptotic Methods in the Theory of Nonlinear Oscillations*. Gordon and Breach, New York, 1961.

21. V.V. Bolotin. *Nonconservative Problems of the Theory of Elastic Stability*. Pergamon Press, Oxford, 1963. Translated from the Russian.

22. V.V. Bolotin. *The Dynamic Stability of Elastic Systems*. Holden-Day, Inc., San Francisco, 1964. Translated from the Russian.

23. P. Bougerol and J. Lacroix. *Products of Random Matrices with Applications to Schrödinger Operators*. Birkhäuser, Boston, 1985.

24. P. Boxler. Lyapunov exponents indicate stability and detect stochastic bifurcations. In P. Krée and W. Wedig, editors, *Probabilistic Methods in Applied Physics*, pp. 97–119, Berlin, 1995. Springer-Verlag.

25. R.M. Christensen. *Theory of Viscoelasticity: An Introduction*. Academic Press, New York, second edition, 1982.

26. H. Cramér. *Mathematical Methods of Statistics*. Princeton University Press, Princeton, 1946.

27. G.J. Creus. *Viscoelasticity : Basic Theory and Applications to Concrete Structures*. Springer-Verlag, Berlin, 1986.

28. C.M. Dafermos and J.A. Nohel. Energy methods for nonlinear hyperbolic volterra integrodifferential equations. *Communication in Partial Differential Equations*, **4**(3), pp. 219–278, 1979.

29. C.M. Dafermos and J.A. Nohel. A nonlinear hyperbolic volterra equation in viscoelasticity. In D.N. Clark, G. Pecelli, and R. Sacksteder, editors, *Contributions to Analysis and Geometry*, pp. 87–116. The John Hopkins University Press, 1981. Supplement to the American Journal of Mathematics.

30. L. Devroye and L. Györfi. *Nonparametric Density Estimation : The L1 View*. John Wiley & Sons, Inc., New York, 1984.

31. W. Feller. *An Introduction to Probability Theory and Its Applications*, vol. 2. John Wiley & Sons, Inc., New York, second edition, 1965.

32. J.D. Ferry. *Viscoelastic Properties of Polymers*. John Wiley & Sons, Inc., New York, third edition, 1980.

33. W. Flugge. *Viscoelasticity*. Blaisdell Publishing Company, 1967.

34. M.I. Freidlin and A.D. Wentzell. *Random Perturbations of Dynamical Systems*. Springer-Verlag, New York, 1984.

35. M.I. Freidlin and A.D. Wentzell. *Random Perturbations of Hamiltonian Systems*, vol. 109 of *Memoirs of the American Mathematical Society, No. 523*. American Mathematical Society, Providence, Rhode Island, 1994.

36. A. Friedman. *Stochastic Differential Equations and Applications*, vol. 1. Academic Press, New York, 1975.

37. Y.C. Fung. *A First Course in Continuum Mechanics*. Prentice Hall, Inc., second edition, 1977.

38. H. Furstenberg and H. Kesten. Products of random matrices. *The Annals of Mathematical Statistics*, **31**(2), pp. 457–469, 1960.

39. H. Furstenberg and H. Kesten. Noncommuting random products. *Transactions of the American Mathematical Society*, **108**(3), pp. 377–428, 1963.

40. C.W. Gardiner. *Handbook of Stochastic Methods : for Physics, Chemistry, and the Natural Sciences*. Springer-Verlag, Berlin, third edition, 2004.

41. I.I. Gihman and A.V. Skorohod. *Stochastic Differential Equations*. Ergebnisse der Mathematik und Ihrer Grenzgebiete, Band 72. Springer-Verlag, Berlin, 1972. Translated by Kenneth Wickwire.

42. B.V. Gnedenko and A.N. Kolmogorov. *Limit Distributions for Sums of Independent Random Variables*. Addison-Wesley Publishing Company, Inc., 1954. Translated from the Russian.

43. A.E. Green and R.S. Rivlin. The mechanics of nonlinear materials with memory. part i. *Archive for Rational Mechanics and Analysis*, **1**(1), 1957.

44. A. Grorud and D. Talay. Approximation of Lyapunov exponents of nonlinear stochastic differential equations. *SIAM Journal on Applied Mathematics*, **56**(2), pp. 627–650, 1996.

45. J. Guckenheimer and P. Holmes. *Nonlinear Oscillations, Dynamical Systems and Bifurcations of Vector Fields*. Springer-Verlag, New York, 1983.

46. I.H. Hall. Viscoelasticity of textile fibers at finite strains. *Journal of Polymer Science Part A-2 : Polymer Physics*, **5**(6), pp. 1119–1144, 1967.

47. A.J. Heunis and M.A. Kouritzin. Strong convergence in the stochastic averaging principle. *Journal of Mathematical Analysis and Applications*, **187**, pp. 134–155, 1994.

48. M. Hijawi, R.A. Ibrahim, and N. Moshchuk. Nonlinear random response of ocean structures using first- and second-order stochastic averaging. *Nonlinear Dynamics*, **12**(2), pp. 155–197, 1997.

49. M.W. Hirsch, S. Smale, and R.L. Devaney. *Differential Equations, Dynamical Systems and An Introduction to Chaos*. Elsevier Academic Press, San Diego, California, second edition, 2004.

50. J. Holzfuss and U. Parlitz. Lyapunov exponents from time series. In L. Arnold, H. Crauel, and J.-P. Eckmann, editors, *Lecture Notes in Mathematics*, vol. 1486, pp. 263–270, Berlin, 1991. Springer-Verlag. Proceedings of a Conference, Oberwolfach, Germany, 1990.

51. W.J. Hrusa. Global existence and asymptotic stability for a semilinear hyperbolic volterra equation with large initial data. *SIAM Journal on Mathematical Analysis*, **16**(1), pp. 110–134, 1985.

52. N. Jacobson. *Lie Algebras*. John Wiley & Sons, Inc., New York, 1962.

53. T. Kawata. *Fourier Analysis in Probability Theory*. Academic Press, New York, 1972.

54. H.K. Khalil. *Nonlinear Systems*. Prentice Hall, Inc., Upper Saddle River, N.J., third edition, 2002.

55. R.Z. Khasminskii and N. Moshchuk. Moment Lyapunov exponent and stability index for linear conservative system with small random perturbation. *SIAM Journal of Applied Mathematics*, **58**(1), pp. 245–256, 1998.

56. R.Z. Khasminskii. A limit theorem for the solutios of differential equations with random right-hand sides. *Theory of Probability and Its Applications*, **11**(3), pp. 390–406, 1966. English translation.

57. R.Z. Khasminskii. On stochastic processes defined by differential equations with a small parameter. *Theory of Probability and Its Applications*, **11**(2), pp. 211–228, 1966. English translation.

58. R.Z. Khasminskii. *Stochastic Stability of Differential Equations*. Kluwer Academic Publishers, Norwell, MA, 1980. English translation.

59. P.E. Kloeden, E. Platen, and H. Schurz. *Numerical Solution of SDE Through Computer Experiments*. Springer-Verlag, Berlin, 1994.

60. P.E. Kloeden and E. Platen. *Numerical Solution of Stochastic Differential Equations*. Springer-Verlag, Berlin, 1992.

61. J.E. Kolassa. *Series Approximation Methods in Statistics*. Springer Science+Business Media, Inc., New York, third edition, 2006.

62. J. Komlós, P. Major, and G. Tusnády. An approximation of partial sums of independent rv's and the sample df. i. *Z. Wahrscheinlichkeitstheorie verw. Gebiete*, **32**, pp. 111–131, 1975.

63. J. Komlós, P. Major, and G. Tusnády. An approximation of partial sums of independent rv's and the sample df. ii. *Z. Wahrscheinlichkeitstheorie verw. Gebiete*, **34**, pp. 33–58, 1976.

64. M.A. Kouritzin and A.J. Heunis. Rates of convergence in a central limit theorem for stochastic processes defined by differential equations with a small parameter. *Journal of Multivariate Analysis*, **43**, pp. 58–109, 1992.

65. M.A. Kouritzin and A.J. Heunis. A law of the iterated logarithm for stochastic processes defined by differential equations with a small parameter. *The Annals of Probability*, **22**(2), pp. 659–679, 1994.

66. N. Krylov and N. Bogoliubov. *Introduction to Nonlinear Mechanics*. Princeton University Press, Princeton, NJ, 1943.

67. H. Kunita. *Stochastic Flows and Stochastic Differential Equations*. Cambridge University Press, Cambridge, 1990.

68. H.J. Kushner. *Stochastic Stability and Control*. Academic Press, New York, 1967.

69. G.S. Larionov. Investigation of the vibrations of relaxing systems by the averaging method. *Mechanics of Composite Materials*, **5**(5), pp. 714–720, 1969. English translation from Mekhanika Polimerov, No. 5, pp. 806¨C813, September¨COctober, 1969.

70. H. Leaderman, F. McCrackin, and O. Nakada. Large longitudinal retarded elastic deformation of rubberlike network polymers. ii. application of a general formulation of nonlinear response. *Journal of Rheology*, **7**(1), pp. 111–123, 1963.

71. H. Leaderman. Large longitudinal retarded elastic deformation of rubberlike network polymers. *Journal of Rheology*, **6**(1), pp. 361–382, 1962.

72. H. Leipholz. *Stability of Elastic Systems*. Sijthoff & Noordhoff, Alphen aan den Rijn, The Netherlands, 1980.

73. Y.K. Lin and G.Q. Cai. *Probabilistic Structural Dynamics : Advanced Theory and Applications*. McGraw-Hill, Inc., New York, 1995.

74. Y.K. Lin and G.Q. Cai. Some thoughts on averaging techniques in stochastic dynamics. *Probabilistic Engineering Mechanics*, **15**(1), pp. 7–14, 2000.

75. Y.K. Lin. *Probabilistic Theory of Structural Dynamics*. McGraw-Hill, Inc., New York, 1967.

76. P. Lochak and C. Meunier. *Multiphase Averaging for Classical Systems : with Applications to Adiabatic Theorems*. Springer-Verlag, New York, 1988.

77. E. Lukacs. *Characteristic Functions*. Charles Griffin & Company Ltd., London, second edition, 1970.

78. A.M. Lyapunov. Problème générale de la stabilité du mouvement. *Communications de la Société Mathématique de Kharkov*, **2**, pp. 265–272, 1892. Reprinted in *Annals of Mathematical Studies*, vol. 17, Princeton University Press, Princeton, 1947.

79. A.M. Lyapunov. *Stability of Motion*. Mathematics in Science and Engineering, vol. 30. Academic Press, New York, 1966.

80. G.N. Milstein. *Numerical Integration of Stochastic Differential Equations*. Kluwer Academic Publishers, Dordrecht, 1995.

81. S.A. Molchanov. The structure of eigenfunctions of one-dimensional unordered structures. *Mathematics of the USSR. Izvestija*, **12**, pp. 69–101, 1978.

82. J.A. Murdock. *Perturbations. Theory and Methods*. Society for Industrial and Applied Mathematics, Philadelphia, 1999.

83. N.S. Namachchivaya, H.J. Van Roessel, and M.M. Doyle. Moment Lyapunov exponent for two coupled oscillators driven by real noise. *SIAM Journal of Applied Mathematics*, **56**(5), pp. 1400–1423, 1996.

84. N.S. Namachchivaya and H.J. Van Roessel. Moment Lyapunov exponent and stochastic stability of two coupled oscillators driven by real noise. *ASME Journal of Applied Mechanics*, **68**(6), pp. 903–914, 2001.

85. N.S. Namachchivaya and H.J. Van Roessel. Stochastic stability of coupled oscillators in resonance : A perturbation approach. *ASME Journal of Applied Mechanics*, **71**, pp. 759–768, 2004.

86. N.S. Namachchivaya and L. Vedula. Stabilization of linear systems by noise : application to flow induced oscillations. *Dynamics and Stability of Systems*, **15**(2), pp. 185–208, 2000.

87. N.S. Namachchivaya. Stochastic bifurcation. *Applied Mathematics and Computation*, **30**, pp. 37–95, 1990.

88. P.J. Olver. *Applications of Lie Groups to Differential Equations*. Springer-Verlag, New York, second edition, 1993.

89. Y.I. Oseledec. A multiplicative ergodic theorem. Lyapunov characteristic number for dynamical systems. *Transactions of the Moscow Mathematical Society*, **19**, pp. 197–231, 1968. English translation.

90. V.D. Potapov. On almost sure stability of a viscoelastic column under random loading. *Journal of Sound and Vibration*, **173**(3), pp. 301–308, 1994.

91. V.D. Potapov. Numerical method for investigation of stability of stochastic integro-differential equations. *Applied Numerical Mathematics*, **24**, pp. 191–201, 1997.

92. M.J. Quinn. *Parallel Programming in C with MPI and OpenMP*. McGraw-Hill, Boston, 2004.

93. J.B. Roberts and J.F. Donne. Literature review : Nonlinear random vibration in mechanical systems. *The Shock and Vibration Digest*, **20**(6), pp. 16–25, 1988.

94. J.B. Roberts and P.D. Spanos. Stochastic averaging : An approximate method of solving random vibration problems. *International Journal of Non-Linear Mechanics*, **21**(2), pp. 111–134, 1986.

95. J.B. Roberts. Techniques for nonlinear random vibration problems. *The Shock and Vibration Digest*, **16**(9), pp. 3–14, 1984.

96. R. Roscoe. Mechanical models for the representation of visco-elastic properties. *British Journal of Applied Physics*, **1**, pp. 171–173, 1950.

97. J.A. Sanders and F. Verhulst. *Averaging Methods in Nonlinear Dynamical Systems*. Springer-Verlag, New York, 1985.

98. K.R. Schenk-Hoppé. Bifurcation scenarios of the noisy duffing-van der Pol oscillator. *Nonlinear Dynamics*, **11**, pp. 255–274, 1996.

99. K.R. Schenk-Hoppé. Stochastic Hopf bifurcation: an example. *International Journal of Nonlinear Mechanics*, **31**(5), pp. 685–692, 1996.

100. R.J. Serfling. *Approximation Theorems of Mathematical Statistics*. John Wiley & Sons, New York, 1980.

101. A.N. Shiryayev. *Probability*. Springer-Verlag, New York, 1984.

102. A.V. Skorokhod, F.C. Hoppensteadt, and H. Salehi. *Random Perturbation Methods with Applications in Science and Engineering*. Springer-Verlag, New York, 2002.

103. A.V. Skorokhod. *Asymptotic Methods in the Theory of Stochastic Differential Equations*. American Mathematical Society, Providence, Rhode Island, 1989.

104. M. Snir, S. Otto, S. Huss-Lederman, D. Walker, and J. Dongarra. *MPI : The Complete Reference*. The MIT Press, Cambridge, Massachusetts, 1996.

105. K. Sobczyk. *Stochastic Differential Equations : with Applications to Physics and Engineering*. Kluwer Academic Publishers, Dordrecht, 1991.

106. R.L. Stratonovich. *Topics in the Theory of Random Noise*, vol. 1. Gordon and Breach Science Publishers, Inc., New York, 1963.

107. R.L. Stratonovich. *Topics in the Theory of Random Noise*, vol. 2. Gordon and Breach Science Publishers, Inc., New York, 1967.

108. D. TALAY AND L. TUBARO. Expansion of the global error for numerical schemes solving stochastic differential equations. *Stochastic Analysis and Applications*, **8**(4), pp. 483–509, 1990.

109. D. TALAY. Approximation of upper Lyapunov exponents of bilinear stochastic differential systems. *SIAM Journal on Numerical Analysis*, **28**(4), pp. 1141–1164, 1991.

110. D. TALAY. Simulation of stochastic differential systems. In P. Krée and W. Wedig, editors, *Probabilistic Methods in Applied Physics*, pp. 54–96, Berlin, 1995. Springer-Verlag.

111. W. WEDIG. Lyapunov exponent of stochastic systems and related bifurcation problems. In S.T. Ariaratnam, G.I. Schuëller, and I. Elishakoff, editors, *Stochastic Structural Dynamics – Progress in Theory and Applications*, pp. 315–327, London, 1988. Elsevier Applied Science.

112. R.E. WHITE. *Computational Mathematics : Models, Methods and Analysis with MATLAB and MPI*. CHAPMAN & HALL/CRC, Boca Raton, Florida, 2004.

113. S. WIGGINS. *Introduction to Applied Nonlinear Dynamical Systems and Chaos*. Springer-Verlag, 1990.

114. A. WOLF, J.B. SWIFT, H.L. SWINNEY, AND J.A. VASTANO. Determining Lyapunov exponents from a time series. *Physica*, **16D**, pp. 285–317, 1985.

115. E. WONG. *Stochastic Processes in Information and Dynamical Systems*. McGraw-Hill, New York, 1971.

116. W.C. XIE. Moment Lyapunov exponents of a two-dimensional system under real noise excitation. *Journal of Sound and Vibration*, **239**(1), pp. 139–155, 2001.

117. W.C. XIE. Moment Lyapunov exponents of a two-dimensional system under bounded noise parametric excitation. *Journal of Sound and Vibration*, **263**(3), pp. 593–616, 616 2003.

118. W.C. XIE. Monte Carlo simulation of moment Lyapunov exponents. *ASME Journal of Applied Mechanics*, **72**(2), pp. 269–275, 2005.

119. W.C. XIE. *Dynamic Stability of Structures*. Cambridge University Press, 2006.

120. E. ZEIDLER. *Nonlinear Functional Analysis and Its Application*, VOL. 1 : FIXED-POINT THEOREMS. Springer-Verlag, New York, 1985.

121. H. Ziegler. *Principles of Structural Stability*. Blaisdell Publishing Company, Waltham, MA, 1968.